IDENTIFICATION OF A NOVEL ERK1/2-INTERACTING A-KINASE ANCHORING PROTEIN

APPROVED BY SUPERVISORY COMMITTEE

Melanie H. Cobb, Ph.D. (mentor)

Joseph P. Albanesi, Ph.D. (chair)

Michael G. Roth, Ph.D.

William J. Snell, Ph.D.

I would like to thank the members of my Graduate Committee, particularly my mentor, Dr. Melanie Cobb, and my parents, Alnasir and Farida Jivan.

IDENTIFICATION OF A NOVEL ERK1/2-INTERACTING A-KINASE ANCHORING PROTEIN

by

ARIF JIVAN

DISSERTATION

Presented to the Faculty of the Graduate School of Biomedical Sciences

The University of Texas Southwestern Medical Center at Dallas

In Partial Fulfillment of the Requirements

For the Degree of

DOCTOR OF PHILOSOPHY

The University of Texas Southwestern Medical Center at Dallas

Dallas, Texas

April 2009

IDENTIFICATION OF A NOVEL ERK1/2-INTERACTING A-KINASE ANCHORING PROTEIN

Arif Jivan, Ph.D.

The University of Texas Southwestern Medical Center at Dallas, 2009

Supervising Professor: Melanie H. Cobb, Ph.D.

Abstract: Initially identified in *Chlamydomonas*, radial spoke protein 3 (RSP3) is one of at least twenty identified radial spoke structural components of motile cilia and is required for axonemal sliding and flagellar motility. The mammalian orthologs for this and other radial spoke proteins, however, remain to be identified and fully characterized.

Mammalian RSP3 was found to interact with ERK2 through a yeast two-hybrid screen designed to identify interactors that have a higher affinity for the phosphorylated, active form of ERK2. Confirming this finding, the human homolog long form, RSP3H, co-immunoprecipitates with ERK1/2 in HEK293 cells. Human RSP3, and its larger alternative start site gene product, radial spoke protein 3 homolog (RSP3H), are phosphorylated by ERK1/2 on threonine 286 *in vitro* and in cells. RSP3/RSP3H are also phosphorylated *in vitro* by cAMP-dependent protein kinase (PKA). Additionally, we showed that human RSP3H functions as an A-kinase anchoring protein (AKAP), and its ability to bind to the regulatory subunits of PKA, RIIα and RIIβ, is regulated by ERK1/2 activity and phosphorylation. Interestingly, expression analysis of mRNA suggests RSP3/RSP3H are also present in cells that are thought to contain a single primary cilium but not motile cilia. Immunofluorescence staining of primary cilia-containing cells indicates that RSP3/RSP3H localize to nuclear punctae, specifically promyelocytic leukemia (PML) bodies, suggesting a non-cilia related role for RSP3/RSP3H in these cells. Functionally, RSP3/RSP3H may localize ERK1/2 to a distinct site of action within the cell and serve as a point of convergence of cAMP-dependent and PKA-mediated influence upon ERK1/2 downstream signaling or vice versa. These data are the first to establish a connection between ERK1/2 and what was once ostensibly thought to only be a ciliary component as well as to identify a novel ERK1/2-interacting AKAP.

TABLE OF CONTENTS

PRIOR PUBLICATIONS

Michael C. Lawrence, **Arif Jivan**, Chunli Shao, Lingling Duan, Daryl Goad, Elma Zaganjor, Jihan Osborne, Kathleen McGlynn, Steve Stippec, Svetlana Earnest, Wei Chen, and Melanie H. Cobb. (2008). The roles of MAPKs in disease. *Cell Research* **18**: 436-442.

Paul L. Shaffer, **Arif Jivan**, D. Eric Dollins, Frank Claessens, and Daniel T. Gewirth. (2004). Structural basis of androgen receptor binding to selective androgen response elements. *Proceedings of the National Academy of Sciences*, **101**: 4758-4763.

Karen L. Soldano, **Arif Jivan**, Christopher V. Nicchitta, and Daniel T. Gewirth. Structure of the N-terminal Domain of GRP94. (2003). *Journal of Biological Chemistry* **279**: 48330-48338.

FIGURES

TABLES

ABBREVIATIONS

AC	adenylyl cyclase
ADP	adenosine diphosphate
AKAP	A-kinase anchoring protein
AKIP	A-kinase interacting protein
AP	adaptor protein
ARF	ADP-ribosylation factor
ATP	adenosine triphosphate
C	catalytic; e.g. subunit of PKA; Cα, β, γ
cAMP	cyclic adenosine 3',5'-monophosphate
CREB	cAMP response element binding protein
D	docking
DAPI	4',6-diamidino-2-phenylindole
DEF	docking site for ERK and FXFP
DUSP1	dual-specificity phosphatase 1
EGF(R)	epidermal growth factor (receptor)
Epac	exchange protein activated by cAMP
ERK	extracellular signal-regulated kinase
FGF(R)	fibroblast growth factor (receptor)
GABA	gamma-aminobutyric acid
GAP	GTPase activating protein
GEF	guanine nucleotide exchange factor
GFP	green fluorescent protein
GGA	Golgi-localized, γ-ear- containing, ARF-binding
GTP	guanosine triphosphate
HEK293	human embryonic kidney 293 cells
IFT	intraflagellar transport

IMCD3	inner-medullary collecting duct cells (mouse)
IP_3R	inositol 1,4,5-trisphosphate receptor
JNK	c-Jun N-terminal kinase
KSR	kinase suppressor of Ras
MAP2	microtubule associated protein 2
MAP(K)	mitogen activated protein (kinase)
MAP2K	MAP kinase kinase
MAP3K	MAP kinase kinase kinase
MEF	mouse embryonic fibroblast
MEK	MAP/ERK kinase
NES	nuclear export signal
NLS	nuclear localization signal
PCD	primary cilia dyskinesia
PDGF(R)	platelet-derived growth factor (receptor)
PDE	phosphodiesterase
PEA/PED-15	phospho-protein enriched in astrocytes/diabetes 15
PKA	cAMP-dependent protein kinase; protein kinase A
PKC	protein kinase C
PKD	polycystic kidney disease
PKI	protein kinase (A) inhibitor
PML	promyelocytic leukemia
PP2B	protein phosphatase 2B; calcineurin
R	regulatory; e.g. subunit of PKA; RIIα, β
RPE1	retinal pigmentosa epithelial 1 cells (human)
RSK	ribosomal S6 kinase
RSP3/RSP3H	radial spoke protein 3; radial spoke protein 3 homolog
RyR	ryanodine receptor
SAM68	Src-associated in mitosis; 68kDa

SAPK	stress-activated protein kinase
SC35	splicing factor; 35kDa
SR3	somatostatin receptor 3
SUMO	small ubiquitin-like modifier
U2OS	osteosarcoma (human) cells

CHAPTER 1. INTRODUCTION

I. MAP kinases

The study of protein phosphorylation can be traced to Levene and Alsberg, who in 1906 described the presence of phosphorous in the protein vitellin, a component of egg yolk (Levene and Alsberg, 1906). Lipmann and Levene later identified the presence of phospho-serine in vitellin, providing the first known example of phosphate-incorporation into a particular amino acid (Lipmann and Levene, 1932). Within 25 years, Burnett and Kennedy described the enzymatic transfer of phosphate from adenosine triphosphate (ATP) to casein, marking a watershed in protein phosphorylation as a critical mechanism by which protein function can be modified within the cell (Burnett and Kennedy, 1954). With the seminal discovery of the first known protein kinase, phosphorylase kinase, an enzyme that catalyzes phosphate transfer and the interconversion of inactive phosphorylase *b* into its active *a* form, Krebs and Fischer established the foundation for the study of reversible phosphorylation as a means to regulate intracellular protein function as well as the enzymes that mediate this reaction (Krebs and Fischer, 1956). Protein kinases are now known to participate in a significant number of signaling events within the cell, culminating in many different cellular outcomes.

The prototypic mitogen-activated protein (MAP) kinase signaling cascade comprises three protein kinases: MAP kinase kinase kinase (MAP3K), MAP kinase kinase (MAP2K), and MAP kinase (MAPK). A classical example of this three kinase cascade is the Raf (MAP3K), MAP/ERK kinase (MEK, MAP2K)) and extracellular regulated kinase (ERK, MAPK) pathway. When activated, the small GTPase Ras, loaded with guanosine triphosphate (GTP), recruits Raf to the membrane, where it is subsequently activated. The serine/threonine kinase Raf,

composed of three family members - A-Raf, B-Raf and C-Raf (also known as Raf-1) - then dually phosphorylates and activates the dual specificity kinases, MEK1/2, which in turn phosphorylate ERK1/2 on threonine and tyrosine residues within their activation loops. The serine/threonine kinases ERK1/2 phosphorylate numerous substrates that participate in a diverse complement of fundamental cellular process including: cell proliferation, survival, differentiation, apoptosis, motility and cytoskeletal dynamics, transcriptional control, and metabolism. In coordinating these processes, the MAP kinase cascades transmit, propagate and amplify signals in responses to diverse extra- and intra-cellular stimuli that are constantly sampled by a cell in a physiological context.

ERK1/2 are members of a larger family of MAP kinases that include the c-Jun N-terminal kinases (JNKs) and stress-activated protein kinases (SAPKs) 1-3, the p38 MAP kinases α, β, γ, δ as well as ERK3, ERK5 and ERK7. (Aouadi et al., 2006). ERK1 and ERK2 are conserved in all eukaryotes and are among the most ubiquitous signaling molecules within diverse cell systems. ERK1 and ERK2 share 84% sequence identity and are 43kDa and 41.2kDa respectively (Boulton et al., 1991). The many cellular processes that these kinases participate in translate into significant and diverse physiological roles, as ERK1/2 are required for normal β-cell function including insulin transcription and secretion, immunological maturation, cognitive function and memory development (Khoo and Cobb, 1997; Berman et al., 1998; Hatano et al., 2003; Khoo et al., 2003; Samuels et al, 2008). Consequently, aberrant signaling by ERK1/2 pathway is implicated in numerous pathologies including: polycystic kidney disease, diabetes, and cancer to name a few (Vigliotta et al., 2004; Lawrence et al., 2005; Omori et al., 2006; Roberts and Der, 2007; Lawrence et al., 2008; Samuels et al, 2008; Shibazaki et al., 2008). Furthermore, microdeletions within the *MAPK1* (ERK2) gene causing decreased ERK2 levels have been found in patients with

DiGeorge syndrome, characterized by craniofacial abnormality and cognitive defects (Newbern et al., 2008).

Despite their sequence identity and significantly similar cellular roles, ERK1/2 are not functionally redundant. ERK2 null mice die during embryonic development by E8.5 due to defects in embryogenesis and placental development. In contrast, ERK1 deficient mice are viable and fertile but have impaired thymocyte maturation. (Pages et al., 1999; Hatano et al., 2003; Saba-El-Leil et al., 2003). Additionally, ERK1 knockout mice display enhanced long-term potentiation in the nucleus accumbens, contributing to hypersensitivity to rewarding cues (Mazzucchelli et al., 2002). As mentioned above, the upstream kinase MEK phosphorylates ERK at the threonine (T) and tyrosine (Y) residues of a threonine, glutamate (E), tyrosine (T^{202}-E-Y^{204} in human ERK1 and T^{185}-E-Y^{187} in human ERK2) motif within the activation loop. Upon activation, ERK1/2 phosphorylate substrates at serine or threonine residues typically followed by a proline (S/T-P sites). Three docking motifs for ERK1/2 binding have been defined in and are critical for determining specificity of substrates. One particular motif is the docking site for ERK and FXFP (DEF, also known as FXF for its amino-acid specificity), which is found in substrates such as the transcription factor c-Fos and the dual-specificity phosphatase DUSP1 (Jacobs et al., 1999). Substrates can also contain the MAPK docking or D motif. These motifs are generally N-terminal to the ERK1/2 phosphorylation site in the substrate and are characterized by the consensus sequence: R/K-X_{4-6}- R/K-ϕ-X-ϕ, where X is any amino acid and ϕ is generally an aliphatic hydrophobic residue such as valine, leucine or isoleucine. The D motif is not only found in ERK1/2 substrates such as ribosomal S6 kinase (RSK) but also in the upstream MAP2Ks MEK1/2 (Yang, Yates et al., 1998; Sharrocks et al., 2000; Tanoue et al., 2000). Finally, a subset of ETS transcription factors contain a leucine-rich motif L-X-L-X_3-F within a conserved 80 amino acid

region termed the pointed domain (Seidel and Graves, 2002). Several ERK1/2 interacting proteins contain combinations of ERK1/2 interacting motifs, in particular both D and FXF sequences in multiple copies, which perhaps function synergistically or contribute to differential interactions with the MAPKs depending on spatiotemporal or cellular context.

II. Regulation of MAP kinases by scaffolding proteins

Despite the linear architecture of this MAP kinase module, signaling through these kinases is not solely manifested in a single series relay of discretized switches, whose resultant outcomes are a consequence of simply turning on or off in the presence or absence of extra- and intra-cellular stimuli. The myriad of heterogeneous outcomes of signaling through these pathways is subject to several modes of regulation including: modulating enzyme kinetics, substrate availability, localization to subcellular compartments and positive and negative feedback loops, and phosphoprotein phosphatases that dephosphorylate and inactivate the pathway as well as allow for rapid reactivation. Analogous to components in an electrical circuit, proteins that regulate MAP kinase pathway signaling in the aforementioned modes can function as transistors, rectifiers and amplifiers, all of which potentiate or attenuate the frequency, duration and amplitude of activation and subsequent activity of these kinases. Here, I will focus on the mechanisms by which ERK1/2 are confined or dynamically distributed to distinct sites of action in the cell, specifically on the regulation by scaffolding and anchoring proteins that not only coordinate ERK1/2 activity, but also integrate multiple inputs into the MAP kinase cascade from other signaling modalities and allow for the divergent responses of the ERK1/2 pathway.

As alluded to earlier, the intracellular and extracellular environments are replete with signals that any given cell constantly samples in time and/or space. How then, do cells: 1. interpret signal from noise while being inundated by stimuli, and 2. integrate multiple signals when necessary to generate the appropriate response or outcome? The cell has evolved numerous mechanisms to connect disparate signaling components into a larger network, like the intricate electric circuit, such that inputs into one particular pathway can be rapidly transduced, amplified, and propagated into other pathways (i.e. cross-talk), resulting in often diverse outcomes. One means of regulation is through scaffolding or anchoring proteins, which can serve as nodes or points of convergence for multiple pathways by binding to components of two or more signaling modules. Examples of these scaffolding proteins are A-kinase anchoring proteins (AKAPs), a particular class of scaffolds that I will elaborate upon later. AKAPs not only bind to cAMP-dependent protein kinase (also known as protein kinase A, PKA), but are also known to interact with other components of signaling pathways including: the β2-adrenergic receptor, β-arrestin, GTPase activating proteins (GAPs), protein phosphatase 2B (PP2B or calcineurin), type I inositol 1,4,5-trisphosphate receptor (IP_3R) as well as other protein kinases such as protein kinase C (PKC) or ERK5 (Coghlan et al., 1995; Faux and Scott, 1997; Nauert et al., 2003; Tu et al., 2004; Houslay and Baillie, 2005). Furthermore, some scaffolding proteins are multifunctional; in addition to anchoring PKA, AKAP-Lbc is also a RhoA guanine nucleotide exchange factor (GEF) (Diviani et al., 2004). Anchoring proteins are not functionally dissimilar from scaffolding proteins, but the word anchor has been historically used to define a non-dynamic protein that serves only to confine enzymes to a particular subcellular locale i.e. in the case of AKAPs. This limited definition has been challenged by many studies suggesting the multifunctional capacities of these proteins (Sette and Conte, 1996; Kapiloff et al., 1999; Dodge-Kafka, 2005).

Scaffolding proteins associated with MAP kinase pathways serve to increase the effective concentration of the kinases in different subcellular locales and assemble kinase cascade components, substrates and downstream effectors in complexes for efficient and rapid phosphorylation and activation of signaling. Through maintaining kinases and their effectors in close proximity, scaffolding proteins facilitate multiple functional interactions and signal transduction in localized microenvironments (Morrison and Davis, 2003; Kolch, 2005). Scaffolds and anchoring proteins affect the magnitude and duration of signals through the MAP kinase pathway, mediate crosstalk with other pathways, and can serve in inhibitory roles, preventing inappropriate action of the kinases in certain cellular compartments. Scaffolds themselves are often subject to multiple post-translational modifications including phosphorylation, sumoylation, and ubiquitylation, which serve to regulate the stability of the scaffolds as well as their roles in interconnecting two or more pathways depending on a particular stimulus or change in cell context (Carnegie et al., 2004; Flotho et al., 2004; Cittero et al., 2006).

The *Saccharomyces cerevisiae* protein Ste5p was the first MAP kinase scaffold discovered. Ste5p assembles the MAP kinase module involved in the yeast pheromone response pathway at the cell cortex and is required for activation of the MAPK cascade in response to mating pheromone (Elion, 2001). Using yeast two-hybrid analysis to test pair-wise interactions, Ste5p was initially found to interact with each kinase in the yeast MAPK module: Ste11p (MEKK), Ste7p (MEK), and Fus3p (MAP kinase homolog) (Printen and Sprague, 1994). Pheromone-induction enhances nuclear export of Ste5p and recruitment to the plasma membrane to modulate the MAPK cascade activation (Mahanty et al., 1999). Ste5p is also phosphorylated by the MAP kinases - primarily by Fus3p and

Kss1p (another MAPK yeast homolog) - in response to pheromone. Additionally, phosphorylation stabilizes Ste5p and causes an accumulation of the scaffold at the cell cortex (Flotho et al., 2004).

Over the years, other scaffolding and anchoring proteins that interact with MAPK components have been identified, connecting the protein kinases to other signaling pathways as well as localizing them to distinct sites within the cell. One such scaffold is kinase suppressor of Ras (KSR), which was initially identified in genetic screens in *Drosophila melanogaster* and *Caenorhabditis elegans* as a positive regulator of activated or constitutively activated Ras. The *KSR* (or *KSR-1*) gene was initially thought to encode a novel putative protein kinase related to the Raf family of Ser/Thr kinases epistatic to Ras (Kornfeld et al., 1995; Sundram and Han, 1995; Therrien et al., 1995). However, KSR lacks a catalytic lysine invariant in all protein kinases - required for coordinating ATP - in its protein kinase domain. KSR1 also interacts with Raf-1, MEK1/2 and ERK1/2, facilitating signal propagation through the kinase module (Therrien et al., 1996; Yu et al., 1998). KSR was shown to modulate MEK localization in cells, shifting the kinase from a primarily cytosolic distribution to a macromolecular membrane-associated complex (Stewart et al., 1999).

Other well-studied MEK/ERK-interacting scaffolds include MEK1 partner (MP1) and paxillin; both are proposed to coordinate ERK signaling at focal adhesions and affect cell migration and spreading. The adaptor protein p14 recruits MP1 and links MEK and ERK activation on late endosomes, where the signaling complex is required for endosomal trafficking and progression of certain receptors (e.g. epidermal growth factor receptor) towards lysosomal degradation (Teis et al., 2002; Teis et al., 2006) MP1 is also suggested to coordinate p21-activated kinase (PAK1) phosphorylation of MEK1 and subsequent activation of ERK to suppress

Rho and Rho kinase function allowing for focal adhesion turnover (Pullikuth et al., 2005). Paxillin, which is also a substrate for ERK, scaffolds Raf, MEK and ERK at focal adhesion sites and its interaction with and phosphorylation by ERK is required for hepatocyte growth factor-induced focal adhesion turnover and tubulogenesis of mouse inner-medullary collecting duct 3 (IMCD3) epithelial cells (Ishibe et al., 2003; Ishibe et al., 2004).

Scaffolds may contribute to the inappropriate regulation of MAPK in certain pathologies. Overexpressing the ERK1/2 scaffold, phospho-protein enriched in astrocytes and diabetes (PEA/PED-15), localizes ERK to the cytoplasm through preventing nuclear transport and promoting nuclear export of ERK, thus impairing its role in transcription (Formstecher et al., 2001; Whitehurst et al., 2004). PEA-15 also scaffolds RSK, allowing for its efficient phosphorylation and activation by ERK (Vaidyanathan et al., 2007). PEA-15 transcript and protein are elevated in type 2 diabetes, contributing to insulin resistance (Condorelli et al., 1998).

To date, only one nuclear ERK1/2 scaffold, Max interactor 2 (Mxi2), has been described (Zervos et al., 1995; Sanz-Moreno et al., 2003; Casar et al., 2007). Mxi2, a p38α isoform, binds to ERK1/2 and modulates their activation of transcription factors in the nucleus (Sanz-Moreno et al., 2003). Furthermore, overexpression of Mxi2 markedly enhances the interaction between ERK1/2 and the nucleoporin, Nup153c, and the nuclear accumulation of the protein kinases (Casar et al., 2007).

III. PKA

To understand signaling cascades and the networks connecting these diverse and often disparate pathways within the cell, one must first appreciate the initial studies elucidating the action of extracellular signals upon intracellular processes and the identification of the mechanisms by which such signals are transduced rapidly and are amplified within the cell.

Cyclic adenosine 3',5'-monophosphate (cAMP) is a ubiquitous intracellular small molecule whose initial discovery by Sutherland and Rall established the classical second messenger theory of signal transduction (Rall et al., 1956; Rall and Sutherland, 1957). Essentially, first messenger extracellular hormones, via their interaction with differently expressed (i.e. cell and tissue-specific) hormone receptors, transmit signals into the cell by the generation of an intracellular second messenger (i.e. cAMP), which in turn can affect a variety of cellular processes. This concept also contributed to the initial understanding of signal transduction cascades in the regulation of many cellular pathways. Expanding on the extensive study of glycogenolysis conducted in the laboratory of Carl and Gerty Cori, Rall and Sutherland showed that the activation of phosphorylase, the enzyme that catalyzes the rate-limiting step in glycogen breakdown and release of glucose 1-phosphate, could be stimulated by epinephrine and glucagon. Sutherland also showed that the activity of purified phosphorylase enzyme from liver extracts was: 1. enhanced in the presence of hormones and 2. dependent upon a heat-labile factor in the particular fraction of the homogenate (Rall and Sutherland, 1957). Initially centrifuging the liver homogenates to remove the assumed cellular-debris-containing particulate fraction abolished the hormonal activation of phosphorylase. The heat-labile factor was identified as cAMP and could be generated by hormonal stimulus in the presence of ATP (Rall et al.,

1957). Sutherland further proved that the accumulation of cAMP was due to the activation of adenylyl cyclase, which, described in subsequent years, was mechanistically linked to extracellular hormonal activation of their cognate G-protein coupled receptors (GPCRs) and downstream heterotrimeric G-protein G_s (Makman and Sutherland, 1957). Through experiments using incorporation of radiolabeled orthophosphate, ^{32}P, Rall and Sutherland also demonstrated that phosphorylase was indeed phosphorylated in the presence of hormone and this correlated with the activation of the enzyme (Rall et al., 1956). Contemporaneous work by Krebs and Fischer indicated that phosphorylation and activation of phosphorylase required ATP and Mg^{2+} and was mediated by phosphorylase kinase (Krebs and Fischer, 1956). Further studies by Krebs and Fischer indicated that phosphorylase kinase activity in rabbit skeletal extracts was dependent upon the presence of ATP, suggesting that the kinase itself was regulated by a phosphorylation event (Krebs et al., 1959). In 1968, Walsh and Perkins in Krebs' laboratory purified phosphorylase kinase kinase, which catalyzed the cAMP-dependent phosphorylation and activation of phosphorylase kinase. Phosphorylase kinsase kinase was referred to in more general terms as adenosine 3',5'-monophosphate-dependent kinase, or cAMP-dependent protein kinase, and later, protein kinase A (PKA), based on greater promiscuity in phosphorylating other substrates such as casein and protamine - in addition to phosphorylase kinase - in its initial identification (Walsh et al., 1968).

We now know that intracellular cAMP is tightly regulated and is typically maintained at a nanomolar concentration in a resting cell. Rapid synthesis by adenylyl cyclases (ACs) causes as much as a 1000-fold increase of cAMP (μM amounts), resulting in pleiotropic cellular outcomes via the action of various cAMP-binding effector proteins including: cAMP-dependent protein kinase (PKA), cyclic nucleotide-gated (CNG) ion channels, and exchange proteins

activated by cAMP (Epacs), which are guanine nucleotide exchange factors for the small GTPases Rap1/2. Intracellular levels of cAMP can be rapidly diminished via the activity of phosphodiesterases (PDEs), which hydrolyze cAMP to 5'AMP, thus rapidly and efficiently terminating cAMP-dependent signaling cascades (Sette and Conte, 1996; Bauman et al., 2006).

In the absence of cAMP, the serine/threonine protein kinase PKA exists as an inactive heterotetrameric complex, composed of two regulatory (R) and two catalytic (C) subunits, R_2C_2 (Reimann et al., 1971; Corbin and Keely, 1977). Upon cAMP induction, two molecules of cAMP bind to each regulatory R subunit in a positively cooperative fashion, releasing the catalytic C subunits from the holoenzyme and allowing for subsequent phosphorylation of neighboring substrates (Corbin, Keely and Soderling et al., 1977; Corbin et al., 1978). There are two classes of PKA, as defined by their regulatory subunits - type I (RI) and type II (RII) (Corbin and Keely, 1977). Four separate gene products give rise to the different mammalian R subunit isoforms, RIα, RIβ, RIIα, RIIβ, and while some are expressed ubiquitously, others are enriched in certain tissues such as RI/IIβ in the brain (Lee et al., 1983; Jahnsen et al., 1986; Sandberg et al., 1987; Scott et al., 1987; Clegg et al., 1988; Øyen et al., 1989; Solberg et al., 1991; McKnight, 1991). Three mammalian C subunits are known: Cα, Cβ, and testis-specific, Cγ (Uhler, Carmichael et al., 1986; Uhler, Chrivia et al., 1986). All of the various isoforms of the regulatory and catalytic subunits can interact to form tetrameric holoenzymes. Increased diversity in PKA complexes arises with the presence of alternatively spliced variants of the regulatory as well as catalytic subunits (Solberg et al., 1997; San Agustin et al., 1998; Reinton et al., 2000). R subunits typically vary from 43-45kDa in size and contain an N-terminal dimerization domain followed by an autophosphorylation or autoinhibitory

domain and two cAMP binding sites. Type I and II regulatory subunits inhibit the catalytic subunits in differing fashions. RII subunits contain a PKA autophosphorylation consensus sequence, R-X-X-S/T-X, in which a serine is phosphorylated upon holoenzyme formation. RIα/β regulatory subunits, however, contain a pseudosubstrate sequence, in which the serine is replaced by either alanine or glycine. Inhibition of the catalytic subunits by the regulatory subunits in the holoenzyme is mediated by these autophosphorylation or autoinhibitory regions, which occlude the substrate binding site of the catalytic subunits; binding of the regulatory subunits to the catalytic subunit also involves other electrostatic interactions (Takio et al., 1984; Titani et al., 1984; Leon et al., 1997).

PKA is a broad-spectrum protein kinase that participates in a multitude of cellular processes, many of which are well characterized, including its roles in glycogen metabolism and transcriptional regulation of various genes through the phosphorylation of a family of transcription factors known as cAMP-response element binding proteins (CREBs). Emerging roles for PKA have been described in other nuclear events including chromosomal condensation during mitosis and pre-mRNA splicing (Collas et al., 1999; Kvissel et al., 2007).

IV. A-kinase anchoring proteins

Site-specific actions of cAMP, particularly those mediated by PKA, can be coordinated by A-kinase anchoring proteins (AKAP), scaffolds that direct the PKA holoenzyme by binding to the RI and RII regulatory subunits. AKAPs target PKA holoenzymes to distinct intracellular locations, where the catalytic subunits can phosphorylate surrounding substrates in response to elevated levels of cAMP, thus providing spatiotemporal specificity to PKA activity and cAMP-dependent signaling (Carlisle and Scott, 2002). AKAPs often contain sequence motifs that

target the scaffolds to subcellular compartments. Alternatively, a teleological explanation is that its interacting partners determine AKAP localization.

Despite the spatial restriction of PKA by AKAPs, it is widely believed that nuclear function of PKA requires the translocation of the free catalytic subunits into the nucleus. Several lines of evidence challenge this notion. Holoenzyme exclusion from the nucleus was first described by the Feramisco and Taylor laboratories, where microinjection experiments of fluorescein-5-isothiocyanate labeled RI and C subunits of PKA into the cytosol of Rat-2 fibroblasts showed the dynamic translocation of free C subunit to the nucleus upon stimulation of cells with 8-bromo-cAMP, a synthetic cAMP analog. RI subunits remained static in the cytoplasm (Meinkoth et al., 1990). From this and similar experiments, they concluded that type I regulatory subunits, as part of the holoenzyme, function as a cytoplasmic anchor for the catalytic subunits in a resting/unstimulated cell. Moreover, the nuclear translocation of the C subunits is thought to occur passively through the nuclear pore, which is diffusion-limited to proteins less than 60kDa in size, thus preventing the larger tetrameric PKA holoenzyme from entering the nucleus. The nuclear restriction of tetrameric PKA was further supported by the identification of a thermostable inhibitor of PKA, protein kinase inhibitor (PKI), which participates in the inhibition and inactivation of the free C subunit of PKA, as well as its subsequent nuclear export through a nuclear export sequence contained in PKI (Walsh et al., 1971; Fantozzi et al., 1994; Wen et al., 1994). In contrast to the differing modalities by which ERK1/2 and activated, phosphorylated ERK1/2 can enter and function in the nucleus – from passive diffusion, interactions with nuclear pore complex proteins, energy-dependent factor-mediated and facilitated transport, as well as the existence of nuclear pools of the kinase – analogous mechanisms for PKA have not been extensively studied (Ranganathan et al., 2006; Yazicioglu et al, 2007). Contrasting these findings,

immunogold staining of RI, RII and C subunits of PKA and electron microscopic imaging of primary hepatocytes, HII4E hepatoma cells, granulosa cells, and spermatogonia indicated the presence of the regulatory subunits as well as the catalytic subunits in the nucleus (Kuettel et al., 1985). C subunits appeared enriched in the nucleus upon treatment of rats with glucagon, whereas treatment of HII4E cells with dibutyryl cAMP, a cell-permeable synthetic analog, caused an apparent increase of R and C subunits in the nucleus, indicating perhaps cell-type, -context and/or ligand-dependent differences in PKA distribution in the cell and its translocation to the nucleus. Furthermore, RIIα has been shown to co-localize with AKAP100 in the nuclei of rat cardiac myocytes and with AKAP150 in the nuclei of chicken limb mesenchymal cells (Zhang et al., 1996; Yang, Drazba et al., 1998).

Early work on PKA suggested that a significant proportion of the enzyme associated with particulate fractions, i.e. microtubules, providing evidence for the theory of compartmentalized cAMP- and PKA-dependent signaling (Goodman et al., 1970; Lohmann et al., 1984). Studies of microtubule-associated PKA also led to the identification of the first known AKAP, microtubule associated protein 2 (MAP2) (Theurkauf and Vallee, 1982). Theurkauf and Vallee showed that type II PKA interacted with MAP2 in bovine brain microtubule preparations and catalytic activity could be released from MAP2 upon stimulation with cAMP, whereas cAMP-binding capacity remained associated with MAP2. These data indicated that upon activation with cAMP, the catalytic subunit of PKA was released and the regulatory subunits were still bound to MAP2.

Over 50 AKAPs have now been identified, most of which have multivalent binding capacity – interacting with PKA as well as other components often of disparate signaling pathways - allowing integration of multiple inputs and signals

and cross-talk of these pathways resulting in unique outcomes in the cell (Figure 1.3). Some of the first AKAPs were identified through the RII overlay technique, where nitrocellulose membranes containing proteins from different cell and tissue lysates were probed with purified ^{125}I-labeled RII subunit or unlabeled RII and iodinated anti-RII antibody to identify bound RII and the associated proteins in the membrane (Fleischer et al., 1981; Lohmann et al., 1984). AKAPs were later shown to bind to a hydrophobic groove between a bundle of four helices at an interface generated by dimerization of the N-terminal domain of the regulatory subunits (Figure 1.1) (Scott et al., 1990). The interaction is mediated by a conserved 14-18 residue amphipathic α-helical domain within the AKAP, which makes extensive hydrophobic contacts via one side of the amphipathic helix as well as Van der Waals interactions with other surfaces of the dimerization interface (Carr et al., 1991). More than 70% of type II PKA (containing RIIα/β dimers) within the cell is associated with organelles or structural components, whereas the majority of type I PKA (containing RIα/β dimers) is primarily soluble (Rubin et al., 1972; Corbin, Sugden et al., 1977; Nigg et al., 1985). Through the cellular distribution of type I and type II PKA and from an inability to identify RI interacting proteins through RI overlay, it was initially believed that AKAP-associated PKA was limited to the type II holoenzyme. However, using yeast two-hybrid analysis, Huang et al., identified a dual-specificity AKAP (D-AKAP1) that interacts with both RI and RII subunits (Huang et al., 1997). In RIIα knockout mice, RIα was sufficient to facilitate the localization of the C subunit with the L-type Ca^{2+} channel and coordinate PKA-dependent potentiation of channel activity in skeletal muscle (Burton et al., 1997). Furthermore, RIα bound to Ht31, a 24 amino acid peptide derived from the amphipathic helical domain of AKAP-Lbc, albeit with approximately 500-fold lower affinity than RIIα.

Biochemical analysis of the interaction between AKAPs and PKA determined that AKAP domains predominantly bind RIIα/RIIβ-containing PKA with nanomolar affinity compared to micromolar affinity towards RIα- or RIβ-containing PKA (Miki and Eddy, 1999). AKAP domains are also thought to be involved in PKA heterotetramer formation, by effectively coordinating binding between the regulatory and catalytic subunits (Gold et al., 2006). AKAP specificity in anchoring type I or type II PKA can be mapped to critical residues within the amphipathic helical domain (Figure 1.2). Aliphatic amino acids at positions 2, 6, and 10 within the amphipathic helix of an AKAP are critical for R subunit binding (Miki and Eddy, 1999). Although not strictly conserved, an aliphatic residue with a longer side chain at position 6 confers specificity for RII over RI subunits – a valine in RII-specific AKAP-Lbc and an alanine in RI-specific AKAP domain B of AKAP82. A similar longer side chain aliphatic residue at position 10 may increase apparent affinity for the RII subunit. D-AKAP2 has an alanine at position 6 in its amphipathic helix, allowing for both RI and RII binding (Kinderman et al., 2006). Additionally, the RI dimerization interface contains a hydrophobic cavity that can accommodate a bulkier side chain amino acid near the end of the AKAP docking helix. Mutating a valine to tryptophan at position 13 in the amphipathic helix of dual-specificity AKAP, D-AKAP2 abolished RII but not RI binding (Burns-Hamuro et al., 2003).

V. AKAPs as signaling loci/nodes

AKAP-mediated signaling complexes were first suggested when it was found that AKAP79 (also known as AKAP5) interacts with calcineurin (Coghlan et al., 1995). The Scott laboratory later showed that AKAP79 also bound PKC (Klauck et al., 1996). Similarly to PKA, AKAPs can directly influence the activity of other associated enzymes. AKAP79 not only coordinates the location of PKA,

calcineurin and PKC to postsynaptic densities (cytoskeletal structures) in cultured hippocampal neurons, but it also inhibits the activity of calcineurin and PKC when the proteins are associated with the AKAP (Faux and Scott, 1997). Furthermore, in the presence of Ca^{2+}, calmodulin binding to AKAP79 releases PKC, resulting in an increase in PKC activity. AKAPs can affect cAMP production and localized cAMP levels within the cell, through their interactions with adenylyl cyclases and phosphodiesterases. AKAP150, the mouse ortholog of AKAP79, was found to co-purify with AC types V and VI in rat brain extracts and coordinate a negative feedback loop that temporally regulates cAMP synthesis (Bauman et al., 2006). PKA bound to AKAP79/150 can phosphorylate the ACs to rapidly terminate cAMP synthesis upon activation of the protein kinase.

AKAPs have also been shown to influence MAP kinase signaling pathways. AKAP79, which is constitutively associated with the β_2-adrenergic receptor (β_2-AR) in HEK293 cells, participates in switching of the GPCR from $G\alpha_s$- to $G\alpha_i$-coupled and subsequent activation of ERK1/2 (Lynch et al., 2005). Upon treatment with the agonist isoproterenol, β_2-AR signals through $G\alpha_s$ to stimulate adenylyl cyclase production of cAMP. Once activated, PKA, scaffolded near the membrane by AKAP79, phosphorylates β_2-AR, switching its coupling to $G\alpha_i$ and causing the $G\beta\gamma$ subunits to dissociate and direct transient ERK1/2 activation in a c-Src- and Ras-dependent manner (Daaka et al., 1997). Knockdown of AKAP79 with double-stranded RNA oligonucleotides or inhibiting the interaction of PKA with AKAP79 with the competitive inhibitor peptide Ht31 diminishes ERK1/2 activation by isoproterenol, supporting the role of AKAP79 in coordinating these signaling events.

Another example is the muscle-specific AKAP, mAKAP, which coordinates a complex containing PKA, ERK5, phosphodiesterase PDE4D3, and Epac1 that spatiotemporally regulates cAMP levels in cardiac myocytes (Figure 1.4) (Dodge-Kafka et al., 2005). mAKAP localizes PKA and PDE4D3 to the perinuclear membrane, where PKA can phosphorylate the phosphodiesterase to enhance cAMP catabolism in a classical negative feedback mechanism (Sette and Conte, 1996). However, PDE4D3 also binds to and recruits ERK5 and the upstream kinase MEK5 to mAKAP, allowing ERK5 to phosphorylate PDE4D3 to suppress its activity. Furthermore, Dodge-Kafka et al. showed that in rat neonatal ventriculocytes, a rise in intracellular cAMP level causes inhibition of serum-stimulated ERK5 activation in a Rap1-dependent manner through the activation of Epac1, a GEF for the small GTPase Rap1 that interacts with mAKAP (Dodge-Kafka et al., 2006). ERK5 inhibits PDE4D3 to allow for cAMP levels to accumulate upon agonist stimulation, after which, PKA and Epac1 can enhance PDE4D3 and suppress ERK5 activity respectively. The decrease in local cAMP concentration by the action of PDE4D3 alleviates the Epac1/Rap1 repression of ERK5, which can subsequently deactivate PDE4D3. Ultimately, the activity of all these enzymes is kinetically regulated in a cAMP concentration- and time-dependent manner.

Through its interaction with the ryanodine receptor (RyR), a calcium release channel, and calcineurin, mAKAP is also involved in integrating cAMP and calcium signaling pathways (Kapiloff et al., 1999). PKA phosphorylates RyR, releasing calcium from intracellular stores and activating calcineurin. Calcineurin dephosphorylates the transcription factor NFAT, allowing it to translocate to the nucleus and mediate transcription of genes involved in cardiac hypertrophy (Pare et al., 2005). Recently, mAKAP was shown to organize ubiquitylating enzymes that participate in a "degradation loop" regulating Hif-1α expression under

normoxic and hypoxic conditions as well as spatially restricting Hif-1α at the perinuclear membrane for rapid translocation into the nucleus upon activation (Wong et al., 2008).

Enzymes associated with AKAPs can often regulate the scaffolding capacity of these proteins. Some AKAPs also contain native enzymatic activity. For example, AKAP-Lbc is a GEF for the small GTPase RhoA and is regulated by phosphorylation by PKA. PKA phosphorylates AKAP-Lbc on Ser 1565, promoting recruitment of the 14-3-3 binding protein which subsequently inhibits AKAP-Lbc RhoA-GEF activity (Diviani et al., 2004). Additionally, PKA phosphorylation of AKAP-Lbc on Ser 2737 causes the release of PKCη-phosphorylated and activated protein kinase D from the scaffolded complex (Carnegie et al., 2004).

PKA is present in the motile cilium or flagellum of cells that contain these appendages and is thought to interact with several different AKAPs. AKAP28, the first identified human ciliary AKAP, is specifically expressed in tissues containing motile cilia or flagella, and is particularly enriched in airway epithelial cilia (Kultgen et al., 2002). Moreover, expression of AKAP28 mRNA increases as human bronchial epithelial cells (HBECs) differentiate into multi-ciliated cells. AKAP4, a RIα-binding AKAP, localizes to the fibrous sheath (an outer matrix surrounding the axoneme) of sperm flagellum, and is implicated in spermatogenesis as well as recruiting PKA to phosphorylate components required for flagellar motility (Miki et al., 2002; Hu et al., 2009). Targeted gene disruption of *AKAP4* in mice led to infertility due to impaired development of the fibrous sheath and shortened and tortuous-appearing flagella resulting in decreased sperm motility.

Of particular interest to our findings, several AKAPs and other PKA binding proteins localize PKA to the nucleus where it is implicated in a variety of processes. AKAP95 localization and interaction with PKA is cell-cycle dependent. During interphase, AKAP95 is in the nucleus in human Hs-68 fibroblasts and HeLa cells, associated with the nuclear matrix fraction. During the onset of mitosis, AKAP95 redistributes to the chromatin fraction, recruits PKA and is required for chromosomal condensation (Eide et al., 1998; Collas et al., 1999).

HA95, a protein homologous to AKAP95, is an atypical PKA scaffold in that it binds to the C subunits of PKA instead of the R subunit dimer. HA95 localizes C subunits to nuclear speckles, sites of pre-mRNA splicing/processing and mRNA export, where it regulates the splicing of E1A, a known PKA-dependent transcript, from an exogenous E1A minigene (Kvissel et al., 2007).

A-kinase interacting protein (AKIP) also binds to the C subunit of PKA and participates in forskolin-stimulated nuclear retention of the activated enzyme (Sastri et al., 2005). However, its role in PKA signaling in the nucleus remains to be determined.

The ADP-ribosylation factor (ARF) 1 GEFs, brefeldin A-inhibited GEFs (BIG) 1 and 2 each contain three putative AKAP domains. BIG1/2 localize to the trans-Golgi network and recycling endosomal systems, where they are involved in the recruitment of the heterotetrameric adaptor protein (AP) 1, 3, 4 and Golgi-localized, γ-ear- containing, ARF-binding (GGA) adaptor proteins for clathrin-mediated vesicle budding (Jones et al., 2005). Mammalian BIG1/2 (~200kDa/190kDa) were initially purified from a large macromolecular complex from bovine brain cytosol, and have since been shown to associate with diverse

interacting partners, indicative of multivalent coordinating capacity. BIG1 interacts with the FK506-binding protein, FKBP13, and Myosin IXB, a RhoA GAP, whereas BIG2 interacts with Exo70, a member of the exocyst complex and the β subunit of the gamma-aminobutyric acid ($GABA_A$) receptor/ion channel (Padilla et al., 2003; Saeki et al., 2005; Xu et al., 2005). BIG1, which contains a nuclear localization signal (NLS), has also been shown to translocate to the nucleus in serum-starved HepG2 cells or upon being phosphorylated by PKA after treating cells with 8-Br-cAMP or forskolin (Cittero et al., 2006). There, BIG1 interacts with nucleolin, fibrallin, which binds U3 small nucleolar RNA required for 18s ribosomal RNA maturation, and the RNA-binding protein La, and is postulated to participate in pre-ribosomal subunit export from the nucleus (Padilla et al., 2008). Evidence of BIG1 function distinct from vesicular trafficking processes at the trans-Golgi is intriguing, as I will later present work suggesting a novel, non-canonical role for another AKAP within the cell.

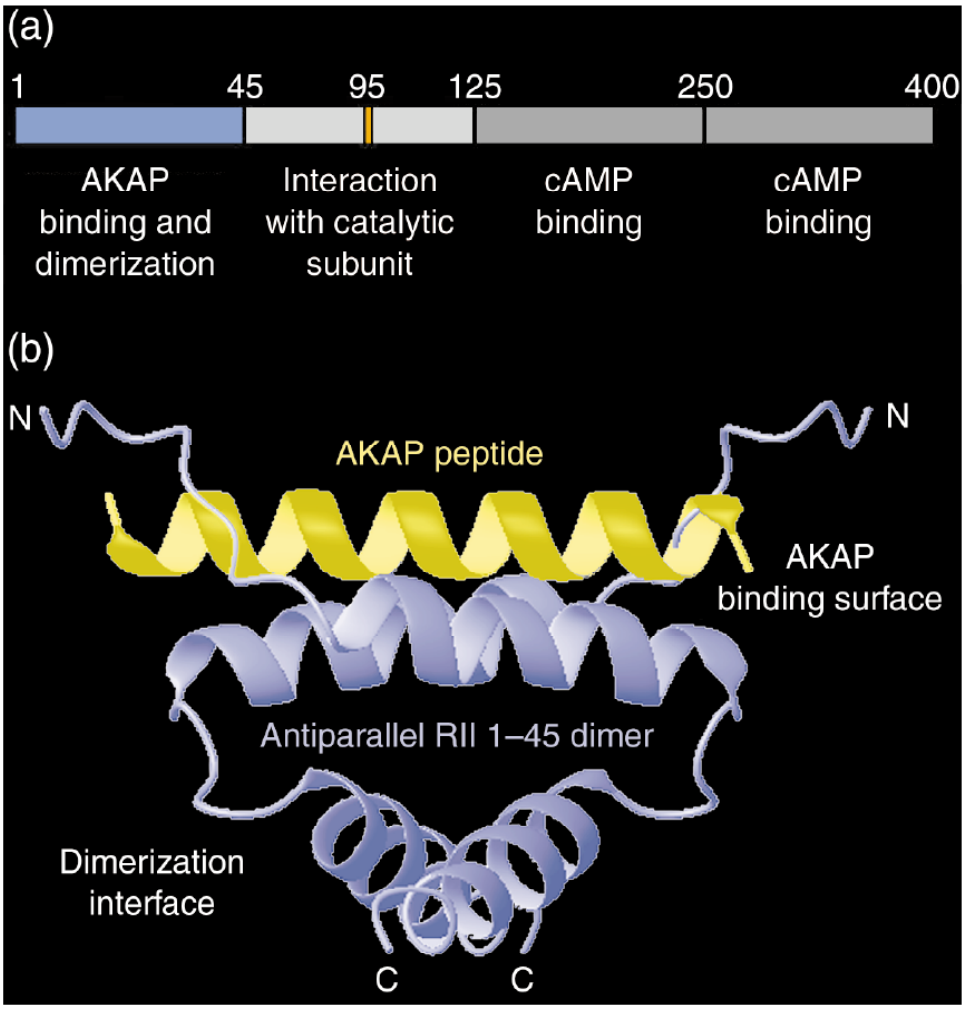

Figure 1.1. RII dimerization interface. Schematic diagram of the RII subunit of PKA. (a) Domain structure of the regulatory subunit. Of note are the N-terminal dimerization domain, and the two cAMP binding domains. Additionally, the orange box, within the C subunit-interacting region, represents the auto-phosphorylation (RII) or pseudo-substrate motif (RI). (b) Structural representation of the RIIα-Ht31 AKAP peptide interaction at the R subunit dimerization interface. Reprinted with permission from Colledge and Scott, 1999.

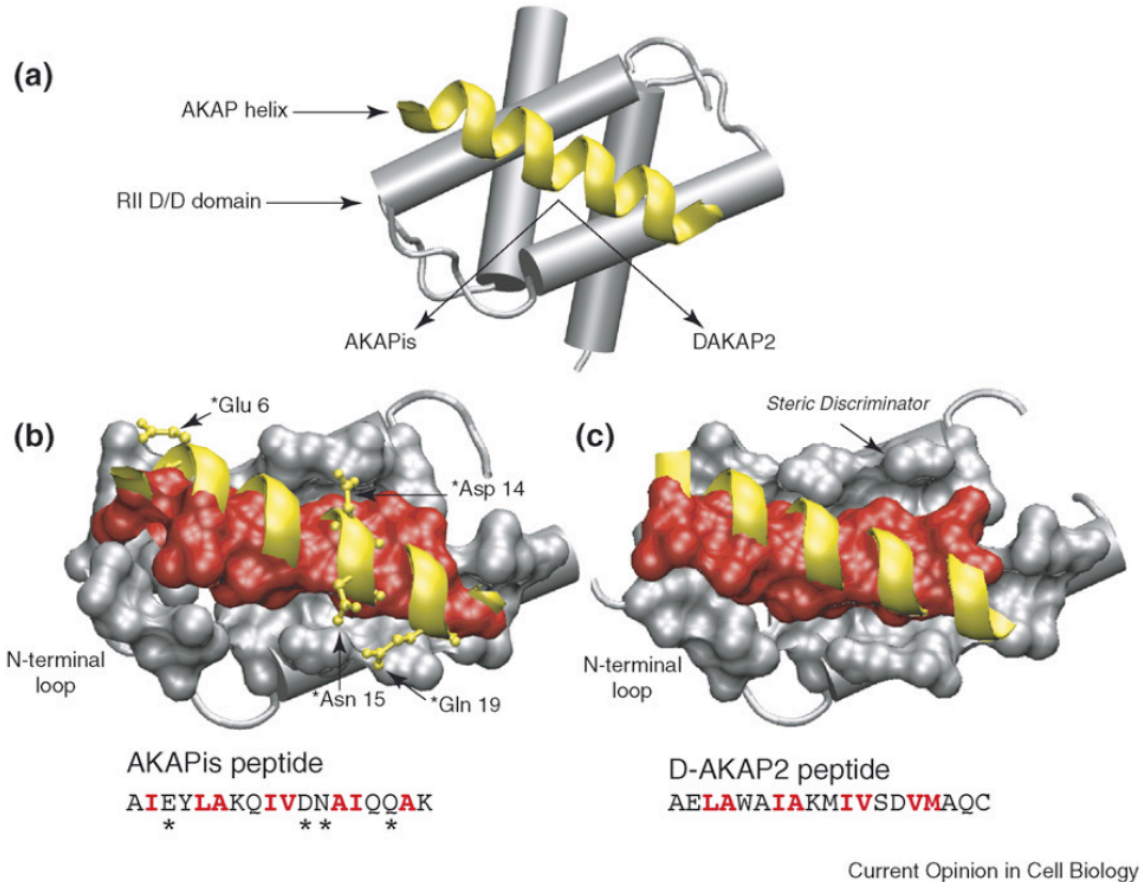

Figure 1.2. RII-AKAP interaction. Ribbon diagram representation of the PKA RII subunit and AKAP binding interface. (a) AKAP helices from both the RII-preferential AKAP*is* and the dual-specificity D-AKAP2 bound to the RII dimerization domain. (b,c) Primary sequence of the AKAP helices indicates the specific residues that mediate the interaction at the interfacial hydrophobic groove of the RII-subunit dimer. Mutation of Val to Trp in position 13 of the D-AKAP2 helix, sterically hinders RII but not RI binding. Reprinted with permission from Beene and Scott, 2007.

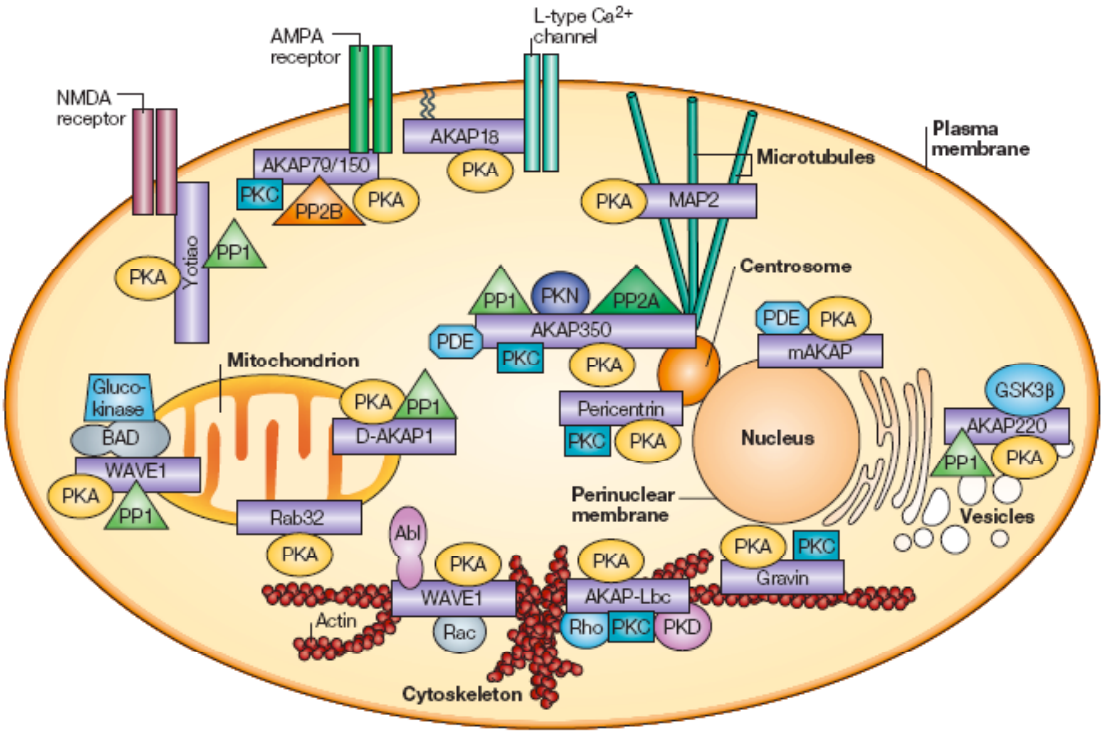

Figure 1.3. AKAP signaling complexes. AKAPs coordinate multiple signaling complexes from disparate pathways and localize PKA to discrete intracellular sites of action. Reprinted with permission from Wong and Scott, 2004.

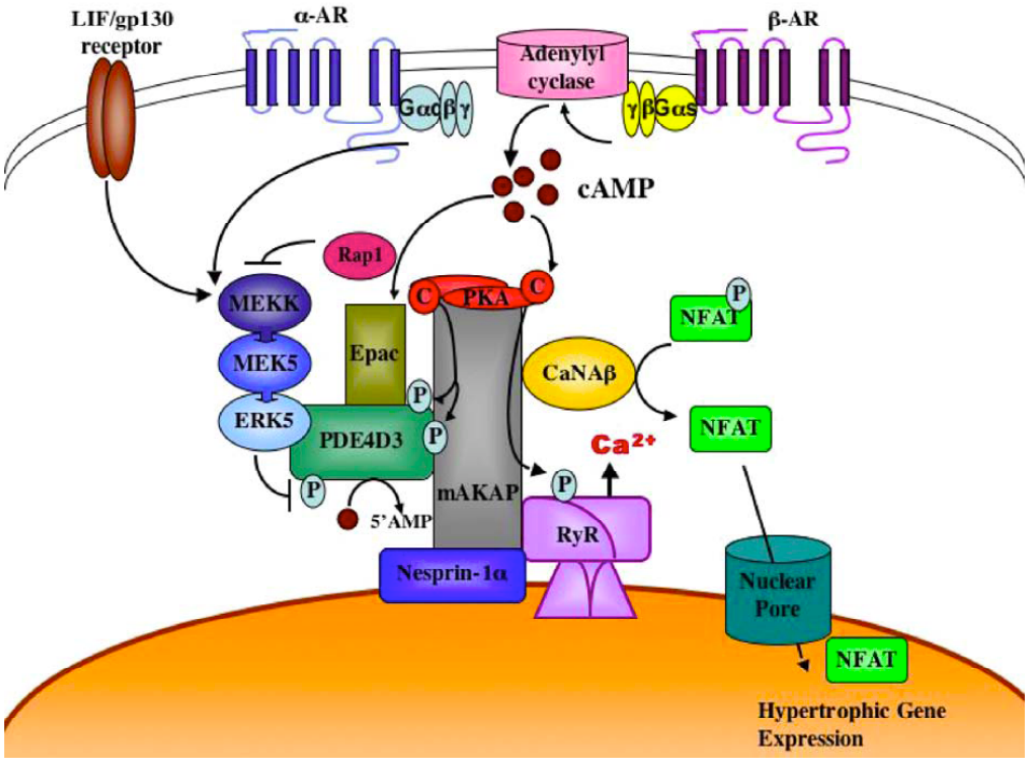

Figure 1.4. mAKAP coordinates MAP kinase signaling. Depiction of the multiple signaling pathways coordinated by mAKAP. ERK5, Epac-Rap1, and PDE4D3 regulated localized cAMP concentration. mAKAP also coordinates calcineurin, affecting NFAT nuclear translocation. Reprinted with permission from Dodge-Kafka and Kapiloff, 2006.

CHAPTER 2: CILIA AND RADIAL SPOKE PROTEIN 3

I. Motile and primary cilia

Motile and primary (typically immotile) cilia are microtubule-based antennae-like projections from the cell and are considered to be sensory organelles, responding to extracellular phenomena and cues. Cilia are generally 10-15μm long, but their length can vary from 2-3μm in some primary-ciliated cells to approximately 45μm for a typical sperm flagellum. Cilia are ensheathed by the plasma membrane, and arise from centrioles in a cell cycle- or differentiation-dependent manner. (Pan and Snell, 2007). Most differentiated cells are thought to have a single primary cilium, whereas motile cilia are expressed in specialized cell types such as sperm, olfactory cells, and airway epithelial cells to name a few (Figures 2.1, 2.2). They receive and integrate signals such as hormones, growth factors, ions, osmotic pressure and fluid flow-related stresses. Cilia also contain the components of many signaling pathways, including: epidermal growth factor receptor (EGFR), platelet-derived growth factor receptor (PDGFR), fibroblast growth factor receptor (FGFR), several ion channels, as well as proteins in the hedgehog and Wnt signaling pathways (Christensen et al., 2007). Defects in cilia signaling due to mutations in ciliary structural components that cause the loss, malformation, or dyskinesia (immotility) of cilia contribute to the etiology of several diseases including: polycystic kidney disease (PKD), pancreatic cyst formation and pancreatitis, Kartagener's and Bardet-Biedel syndrome (BBS) (Lin et al., 2003; Cano et al., 2006; Nachury et al., 2007). Pathologies that result in defective motile cilia are referred to as immotile-cilia syndrome and are also known as primary cilia dyskinesia (PCD). PCD is typically characterized by sinusitis, bronchiectasis, and mucus buildup, as a result of an impaired clearance by the bronchial airway epithelial cilia, as well as infertility due to immotile

spermatozoa (Afzelius, 2004). Kartagener's patients present the respiratory hallmarks of PCD as well as situs inversus totalis, the disruption of left-right axis symmetry in the body. This symmetry inversion is caused by defects in nodal cilia that adversely affect hedgehog or Wnt morphogenic gradient distribution during development. Bardet-Biedel syndrome is characterized by macular degeneration, polydactyly, nephropathy, obesity, and diabetes. Mutations to components regulating membrane trafficking into the primary cilium have been linked to the pathogenesis of BBS (Nachury et al., 2007; Loktev et al., 2008). An extensively studied cilia-signaling disease is autosomal dominant polycystic kidney disease (ADPKD). ADPKD is an extremely common genetic disease, having an incidence of 1 in 500 to 1 in 1000 in the population. Human mutations within the ciliary G-protein coupled receptor, polycystin 1, and its interacting partner, polycystin 2, a calcium channel, have been shown to contribute to the hyperplastic-growth cyst phenotype (Igarashi and Somlo, 2002). Furthermore, mutations that affect the structural integrity or formation of cilia can recapitulate the PCD and ADPKD phenotypes. Mice lacking KIF3A, a subunit of the anterograde motor protein, kinesin-II, fail to form or have shortened cilia and display situs inversus as well as other hallmarks of PCD (Takeda et al., 1999). Kidney-specific deletion of the *Kif3a* gene results in renal cyst formation characteristic of PKD. Loss of KIF3A in the pancreas causes pancreatitis, fibrosis and ductal metaplasia characterized by hyperactivation of ERK1/2 in the pancreas (Lin et al., 2003; Cano et al., 2006).

The motile cilia/flagellar axoneme, the structural core or skeleton, is composed of an outer ring of nine doublets of microtubules surrounding an inner pair of microtubules (9+2) (Satir and Christensen, 2007). The outer microtubule doublets are linked to the inner pair via radial spoke complexes that are required for regulation of dynein-mediated microtubule sliding and subsequent motility. Primary cilia (9+0) are structurally different from motile cilia in that they lack the

inner pair of microtubules, dynein arms, as well as the radial spoke components (Figure 2.3). Thus, primary cilia are conventionally deemed immotile due to this distinction in structure. Nodal cilia, which are important for left/right asymmetrical patterning in development, are an exception. They display a 9+0 structure and are still able to generate rotational motility, albeit distinct from the canonical flagellar sinusoidal wave motion.

Cilia are emerging as important regulators of the MAP kinase signaling pathway, potentially affecting transcriptional control, cell motility, proliferation, and differentiation through providing inputs and/or modulating activity of these kinases (Schneider et al., 2005; Cowley, 2008; Nagao et al., 2008). Stimulation with PDGF-AA in the NIH3T3 fibroblast cell line as well as in primary mouse embryonic fibroblasts (MEFs) leads to the activation of PDGFRα and downstream activation of MEK1/2 (Schneider et al., 2005). Furthermore, p-MEK1/2 localizes to the primary cilium. In MEFs derived from intraflagellar transport protein 88 (IFT88) knockout mice, which fail to properly assemble primary cilia, PDGFRα is mislocalized and PDGF-AA fails to activate the PDGFRα and downstream MEK1/2 pathways. Inappropriately regulated and increased ERK1/2 activity is thought to underlie the proliferation of kidney ductal epithelial cells and the resulting aberrant changes in epithelial cell morphology associated with cyst formation in PKD (Yamaguchi et al., 2000; Nagao et al., 2003). The disruption of cilia signaling alters the relationship between cAMP, calcium, and growth factor signaling pathways and their combined effects on ERK1/2. In normal kidney epithelial cells, factors that stimulate cAMP production regulate epithelial transport without causing cell proliferation. In PKD, however, cAMP causes the ERK1/2-dependent proliferation of kidney epithelial cells, leading to cyst formation, presumably due to a loss of calcium-mediated inhibition of cAMP stimulation of MAP kinase activation (Yamaguchi et al.,

2003; Yamaguchi et al., 2004; Belibi et al., 2004). This switch in cAMP response results from the loss of function, misregulation or mislocalization of effectors in both the calcium and cAMP signaling pathways. Our lab has extensively studied the connection of these disparate signaling pathways influencing the activity and activation of ERK1/2 and of other MAP kinases including ERK5. Combinatorial inputs eliciting responses from the MAP kinase pathways are often cell type-, state-, and context-dependent (Dugan et al., 1999). For example, cAMP reduces serum-stimulated proliferation in many cell types, and while ERK5 is inhibited by cAMP in most contexts, ERK1/2 may be inhibited, unaffected or stimulated by cAMP, depending on growth conditions (Pearson et al., 2006). As mentioned above, an imbalance in cAMP and ERK1/2 signaling is believed to contribute to the progression of ADPKD.

II. Radial spoke protein 3

Initially identified in *Chlamydomonas reinhardtii*, RSP3 is one of at least 23 known radial spoke proteins assembled in a large multi-subunit complex required for eukaryotic ciliary or flagellar motility (Yang et al., 2006). Radial spoke proteins are thought to be important in transducing signals from the inner pair of microtubules to the outer doublets, regulating dynein-mediated axonemal sliding and subsequent flagellar motility (Figure 2.4). Using mass-spectrometry, Yang et al. identified several novel radial spoke proteins that are thought to contain unique enzymatic and regulatory functions based on sequence and predicted-domain structure analysis (Figure 2.5). Of note include: RSP7, which contains a homologous domain to the RIIα regulatory subunit of PKA as well as several Ca^{2+}-binding EF hand domains, RSP11, which also contains a RIIα-like domain, and RSP23, which contains a putative peptidyl-prolyl isomerase domain.

Genetic analysis of RSP3 function in *Chlamydomonas* indicates that loss of RSP3 results in paralyzed flagella and unassembled radial spokes (Luck et al, 1977; Piperno et al., 1981). Additionally, biochemical studies of *Chlamydomonas* RSP3 show that it functions as an AKAP, and loss of its ability to bind to PKA also results in abnormal flagellar motility and paralyzed flagella (Gaillard et al., 2001; Gaillard et al., 2006). More recently, RSP3 has been shown to form a homodimer within the radial spoke structure. This dimer is proposed to provide the base for radial spoke assembly (Wirschell et al., 2008).

Through proteomic analysis of human bronchial epithelial cells and immunofluorescence staining of mouse tracheal epithelial cells, RSP3 has been shown to localize to motile cilia in mammals (see Figure 2.2) (Ostrowski et al., 2002; Wirschell et al., 2008). Furthermore, Koukoulas et al., showed through Northern blot analysis that two RSP3 mRNA transcripts, 2.2kb and 1.8kb in size, are present in mouse brain, kidney, liver, spleen, and testis (Koukoulas et al., 2004). The presence of mRNA transcript in developing and mouse neonatal cortex is suggestive of a non-motile ciliated role for RSP3. The mammalian *RSP3* gene consists of 8 exons and 7 introns, while the *Chlamydomonas* gene is comprises 4 exons separated by 3 intronic regions. Mammals contain one *RSP3* gene (mapped to chromosomal locus 6q25.3), which is believed to contain alternative start sites that generate two transcripts – a long and short form. The short form is made up of 418 amino acids, while the 560-amino acid long form, extended by 142 amino acids at the N terminus, is referred to as radial spoke protein 3 homolog (RSP3H or RSPH3 as annotated by NCBI). Human and mouse RSP3 are approximately 84% similar at the amino acid level and share 67% similarity within the radial spoke domain to *Chlamydomonas* RSP3. The radial spoke domain and the AKAP domain of RSP3 are conserved among a variety of

species (Table 2.1). The mammalian orthologs for this and other radial spoke proteins, however, remain to be identified and fully characterized.

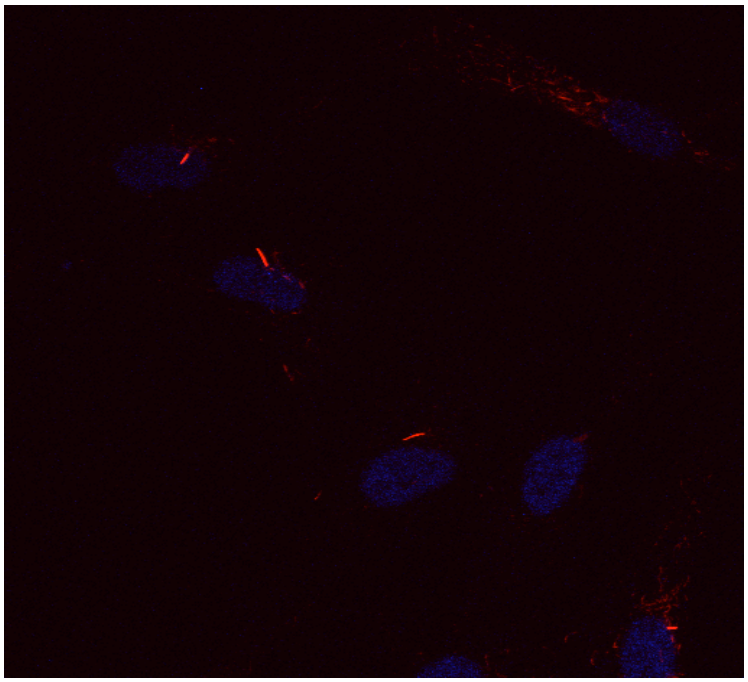

Figure 2.1. Human retinal pigmented epithelial cells have a single primary cilium. Telomerase immortalized human retinal pigmented epithelial (RPE1) cells were plated on 0.5% gelatin-coated coverslips and fixed in 4% paraformaldehyde. Cells were stained with 1:10,000 mouse anti-acetylated tubulin antibody and goat anti-mouse Alexa Fluor 546 nm-conjugated secondary antibody. DNA was visualized using 4',6-diamidino-2-phenylindole (DAPI). Stabilized microtubule structures such as acetylated and glutamylated tubulin are enriched in cilia, and as such, are used as markers for the primary cilium. Images were taken at 63x under oil immersion (n_a=1.518) on a Zeiss LSM 510 META LSM with a Chameleon XR NIR laser two-photon confocal microscope.

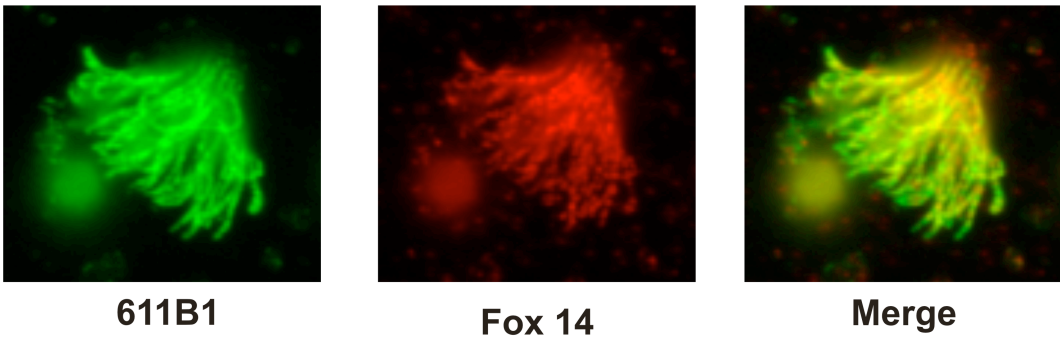

Figure 2.2. Mouse tracheal epithelial cells contain multiple motile cilia. Specialized cell types have motile cilia, and some have multiple motile cilia. Images represent isolated cilia from mouse tracheal epithelial cells. In panel 1, cilia were stained with an anti-acetylated tubulin (611B1) antibody. Panel 2 represents anti-RSP3 antibody (Fox 14) staining of the tracheal cilia. Reprinted with permission from Wirschell et al., 2008.

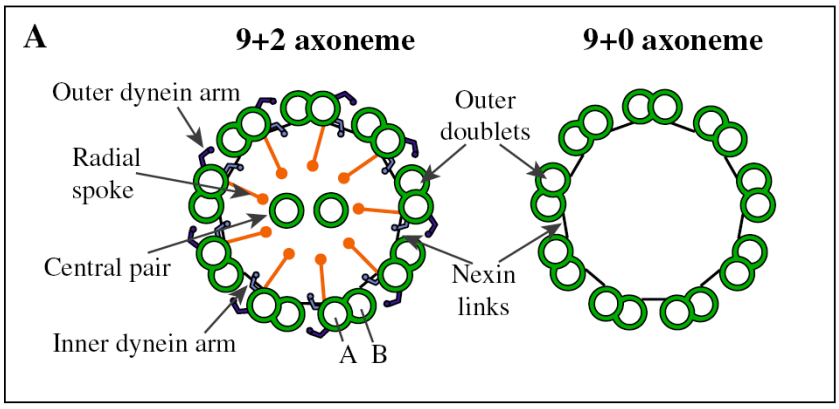

Figure 2.3. Cross-section of the ciliary axoneme. Motile cilia have a 9+2 structure, consisting of an outer ring of 9 pairs of microtubules surrounding an inner pair of microtubules. The outer ring is connected to the inner doublet by radial spoke proteins, which allow for axonemal sliding and subsequent ciliary motility. The primary cilium is characterized by a 9+0 structure, with "0" indicating a lack of the inner pair of microtubules. Additionally, the primary cilium does not contain the radial spoke complexes. Reprinted with permission from Dawe et al., 2007.

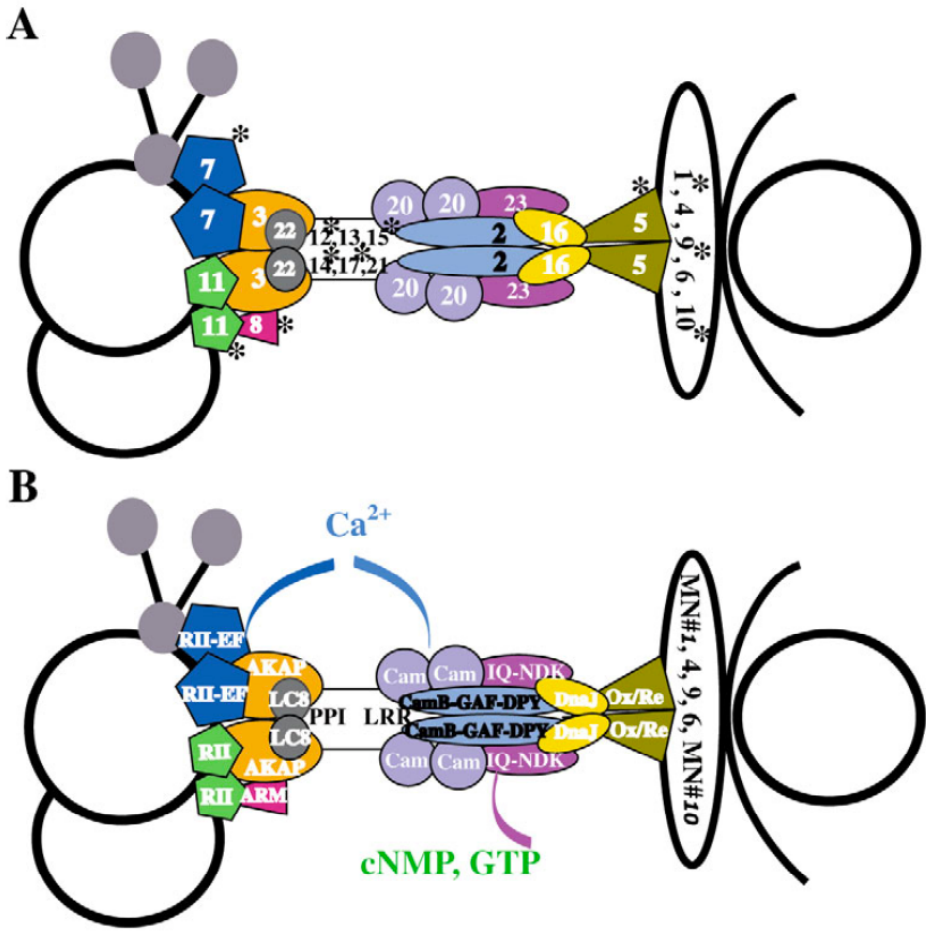

Figure 2.4. Model of the radial spoke complex. A. Proposed architecture of the radial spoke complex. Radial spoke protein 3 is thought to form a nucleating dimer at the base of the spoke complex on the outer microtubule pair (left circles) (Wirschell et al., 2008). The radial spoke extends to the inner microtubule doublet (right). Asterisks indicate novel, uncharacterized radial spoke proteins (Yang et al., 2006) **B.** Proposed function for each of the radial spoke proteins based on sequence and domain structure analysis. Reprinted with permission from Yang et al., 2006.

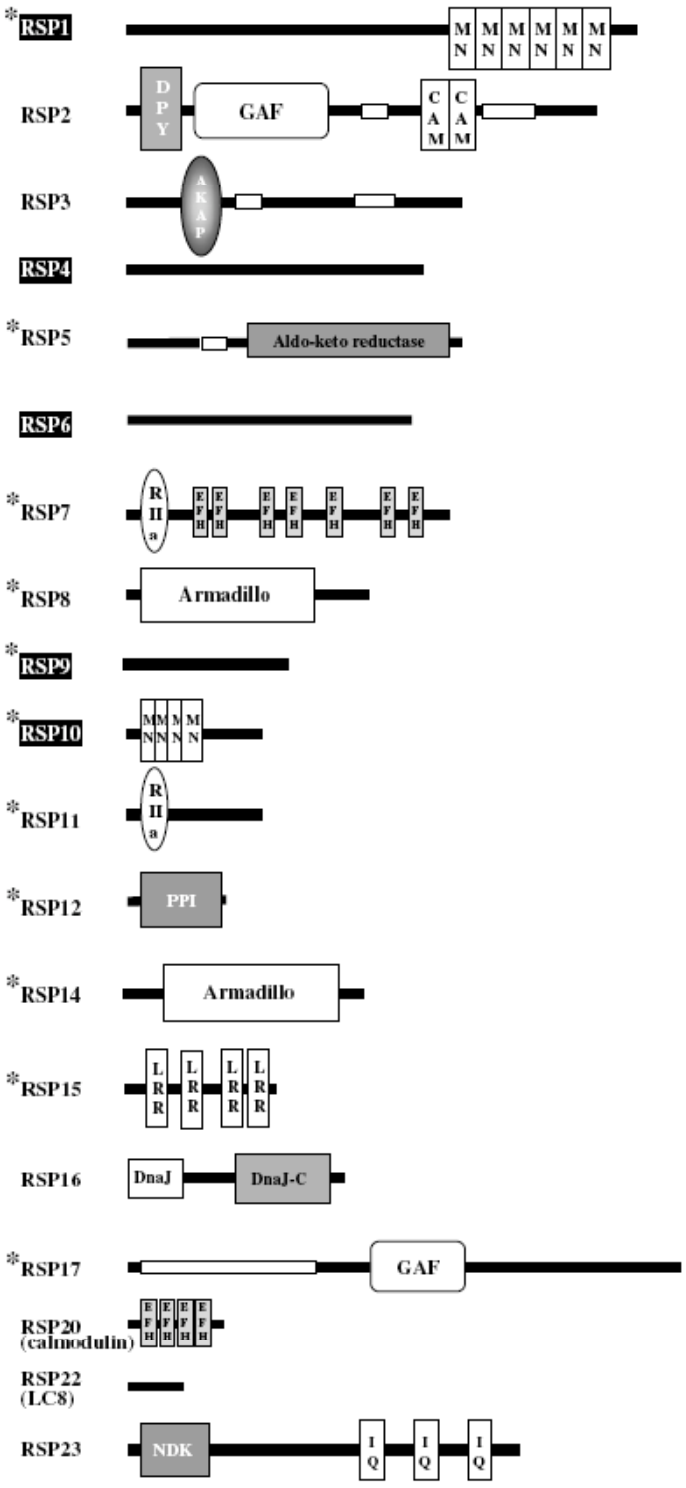

* Newly Identified protein

Figure 2.5. Previously characterized and predicted domains of radial spoke proteins. Potential functional roles of radial spoke proteins identified through mass-spectrometric and domain prediction analysis. Reprinted with permission from Yang et al., 2006.

Species	% Conserved for *radial_spoke_3* domain	% Conserved for PKA-binding domain
Anopheles gambiae	59	83
Trypanosoma brucei	59	89
Apis mellifera	61	89
Leishmania major	62	89
Canis familiaris	66	89
Mus musculus	67	89
Pan troglodytes	67	89
Homo sapiens	67	89
Gallus gallus	68	89
Xenopus tropicalis	69	89
Danio rerio	69	89
Ciona intestinalis	71	89

Table 2.1. RSP3 orthologs in various species. Percent conservation represents similarity (identical and conserved residues) at the amino acid level relative to *Chlamydomonas* RSP3. Reprinted with permission from Gaillard et al., 2006.

CHAPTER 3. RSP3 IS A SCAFFOLD FOR ERK1/2 AND PKA

I. Abstract

Mammalian RSP3 was found to interact with ERK2 through a yeast two-hybrid screen designed to identify interactors that have a higher affinity for the phosphorylated, active form of ERK2. Confirming this finding, the human homolog long form, RSP3H, co-immunoprecipitates with ERK1/2 in HEK293 cells. Human RSP3, and its larger alternative start site gene product, radial spoke protein 3 homolog (RSP3H), are phosphorylated by ERK1/2 *in vitro* and in cells on threonine 286. RSP3/RSP3H are also phosphorylated *in vitro* by cAMP-dependent protein kinase (PKA). Additionally, we show that the human RSP3H functions as an A-kinase anchoring protein (AKAP), and its ability to bind to the regulatory subunits of PKA, RIIα and RIIβ, is regulated by ERK1/2 activity and phosphorylation.

II. Introduction

Radial spoke protein 3 is a component of the radial spoke complex contained within motile cilia. Identifying RSP3 as an interacting protein for the MAP kinases ERK1/2 was quite intriguing, since the finding initially suggested a possible role for ERK in cilia or a means of compartmentalized regulation of signaling through the MAP kinase pathway. The Sale laboratory initially characterized the *Chlamydomonas* ortholog of RSP3 as an AKAP and showed that its AKAP activity was required for normal flagellar motility (Gaillard et al., 2001; Gaillard et al., 2006). *Chlamydomonas* containing an AKAP-defective RSP3 mutant, displayed paralyzed flagella. Interestingly, inhibiting PKA activity with PKI rescued paralysis, suggesting that a loss of PKA-binding by RSP3 causes a mislocalization or unregulated activation of PKA within the cilium. To date, however, the catalytic subunits of PKA have not been identified in the *Chlamydomonas* genome and limited predicted sequence homology to radial spoke components (see Figure 2.5) suggests the presence of regulatory subunits of PKA. This paradox obscures the role of AKAP complexes, furthermore PKA signaling within the *Chlamydomonas* flagellum. RSP3 as well as its PKA binding domain are conserved among a variety of species (see Table 2.1), and its AKAP domain is homologous to several known AKAPs (Figure 3.1). RSP3 AKAP sequence is conserved among higher eukaryotes, however the AKAP function of the mammalian orthologs has not been characterized (Figure 3.2). The *Chlamydomonas* RSP3 protein is 516 amino acids, with a theoretical molecular weight of 57 kDa, and was first identified as AKAP97 based on its apparent molecular weight by sodium dodecyl sulfate polyacrylamide gel electrophoresis (SDS-PAGE). This anomalous migration is characteristic of other AKAPs and is attributed to the exposed amphipathic helical R-subunit binding domains (Lester et al., 1996).

Human RSP3/RSP3H are thought to be derived from alternative start sites within a single gene, encoding proteins of 418 amino acids and 560 amino acids respectively. RSP3H, the long form, is extended by 142 amino acids at the N-terminus and is referred to as radial spoke protein 3 homolog (RSP3H or RSPH3 as annotated by NCBI). We utilized constructs expressing the long form in most of our experiments characterizing binding and function of RSP3H. Human RSP3H has a theoretical molecular weight of 64 kDa but migrates between 75-100 kDa on a 12% SDS-polyacrylamide gel, similarly to *Chlamydomonas* RSP3. RSP3/RSP3H contain consensus PKA and ERK1/2 phosphorylation sites and a homologous RII-binding AKAP domain (Figure 3.3). As I will discuss later in the chapter, we found RSP3/RSP3H to be substrates for PKA and ERK1/2 and mapped the major ERK phosphorylation site, however other sites may exist and remain to be determined.

Several prevalent ERK1/2 interaction motifs have been mapped to known substrates - these include the FXF, D, and leucine rich motifs. Sequence analysis of RSP3/RSP3H suggests the possibility of all of these regions, however the putative FXF and D motif(s) are the most apparent (see Figure 3.3). Aside from the FXF motif, these regions are often degenerate and non-obvious. RSP3/RSP3H may also contain combinations of these ERK1/2 interacting motifs, which could function synergistically or contribute to differential interaction with the MAPKs depending on cellular context.

Phosphorylation is a key reversible regulatory mechanism to modulate protein function within the cell. However, not all phosphorylation events, moreover sites, are created equal. Spurious phosphorylation *in vitro* can occasionally lead one to believe that a protein is indeed a substrate of a particular protein kinase. As

Gustav Lienhard postulates, due to the limited energetic consequence of percent total ATP consumption of all kinase enzymatic reactions in the cell, non-functional phosphorylation is tolerated *in vivo* (Lienhard, 2008). Additionally, there is limited selective pressure to eliminate an inconsequential site, particularly if the stoichiometry of the phosphate incorporation is low. Thus, identifying the functional consequence of a given phosphorylation event is of utmost importance.

III. Materials and Methods

Cell culture, transfection, harvest

Human embryonic kidney (HEK) 293 cells were cultured in Dulbecco's Modified Eagle's Medium (DMEM) containing 10% fetal bovine serum (FBS) and 1% L-glutamine at 5% CO_2. Generally, cells were reverse-transfected using Fugene 6 according to manufacturer's protocol. 1.5 μg of plasmid(s) was used in transfections, and cells were harvested 36-40 hours post-transfection. After indicated treatments as described in the results section and figure legends, cells were washed twice with cold phosphate-buffered saline (PBS) and lysed on ice using cold lysis buffer (50 mM HEPES pH 7.5, 150 mM NaCl, 1.5 mM $MgCl_2$, 1 mM EGTA, 0.2 mM Na_3VO_4, 100 mM NaF, 50 mM β-glycerophosphate, 10% glycerol, 0.1% Triton X-100, 1.6 μg/mL aprotinin, 0.1 mM phenylmethylsulfonyl fluoride, and 10 μg/mL each: N^a-p-tosyl $_L$-lysine chloromethyl ester, N^a-p-tosyl $_L$-arginine methyl ester, N^a-p-tosyl $_L$-lysine chloromethyl ketone, pepstatin A, leupeptin). After 15 minutes on ice, lysates were quick frozen in N_2 (l) and thawed on ice, followed by centrifugation for 15 minutes at 16,000 xg in a microfuge at 4^o C. Supernatants were stored at -80^o C until further analysis.

Plasmids and antibodies

Human RSP3H in a pSPORT6 vector was obtained from ATCC and cloned into pCMV7.1 N-terminal 3xFLAG vector for mammalian expression. Site-directed mutagenesis was performed to generate RSP3H ERK1/2 phosphorylation site and AKAP-binding mutants. pCMV7.1 3xFLAG-RSP3H truncation mutants were also generated. Mouse monoclonal antibodies against PKA RIIα or RIIβ were obtained from BD Biosciences Transduction Laboratories (San Jose, CA). Rabbit anti-PRKAR2A/PKA-RIIalpha antibody was obtained from Bethyl Laboratories Inc (Montgomery, TX). Normal mouse or rabbit control IgG were purchased from

Santa Cruz Biotechnology (Santa Cruz, CA). The anti-Myc antibody was obtained from the National Cell Culture Center. Mouse monoclonal anti-MAP kinase, activated (diphosphorylated) ERK-1&2 and mouse monoclonal anti-FLAG M2 antibodies were obtained from Sigma-Aldrich (St. Louis, MO). The ERK1/2 antibodies Y691 and X837 are as described (Boulton and Cobb, 1991). The MEK inhibitor, U0126, was obtained from Promega (Madison, WI).

Purification of recombinant His_6-RSP3

Rosetta *Escherichia coli* cells were transformed with pHis-parallel vector containing RSP3 and grown in culture until a turbidity measuring of $OD_{600} = 0.5$. Cells were induced with 400 μM isopropyl β-D-1-thiogalactopyranoside (IPTG) and grown at 30° C overnight (~20 hours). Cells were pelleted (3,000 rpm for 20 minutes), resuspended in GTE (50 mM glucose, 25 mM Tris pH 8.0 and 10 mM EDTA pH 8.0), subjected to centrifugation and pelleting once more, flash frozen in N_2 (l) and stored overnight at -80° C. The next day, samples were thawed on ice and mixed with 1 mL of sonication buffer (20 mM HEPES pH 8.0, 0.1 M NaCl, 1 mM β-mercaptoethanol) and 2 μg of Tris-saturated lysozyme. Samples were vortexed and incubated on ice for 60 minutes prior to sonication using a microprobe tip. Samples were subjected to four 10-second on/off pulses at 50% amplitude. Next, disrupted samples were centrifuged at 35,000 rpm for 45 minutes using a TLA45 rotor. Both pellet and supernatant were saved/stored at -80° C. His_6-RSP3 was found predominantly in the cell pellet, most likely in inclusion bodies or aggresomes, thus the pellet was subjected to 8 M guanidine-HCl extraction and stepwise dialysis. Briefly, the previous cell pellet was resuspended in 40 mL resuspension buffer (20 mM HEPES pH 8.0, 0.1 M NaCl, 0.1% Triton X-100, and 1 mM β-mercaptoethanol) with PMSF, leupeptin, aprotinin and a protease inhibitor cocktail (as described in the cell harvest methods). The resuspension was sonicated and re-centrifuged at 30,000 rpm in a

Ti45 rotor for 40 minutes. The pellet was then resuspended in 20 mL extraction buffer (50 mM HEPES pH 8.0, 5 mM EDTA, 8 M guanidine-HCl and 1 mM β-mercaptoethanol), homogenized using a Polytron homogenizer and centrifuged at 30,000 rpm for 40 minutes in a Ti45 rotor. The subsequent supernatant was diluted to 4 M guanidine-HCl prior to attempting to load sample onto a Ni-NTA agarose gravity-flow column and eluting with a two-step 30 mM and 150 mM imidazole wash. Assaying the eluate indicated that His_6-RSP3 did not bind to the column during sample loading prior to imidazole elution. Thus, the unbound material was collected and stepwise dialyzed to 2 M and then guanidine-HCl-free buffer. However, protein precipitated during the last dialysis step. Finally, precipitated His_6-RSP3 was resuspended in 1 mL 1xPBS. Protein concentration was determined to be approximately 1 mg/mL by Coomassie blue staining of proteins resolved on a 12% SDS-polyacrylamide gel loaded with increasing volumes of His_6-RSP3 compared to known amounts of bovine serum albumin (BSA).

Immunoprecipitation

For immunoprecipitations, cell extracts containing 1 mg total protein were pre-cleared with 30 μL of protein A-Sepharose beads for 1 hour at 4^oC prior to incubation with the indicated primary antibodies (1:250 dilution) at 4^oC overnight. The following day, 30 μL of protein A-Sepharose beads was incubated with the lysate for 2 hours at 4^oC. The beads were centrifuged at 5000 xg for 3 minutes prior to three 10-minute washes with IP wash buffer (10 mM Tris pH 7.4, 5 mM $MgCl_2$, 500 mM NaCl). The beads were subsequently boiled in Laemmli sample buffer (2% SDS, 10% glycerol, 5% β-mercaptoethanol, 0.01% bromophenol blue, 50 mM Tris HCl) and subjected to SDS-PAGE. Proteins were electrotransferred to nitrocellulose membranes (Millipore, Billerica, MA).

Membranes were blocked with 5% nonfat powdered milk in 20 mM Tris, pH 7.5, 0.15 M NaCl (TBS) for 2 hours at 4^{o} C, incubated with the primary antibody overnight at 4^{o} C, followed by incubation with horseradish peroxidase-conjugated secondary antibody diluted 1:2000 in 5% milk in TBS for 1 hour at room temperature. Proteins were detected by enhanced chemiluminescence. In some cases, immunoblots were analyzed by densitometry using Image J.

Immunoprecipitation kinase assays

After washing the immunoprecipitates with IP wash buffer, protein A-Sepharose beads were washed with kinase wash buffer (10 mM HEPES pH 8.0, 10 mM $MgCl_2$). Beads were subsequently resuspended in kinase buffer (10 mM HEPES pH 8.0, 10 mM $MgCl_2$, 1 mM 1,4-dithiothreitol, 1 mM benzamidine). Recombinant active, phosphorylated ERK2 and purified catalytic subunit of PKA were used as enzymes. IP kinase assays were performed at 30^{o} C for 10 minutes. Reactions contained 10 μCi of [γ-^{32}P]-ATP and a final concentration of 10 μM ATP in a 30 μL total reaction volume (300 pmol of total ATP, 0.033 μCi/pmol ATP, resulting in ~69597 cpm/pmol ATP; 2.22*10^{6} dpm/μCi and assuming a counting efficiency of 0.95). Reactions were quenched with Laemmli sample buffer and boiled at 100^{o} C for 5 minutes. Samples were resolved on 12% SDS-polyacrylamide gels, stained with Coomassie blue, dried and analyzed using autoradiography.

Phosphoamino acid analysis

1μg of His_6-RSP3 phosphorylated *in vitro* with pERK2 was hydrolyzed with 6 N HCl and the products were resolved by electrophoresis on a thin layer plate using a Hunter apparatus as previously described (Hunter and Sefton, 1980; Kamps and Sefton, 1989). Phosphorylated residues were compared to migration of known

phosphoamino acid standards: phosphoserine, phosphothreonine and phosphotyrosine visualized with ninhydrin.

Quantification and statistical analyses

Results are expressed as means ± SEM determined from at least three independent experiments. Statistical significance was calculated using paired or unpaired two-tail t-tests and is indicated in the figure legends. Densitometric quantification of immunoblots was performed using Image J. Scanned images of film exposed with intensities of bands in the linear range as determined by exposure of a sensitometer imprinting an intensity gradient on the film were used for all quantification analyses.

IV. Results

RSP3/RSP3H are interacting proteins and substrates for ERK1/2

The interaction between ERK2 and RSP3 was found by our lab through a yeast two-hybrid screen designed to identify interacting proteins that have a higher affinity for the phosphorylated, active form of ERK2. Yeast were transformed with bait vectors, either containing an ERK2 and constitutively active MEK1 (MEK1R4F) co-expression plasmid, ERK2 or MEK1R4F alone, along with a mouse brain cDNA library as prey. Growth on restrictive medium and β-galactosidase activity were used as readouts for an interaction (Table 3.1). To confirm the yeast two-hybrid finding, 3xFLAG-tagged RSP3H, the longer human isoform, and Myc epitope-tagged ERK2 were overexpressed in HEK293 or HeLa cells and reciprocally co-immunoprecipitated. Overexpressed RSP3H also co-immunoprecipitated with endogenous ERK1 (Figure 3.4). Despite a theoretical molecular weight of 64 kDa (67 kDa with the 3xFLAG epitope), 3xFLAG-RSP3H migrates between 75-90 kDa on a 12% SDS-polyacrylamide gel. This slower migration is a characteristic of other AKAPs, and is due to the exposed charge of the amphipathic helical domain.

FLAG-tagged truncation mutants of RSP3H, amino acids 1-476, 1-187, and 187-476 all co-immunoprecipitated with endogenous ERK1, suggesting that multiple, different ERK1/2 binding motifs may exist in RSP3H (Figure 3.5). However, binding of 187-476 to ERK1 was significantly diminished. Thus, the first 187 amino acids of RSP3H appear to primarily contribute to the affinity of the RSP3H-ERK interaction. Numerous substrates, including RSP3H, contain multiple binding domains for ERK. Consequently, three apparent putative FXF motifs within RSP3H were mutated; however, all resulting mutants were able to co-immunoprecipitate with ERK1 (Figure 3.6). To test whether ERK1/2 activity

affected the interaction in a mammalian cell system, HEK293 cells expressing 3xFLAG-RSP3H were treated with the MEK1/2 inhibitor, U0126, which inhibits the subsequent activation of ERK1/2, or DMSO as a control for 10 minutes prior to immunoprecipitation of endogenous ERK1. No apparent difference in co-immunoprecipitation of RSP3H with ERK1 was observed between the control- and U0126-treated samples.

In vitro kinase assays performed with recombinant phosphorylated ERK2 (pERK2) and immunoprecipitated RSP3H from HEK293 lysate or recombinant His_6-RSP3 showed that RSP3 and RSP3H are indeed substrates. Recombinant His_6-RSP3 was generated for antibody production and for use in *in vitro* kinase assays for phospho-residue identification (Figure 3.8). Phosphoamino acid analysis indicates that pERK2 phosphorylates predominantly threonine in RSP3/RSP3H, and *in silico* prediction of consensus ERK1/2 phosphorylation motifs suggested the major site to be threonine 286. Mutation of threonine 286 to alanine in RSP3H (T286A) attenuated phosphorylation by ERK2 greater than 60% in immunoprecipitation kinase assays (Figure 3.9). ^{32}P labeling indicated that RSP3H is phosphorylated upon stimulation of cells with EGF (Figure 3.10). Radiolabeled phosphate incorporation into RSP3H was diminished by pre-treatment with the MEK1/2 inhibitor U0126, suggesting that at least a portion of this phosphorylation is ERK1/2 dependent. Furthermore, the extent of radiolabeled phosphate incorporation into RSP3H T286A was much less than that into wild-type, suggesting that threonine 286 is the major ERK1/2 phosphorylation site in cells. Radiolabled phosphate incorporation was not completely abolished, indicating that threonine 286 may not be the only site that is phosphorylated upon stimulus with EGF and that ERK1/2 are presumably not the only protein kinases that phosphorylate RSP3H in cells. Truncation mutants of

3xFLAG-RSP3H were also used as substrates for pERK2 in immunoprecipitation kinase assays, and all were phosphorylated *in vitro* (Figure 3.11).

Mammalian RSP3H is an AKAP and a substrate for PKA

Chlamydomonas RSP3 has been shown to bind to the regulatory subunits of PKA *in vitro* in a similar manner to other known AKAPs. Orthologs of RSP3 exist in a variety of species, all of which contain a highly conserved similar sequence in the AKAP R-subunit binding domain (see Figure 3.2). Along these lines, we tested whether the human isoform of RSP3H has a similar AKAP function. Overexpressed RSP3H co-immunoprecipitated with endogenous RIIα and RIIβ - the regulatory subunits of PKA known to sequester the tetrameric holoenzyme to discrete subcellular locales (Figure 3.11). Mutation of residues threonine 325 and isoleucine 326 to alanines within the amphipathic helix of RSP3H, which are critical for PKA regulatory subunit binding, disrupted the co-immunoprecipitation interaction observed with overexpressed wild-type RSP3H (Figure 3.13; Figure 3.14). *In vitro* kinase assays indicated that the purified catalytic subunit of PKA (PKAc) phosphorylates both wild-type and T286A mutant 3xFLAG-RSP3H similarly, although the site(s) remain to be determined (Figure 3.15).

ERK1/2 phosphorylation regulates AKAP function

We next decided to pursue whether phosphorylation of RSP3H by ERK1/2 has any consequence on RSP3H function. Mutating the ERK1/2 phosphorylation site in RSP3H affects its ability to co-immunoprecipitate with the regulatory subunits of PKA. Co-immunoprecipitation of the T286A mutant with endogenous RIIα or RIIβ was enhanced by approximately 1.8 fold compared to wild-type overexpressed 3xFLAG-RSP3H (Figure 3.16). However, treating cells with the MEK1/2 inhibitor, U0126, which inhibits the subsequent activation of ERK1/2,

diminished the interaction of RSP3H with endogenous RIIα. HEK293 cells expressing 3xFLAG-RSP3H were treated with fresh medium (containing 10% fetal bovine serum) and 10 μM U0126 or DMSO as a control for 10 minutes prior to immunoprecipitation of RIIα (Figure 3.17). Stimulation with fresh serum-containing medium caused an expected increase in phospho-ERK1/2 and this activity was decreased in U0126-treated samples. Treatment with U0126 caused an approximate 67% decrease in RSP3H pull-down with RIIα, suggesting that inhibiting ERK1/2 activity correlates with decreased AKAP function of RSP3H, contrary to what is expected based on the results obtained from the RSP3H T286A mutant interaction with RIIα. To further examine the interaction between RSP3H and RIIα, a time course analysis of the effects of serum and U0126 treatment upon the interaction was performed. In this experiment, the culture medium of RSP3H-transfected HEK293 cells was changed to fresh serum-containing medium supplemented with 10 μM U0126 or DMSO as a control for the indicated times – 1, 2.5, 5, 10, 30, and 60 minutes – prior to lysis (Figure 3.18). The difference in the amount of RSP3H that co-immunoprecipitated with endogenous RIIα was negligible between untreated and samples treated with serum plus DMSO (control) for 1 minute, however, the amount of co-immunoprecipitated RSP3H decreased from 1 minute up to 5 minutes after new serum-containing medium was added to the cells. The interaction between RIIα and RSP3H was consistently diminished in the presence of U0126 over the time course of the experiment with an average two-fold reduction in RSP3H pulled down with RIIα at all time points measured (Table 3.2). Thus, inhibiting ERK1/2 activity appears to negatively regulate the AKAP function of RSP3H.

V. Discussion

Mammalian RSP3H is a novel ERK1/2 interacting AKAP; mutating residues within the amphipathic helix of RSP3H, disrupted its interaction with RIIα, indicating that human RSP3H is a bona fide AKAP. The ERK-RSP3H interaction is likely to be due to direct binding, as it was initially identified through yeast two-hybrid analysis. This is the first evidence indicating that the human ortholog of RSP3 is an AKAP as well as the first describing it to directly bind to the ERK1/2 MAP kinases. *In vitro* binding studies of purified proteins need to be performed to definitively confirm the nature of this interaction. The yeast two-hybrid screen that produced RSP3 as an interacting protein was designed to identify proteins that have a higher affinity for the phosphorylated and active form of ERK2. Based on β-galactosidase activity, mammalian RSP3 bound 2.5 times better to pERK2 compared to inactive ERK2 under the assay conditions. We confirmed this interaction through co-immunoprecipitation studies and have discerned the minimal interacting region, amino acids 1-187, that appears to contribute to the majority of the affinity of the ERK-RSP3H interaction. Inhibiting ERK1/2 activation with U0126 did not disrupt the ability of RSP3H to co-immunoprecipitate with endogenous ERK. Corollary experiments using EGF and forskolin to activate the ERK1/2 and PKA signaling pathways respectively, did not cause an apparent change in co-immunoprecipitation (data not shown). We have not been successful in determining whether the RSP3H-ERK interaction is affected by modulating ERK1/2 activity in the cell, as it has proved difficult to measure changes in amounts of overexpressed RSP3H co-immunoprecipitating with endogenous ERK1. Titrating levels of transfected plasmids encoding RSP3H transcripts may prove useful in enhancing the sensitivity of the interaction to ligands that stimulate cAMP production or cause downstream activation of ERK1/2.

RSP3H contains several FXF sequences, however mutating these individually did not disrupt the interaction as observed by co-immunoprecipitation. These data as well as the truncation mutant co-immunoprecipitation experiments suggest the presence of another ERK1/2 interacting motif within RSP3H as well as the possibility of multiple binding motifs that contribute to the interaction. Amino acids 15-20 of RSP3H may encode a putative D-domain; mutagenic analysis of this region and the combinatorial disruption of all three FXF sequences require further exploration.

Here we pinpoint the major ERK1/2 phosphorylation site in RSP3H, threonine 286 (within a P-P-T-P motif), *in vitro* and in cells. Mutating threonine 286 to alanine, however, only decreased ^{32}P-incorporation *in vitro* by approximately 69%, suggesting that other ERK1/2 phosphorylation sites may exist. ^{32}P-labeling experiments of cells transfected with wild-type or T286A mutant RSP3H also support this notion. EGF treatment resulted in some ^{32}P incorporation into RSP3H T286A, although less than into wild-type. EGF-stimulated phosphorylation of RSP3H T286A was marginally decreased with pretreatment with U0126, indicating that an additional site in RSP3H was phosphorylated in an ERK1/2-dependent manner. U0126 treatment did not completely reduce EGF-stimulated ^{32}P incorporation to basal levels in both wild-type and T286A RSP3H, arguing that other kinases may be phosphorylating RSP3H upon treatment with EGF. Additionally, ^{32}P incorporation in RSP3H T286A was further suppressed compared to wild-type under basal conditions (treatment with U0126 alone), indicating that other stimuli may induce ERK1/2 to phosphorylate RSP3H. Further examination of the cell context- and ligand-dependent manner by which ERK1/2 and other protein kinases phosphorylate RSP3/RSP3H is required.

Truncation mutants of RSP3H were phosphorylated *in vitro*, and despite the artificial nature of such reactions, all contain putative ERK1/2 phosphorylation sites. Serine 99 is one such site and could account for ERK phosphorylating the 1-187 amino acid truncation mutant. Phosphoamino acid analysis performed on recombinant His_6-RSP3, the short form, only indicated ^{32}P-labeled threonine, but as it lacks the N-terminal 142 amino acids of RSP3H, serine 99 (L-L-S-P) could have been missed. Immunoprecipitated full-length 3xFLAG-RSP3H did not yield sufficient radiolabel counts to determine site-specific phosphate incorporation using phosphoamino acid analysis. Threonine 243, within a P-Q-T-P motif, is another likely ERK1/2-phosphorylation site.

PKA phosphorylates RSP3H *in vitro*, and this phosphorylation is not dependent on ERK1/2 phosphorylation at least *in vitro*, as T286A and wild-type RSP3H were equally phosphorylated by PKA. RSP3/RSP3H contain multiple PKA phosphorylation consensus motifs, R-X-X-S/T-ϕ, with threonine 21 being a high stringency Scansite 2.0 predicted PKA phospho-site (Obenauer et al., 2003). Other potential sites within consensus motifs include: S156, T202, S216, T243, T286, and S530. From the *in vitro* immunoprecipitation kinase assay, threonine 286 is most likely not a PKA phosphorylation site; however, it could be phosphorylated by PKA *in vivo*, as certain residues can be phosphorylated by multiple kinases, providing additional layers of complexity in regulating protein function. PKA phosphorylation sites need to be further explored using mass-spectrometric or phosphoamino acid analysis.

Inhibiting ERK1/2 activation and subsequent activity decreases the amount of overexpressed RSP3H that co-immunoprecipitates with endogenous RIIα. Mutating the ERK1/2 phosphorylation site in RSP3H to an alanine, however, increases the capacity of RSP3H to co-immunoprecipitate with RIIα. A few

possibilities might explain the apparently incongruous outcomes of these two experiments. Firstly, mutating the ERK1/2 phosphorylation site in RSP3H to an alanine may cause a conformational change that affects RIIα binding in a distinct manner from (de)-phosphorylation of the residue. The T286A mutation could result in a conformational rearrangement in RSP3H that is more conducive to binding to RIIα, independent of phospho-regulation of that site. Moreover, the structurally distinct RSP3H T286A could have a higher affinity for the regulatory subunits of PKA than wild-type RSP3H. Secondly, as seen in the serum-stimulation time course experiments, increased ERK1/2 activity could result in increased phosphorylation of RSP3H and dissociation from the PKA holoenzyme. Alternatively, PKA could be activated by serum stimulation, releasing the C subunits and causing a concomitant dissociation from its cognate AKAP. However, it is believed that the R subunits remain dimerized even as the C subunits are released, so the R subunit-AKAP interaction may not be impaired (Zhao et al., 1998). The decreasing interaction of RSP3H with RIIα observed at early time points after addition of fresh serum-containing medium was consistent with the T286A mutant experiments, and U0126 treatment appeared to reverse this phenomenon – U0126 treatment for 1 and 2.5 minutes caused greater than 50% reduction in RIIα co-immunoprecipitation, whereas U0126 treatment for 5 and 10 minutes resulted in 25% and 38% reduction respectively (Figure 3.17; Table 3.2). Thirdly, the diminishing interacting capacity caused by U0126 may be due to the fact that U0126 may have additional effects upon the function of RSP3H, perhaps conformationally or spatially inhibiting its interaction with the regulatory subunits of PKA. Fourthly, mutating the major ERK1/2 phosphorylation site within RSP3H could release its subcellular restriction, altering the localization of RSP3H within the cell, causing an increased availability to a greater pool of PKA and the observed increase in co-IP with

RIIα. The dynamic and regulated localization of RSP3H by ERK1/2 is an intriguing hypothesis, as RSP3H contains several regions that may encode a putative monopartite or bipartite nuclear localization signal (NLS). How mutating the ERK1/2 phosphorylation site and other pharmacological manipulations affect the AKAP function of RSP3H remains to be elucidated, particularly through more extensive structure-function and cell biological studies.

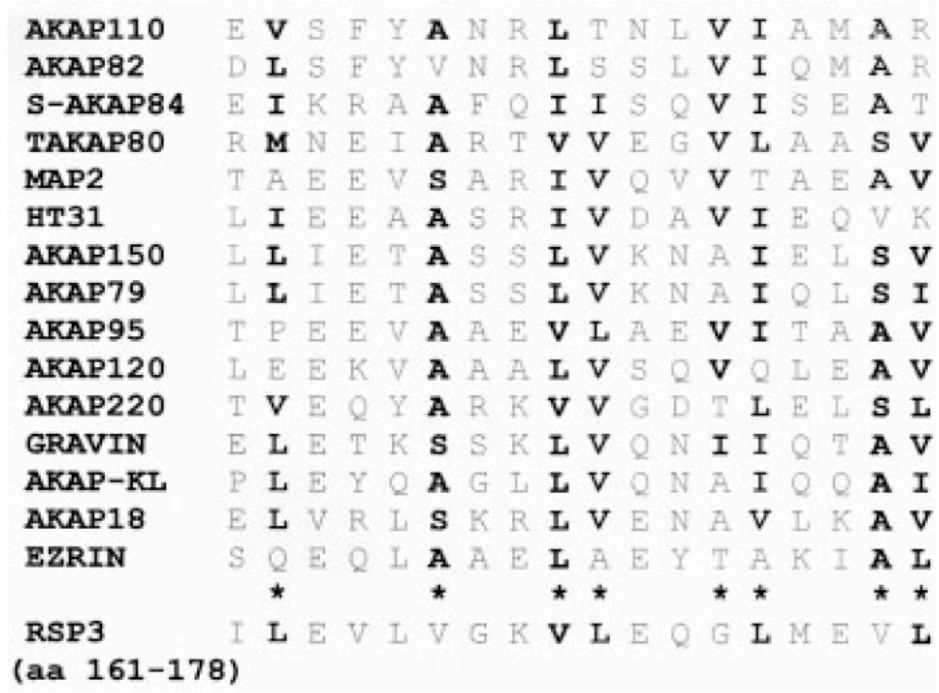

Figure 3.1. Alignment of RSP3 AKAP domain with known AKAPs.
Alignment of *Chlamydomonas* RSP3 AKAP amphipathic helix (amino acids 161-178) with the RII-binding domains of known AKAPs. Residues in bold indicate identical or conservatively substituted amino acids, and residues with an asterisk above indicate residues required for RII-binding. Reprinted with permission from Gaillard et al., 2001.

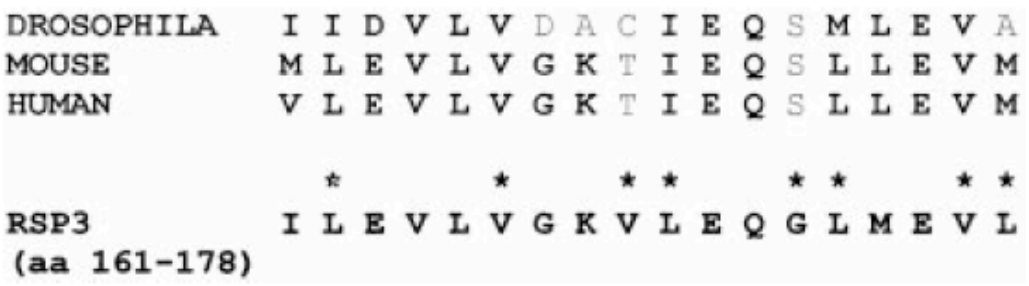

Figure 3.2. Higher eukaryotic orthologs of RSP3. Alignment of *Chlamydomonas* RSP3 AKAP domain with a proposed similar region in drosophila, human, and mouse. Residues in bold indicate identical or conserved amino acids, while the residues with asterisks above are required for RII-binding.

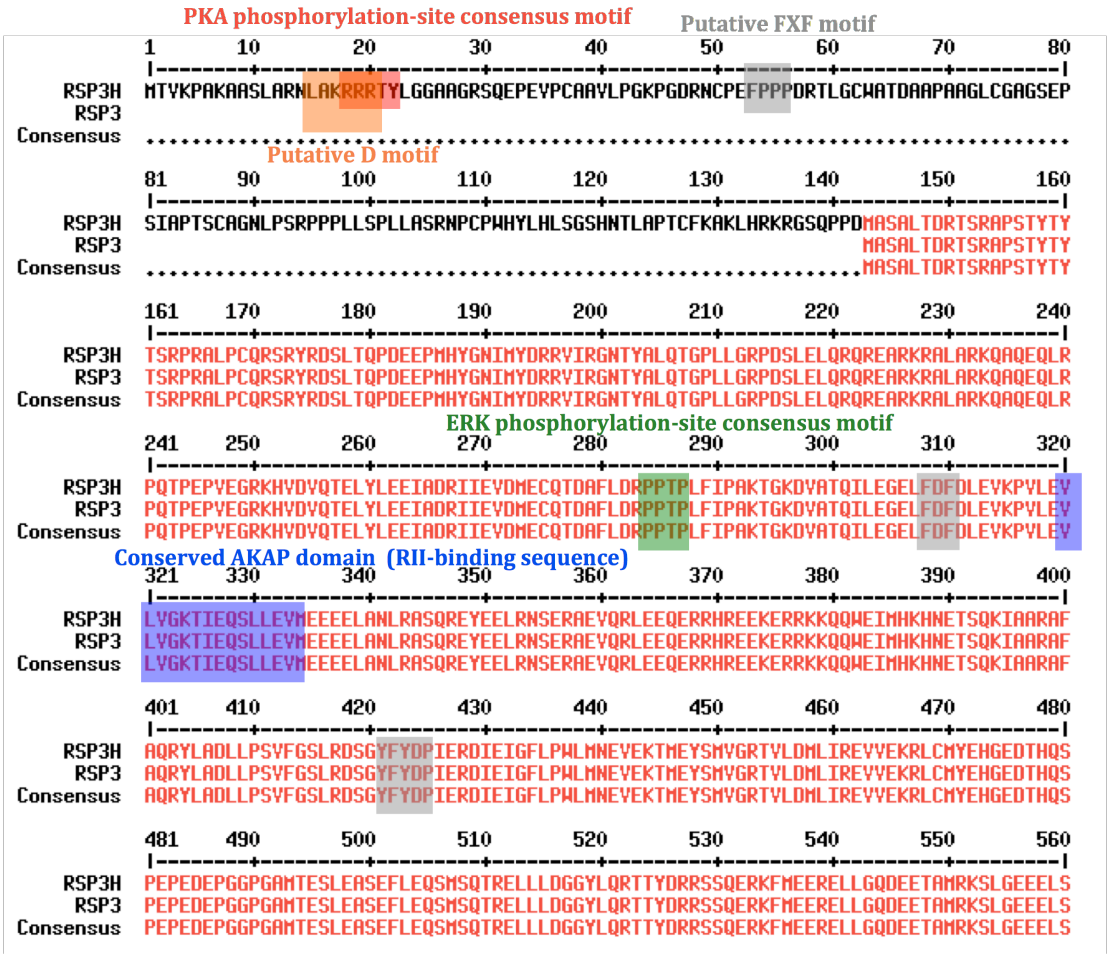

Figure 3.3. Amino acid sequence of human RSP3/RSP3H. Sequence analysis of RSP3/RSP3H indicated several regions of interest, including PKA (highlighted in red) and ERK (highlighted in green) phosphorylation site consensus motifs as well as a conserved RII-binding region (blue). Threonine 21, within a R-R-X-S/T-ϕ region, is a putative PKA phosphorylation site while ERK phosphorylates threonine 286. Threonine 243 (P-Q-T-P) is a putative ERK phosphorylation site as well. ERK-interacting domains include three putative FXF motifs (highlighted in grey) – phenylalanines (F) at positions 53, 308, and 422 in the primary sequence. Highlighted in orange is the putative D motif, LAKRRR.

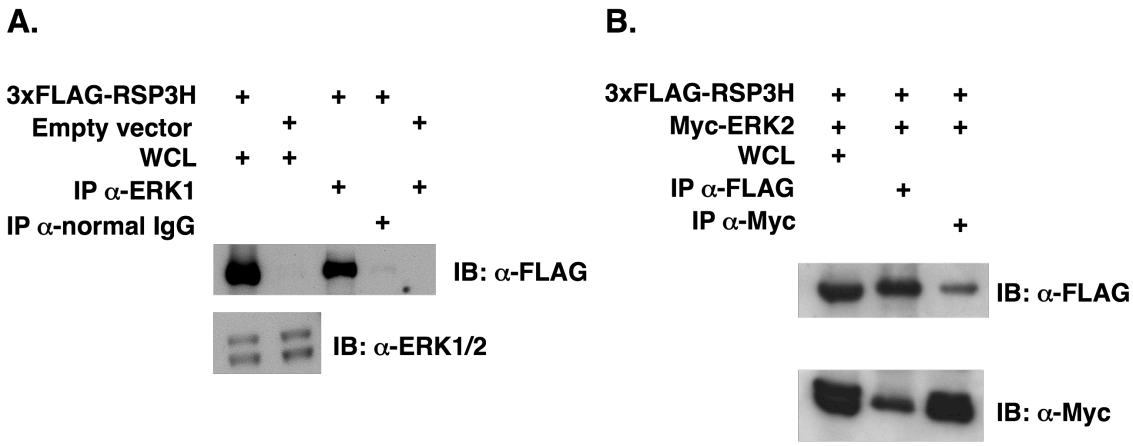

Figure 3.4. RSP3H and ERK1/2 co-immunoprecipitate. A. 3xFLAG-tagged RSP3H was expressed in HEK293 cells and co-immunoprecipitated with endogenous ERK1 (X837 antibody as described in the methods). **B.** Reciprocal immunoprecipitation of RSP3H and ERK2. 3xFLAG-RSP3H was co-expressed with Myc-ERK2 in HeLa cells and immunoprecipitated (IP) and immunoblotted (IB) with the indicated antibodies. WCL = whole cell lysate, IgG = normal rabbit IgG control antibody.

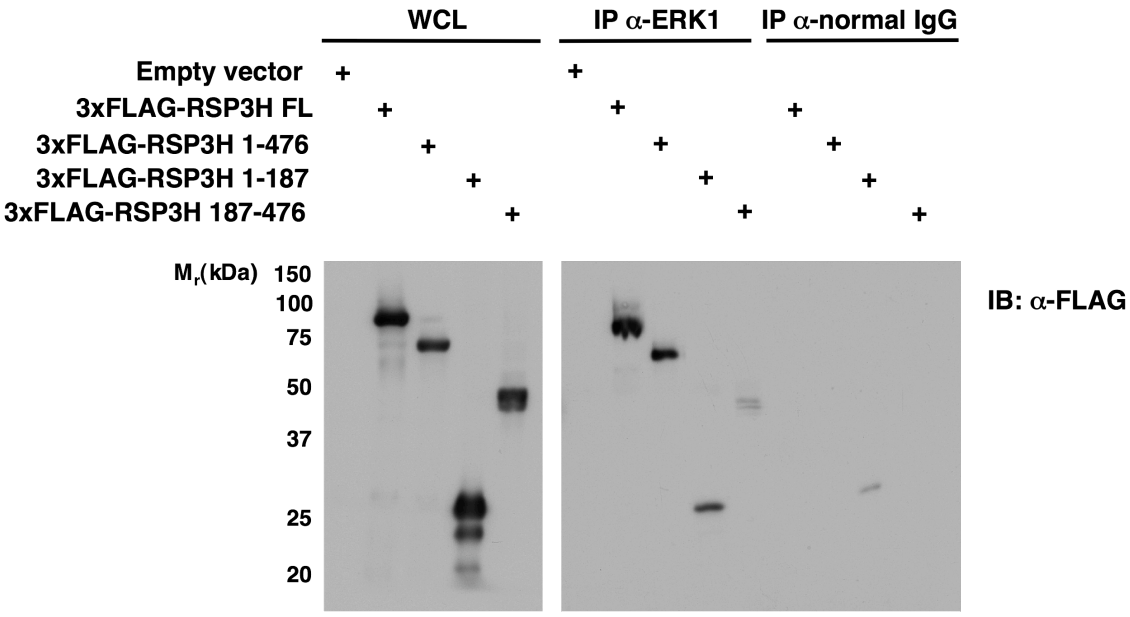

Figure 3.5. Domain analysis of RSP3H interaction with ERK. Truncation mutants of 3xFLAG-RSP3H were expressed in HEK293 cells and co-immunoprecipitated with endogenous ERK1. FL = full length. Amino acids 1-187 correspond to the sequence N-terminal to the conserved radial spoke protein domain, which spans amino acids 187-476.

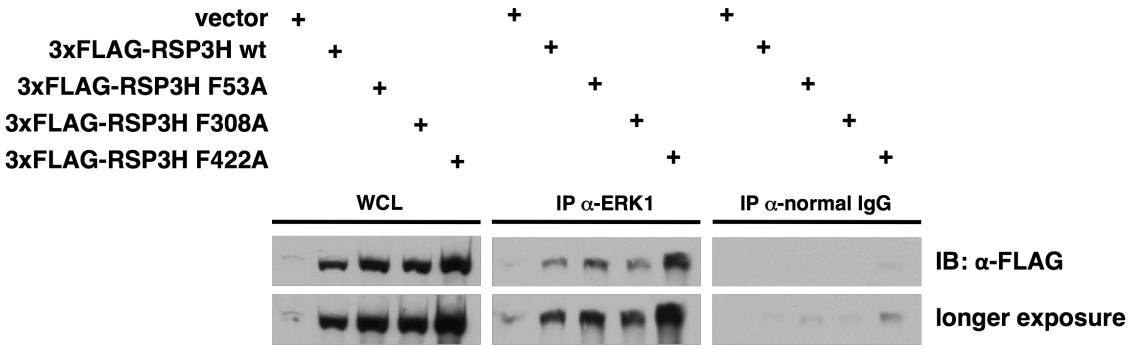

Figure 3.6. FXF mutants co-immunoprecipitate with ERK1. Three F to A substitutions within putative FXF motifs of full-length RSP3H were generated using site-directed mutagenesis. 3xFLAG-RSP3H FXF mutants were expressed in HEK293 cells and co-immunoprecipitated with endogenous ERK1.

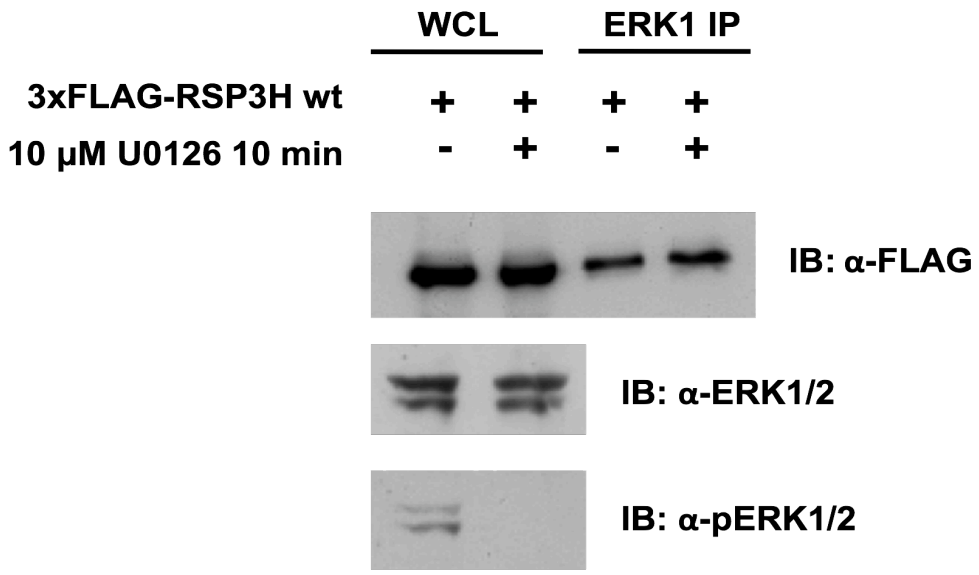

Figure 3.7. Inhibiting ERK1/2 activity does not disrupt the RSP3H-ERK interaction. HEK293 cells expressing 3xFLAG-RSP3H were treated with 10 μM U0126 or DMSO as a control for 10 minutes prior to lysis and immunoprecipitation of endogenous ERK1. Samples were immunoblotted (IB) with the indicated antibodies. WCL = whole cell lysate. No apparent difference in co-immunoprecipitation was observed between the control- and U0126-treated samples.

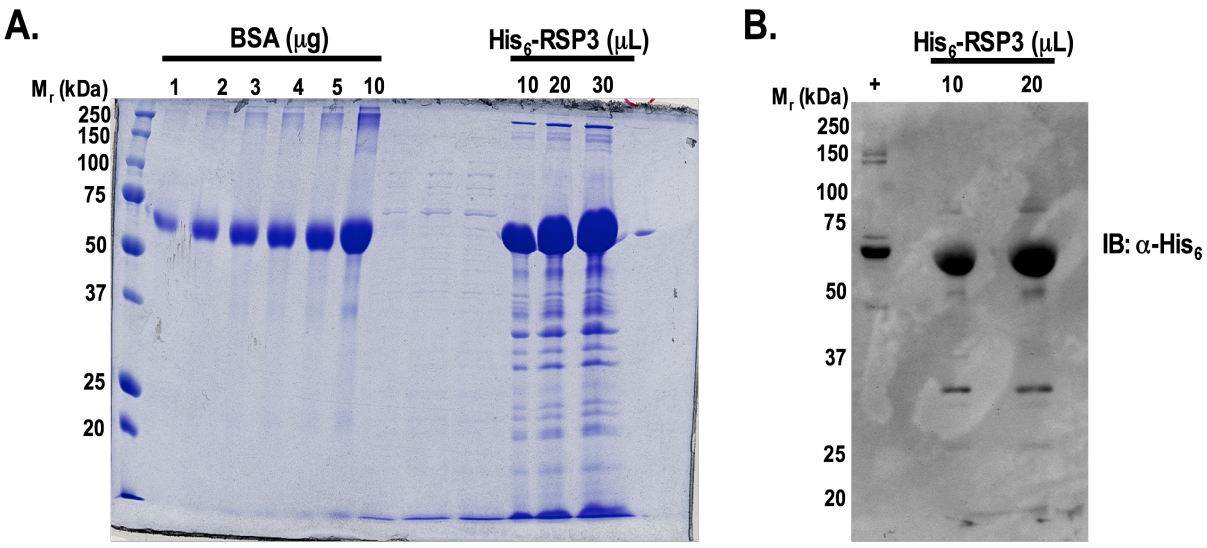

Figure 3.8. Purification of His_6-RSP3. Human 6x-histidine-tagged RSP3 (418 amino acids) was purified for use in *in vitro* kinase assays as well as to generate rabbit antisera (polyclonal antibody population) to detect endogenous protein. **A.** Semi-quantitative determination of purified, recombinant His_6-RSP3 sample concentration. Coomassie stain of a 12% SDS-PAGE loaded with increasing volumes (μL) of His_6-RSP3 compared to increasing amounts of BSA (μg). **B.** Immunoblot of purified His_6-RSP3 using an anti-His_6 antibody. A His_6-Tao2 fragment was used as a positive control (+)

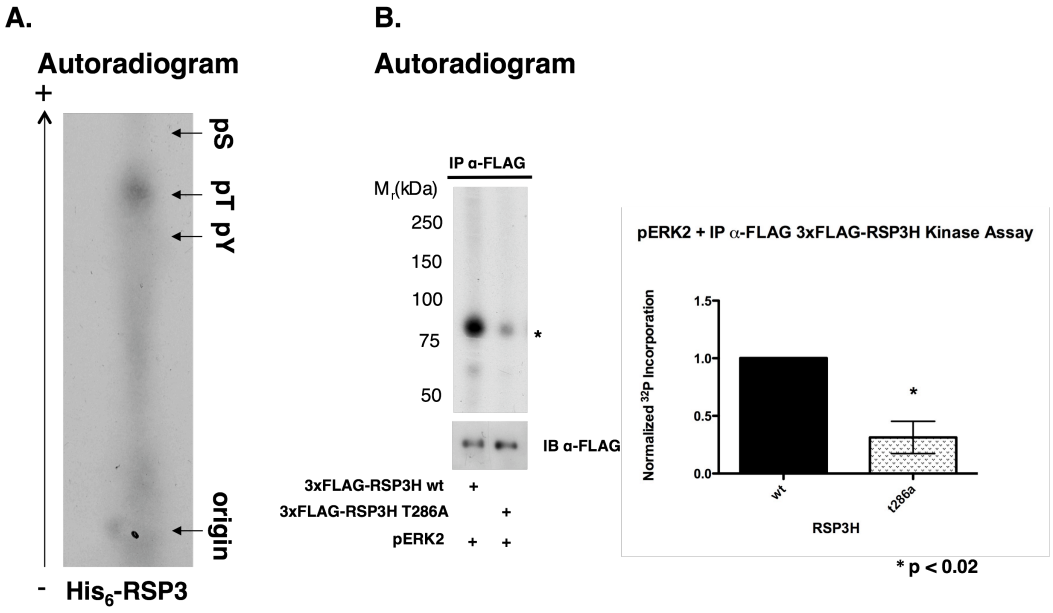

Figure 3.9. ERK phosphorylates RSP3H on threonine 286. A. Phosphoamino acid analysis of RSP3. *In vitro* pERK2 phosphorylated His_6-RSP3 was hydrolyzed with 6 N HCl and the products were resolved using thin layer electrophoresis on a Hunter apparatus. Phosphorylated residues were compared to migration of known phosphoamino acid standards visualized with ninhydrin. **B.** Overexpressed 3xFLAG-RSP3H wild-type (wt) or T286A mutant was immunoprecipitated (IP) from HEK293 cells and used as substrate for an *in vitro* immunoprecipitation kinase reaction with recombinant phosphorylated, active ERK2 (pERK2) as the kinase. Graph represents quantification of ^{32}P-incorporation of RSP3H bands via scintillation counts, normalized to wild-type. Mean of T286A = 0.31. Data represents mean ± SEM. n = 3. Significance was determined using a one-tailed t-test with an obtained p-value = 0.0196.

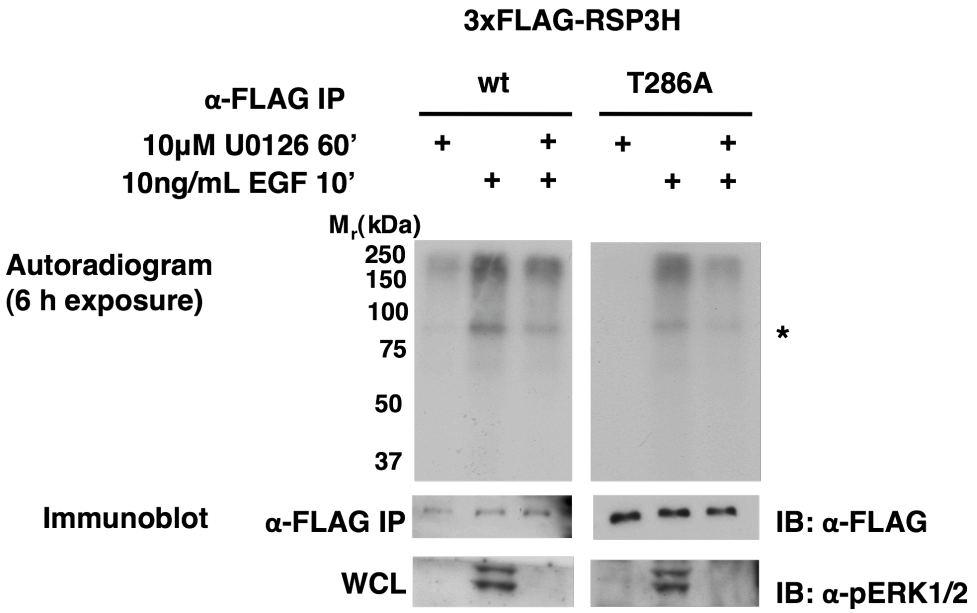

Figure 3.10. ERK1/2 phosphorylate RSP3H in cells. HEK293 overexpressing 3xFLAG-RSP3H wt or T286A were serum starved in 0% FBS for 20 hours, labeled with 1 mCi/mL ^{32}P orthophosphate and treated with 10 μM U0126 (as indicated) for 60 minutes followed by stimulation with 10 ng/mL EGF for 10 minutes (as indicated). 3xFLAG-RSP3H was immunoprecipitated (IP) and assayed for radiolabeled-phosphate incorporation. Immunoblots (IB) with the indicated antibodies were performed on the IP and whole cell lysate (WCL) samples. Graph represents fold ^{32}P-incorporation based on a ratio of CPM (determined via scintillation counts) to IP band (determined via densitometry) normalized to U0126-treated wild-type sample.

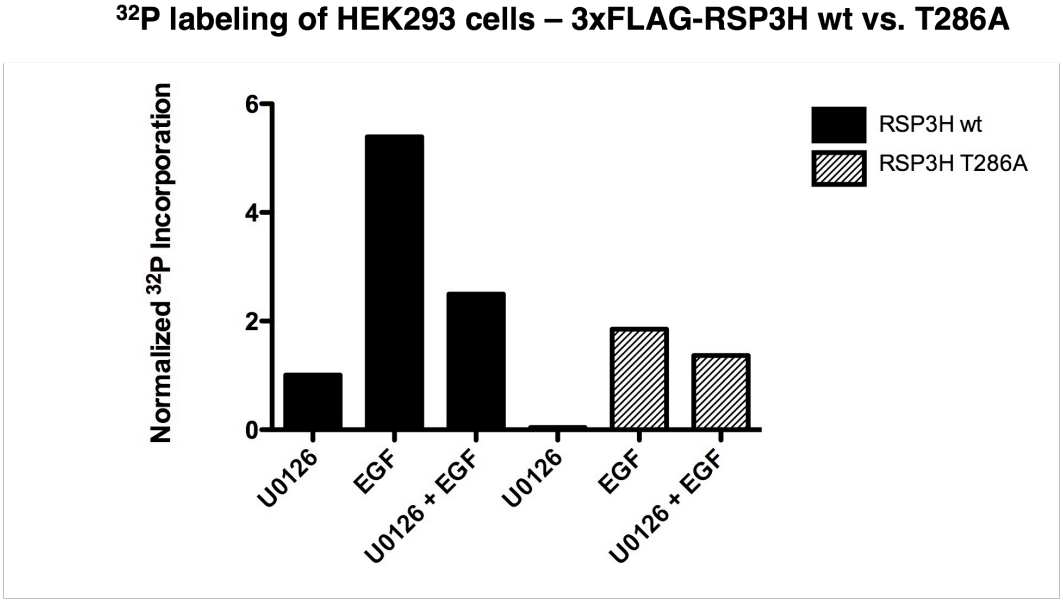

Figure 3.10. ERK1/2 phosphorylate RSP3H in cells (continued).

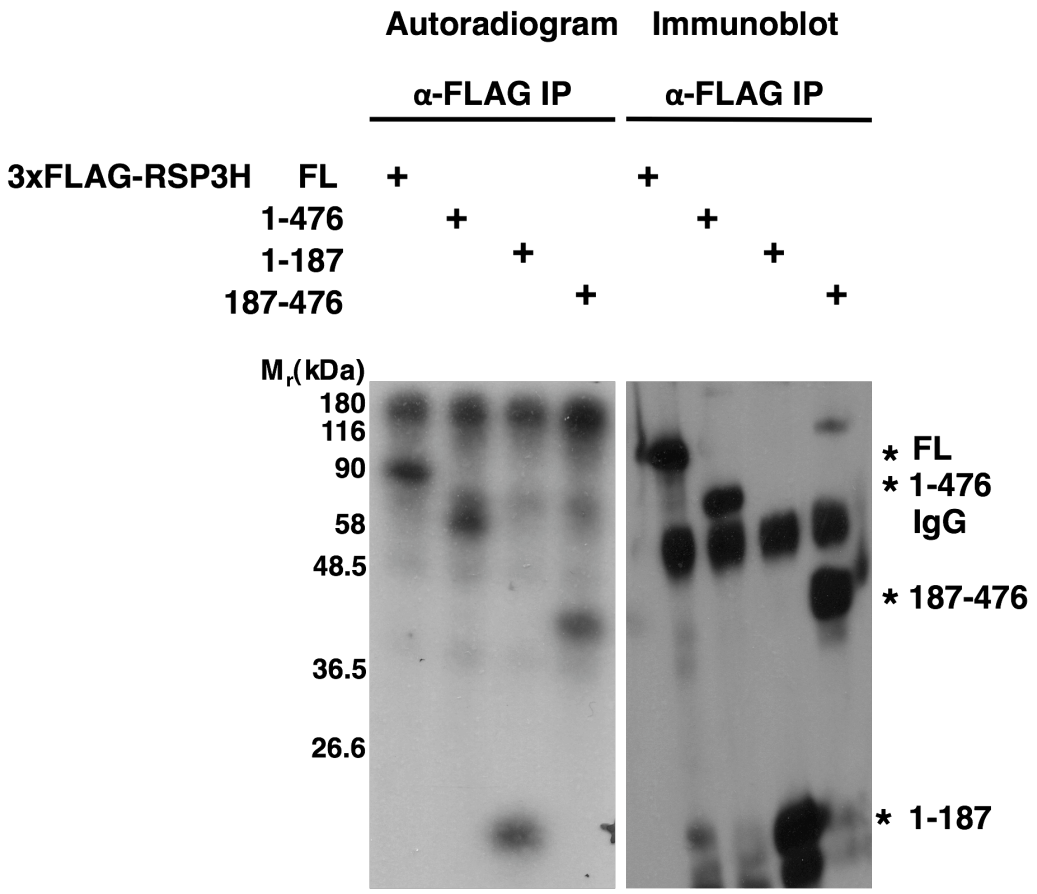

Figure 3.11. Immunoprecipitation kinase assays of RSP3H truncation mutants. Overexpressed 3xFLAG-RSP3H full-length (FL) or indicated truncation mutants were immunoprecipitated with α-FLAG antibody and subjected to *in vitro* kinase assays with recombinant phosphorylated, active ERK2 (pERK2) as the kinase. Graph represents quantification of ^{32}P-incorporation into RSP3H bands via scintillation counts. CPM = counts per minute.

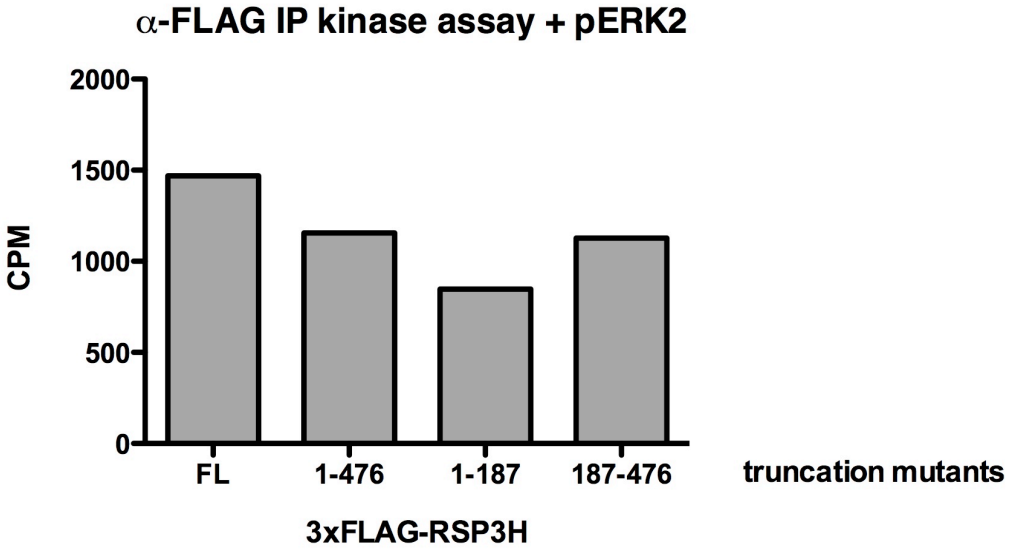

Figure 3.11. Immunoprecipitation kinase assays of RSP3H truncation mutants (continued).

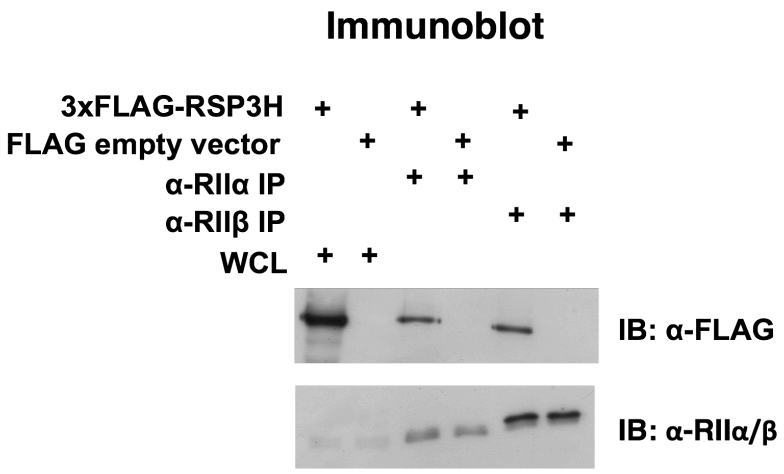

Figure 3.12. RSP3H co-immunoprecipitates with endogenous RIIα/β.
Endogenous RIIα or RIIβ were immunoprecipitated (IP) from the HEK293 cells expressing 3xFLAG-RSP3H. Samples were immunoblotted (IB) with the indicated antibodies. WCL = whole cell lysate.

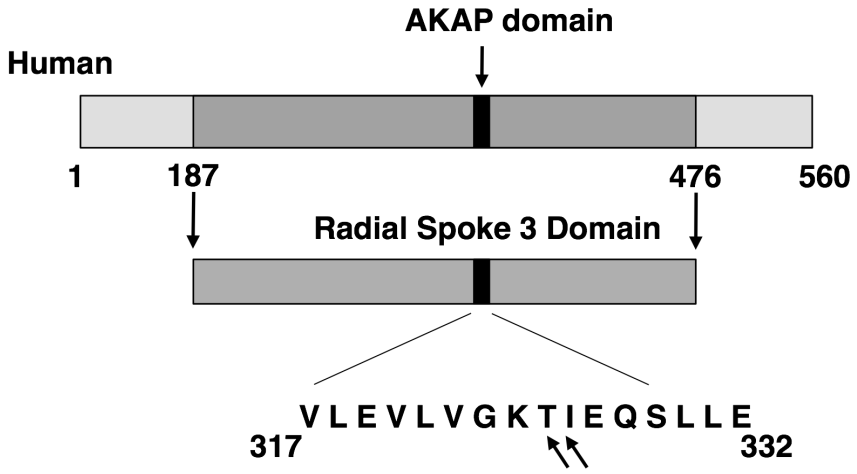

Figure 3.13. Human RSP3H contains an AKAP (RII-binding) domain. Domain structure of the AKAP domain of human RSP3H. Site-directed mutagenesis of threonine 325 and isoleucine 326 to alanine disrupted the R-subunit interaction.

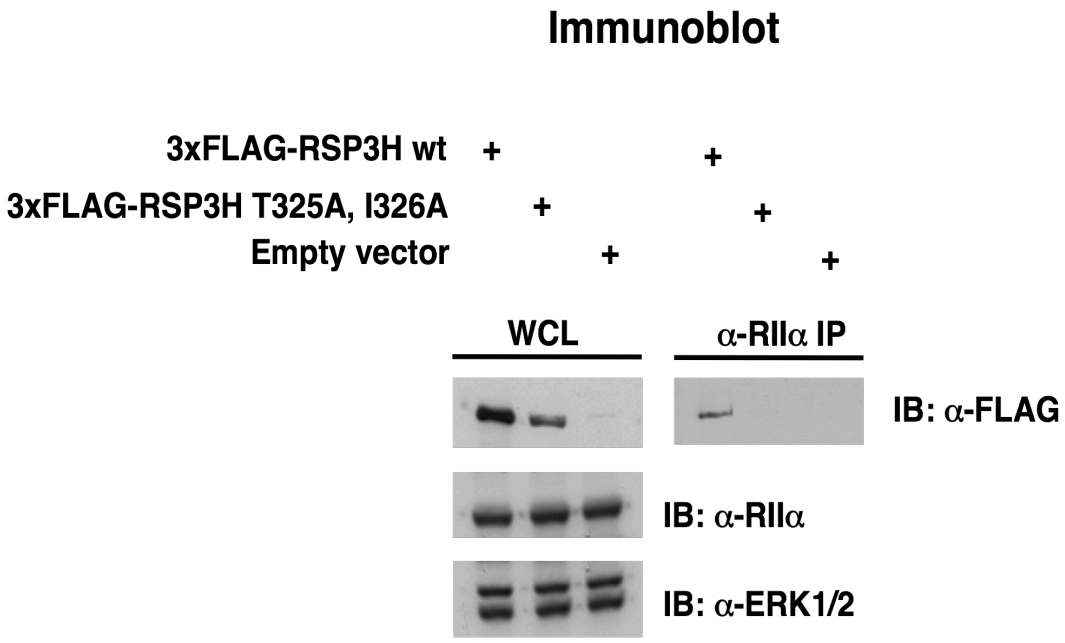

Figure 3.14. RSP3H is an A-kinase anchoring protein. Endogenous RIIα was immunoprecipitated (IP) from the HEK293 cells expressing 3xFLAG-RSP3H wt or the AKAP-defective mutant, T325A, I326A, isoform. Empty vector was used as a negative control. Samples were immunoblotted (IB) with the indicated antibodies. WCL = whole cell lysates. Data represents mean ± SEM. n = 3. The fold change in interaction was determined by normalizing arbitrary units (AU) of intensity (measured by densitometry) of the α-FLAG IP band to the intensity of WCL band and calculating fold difference. T325A, I326A mean value = 0.33. Significance was analyzed using a one-tailed t-test with an obtained p-value = 0.0015.

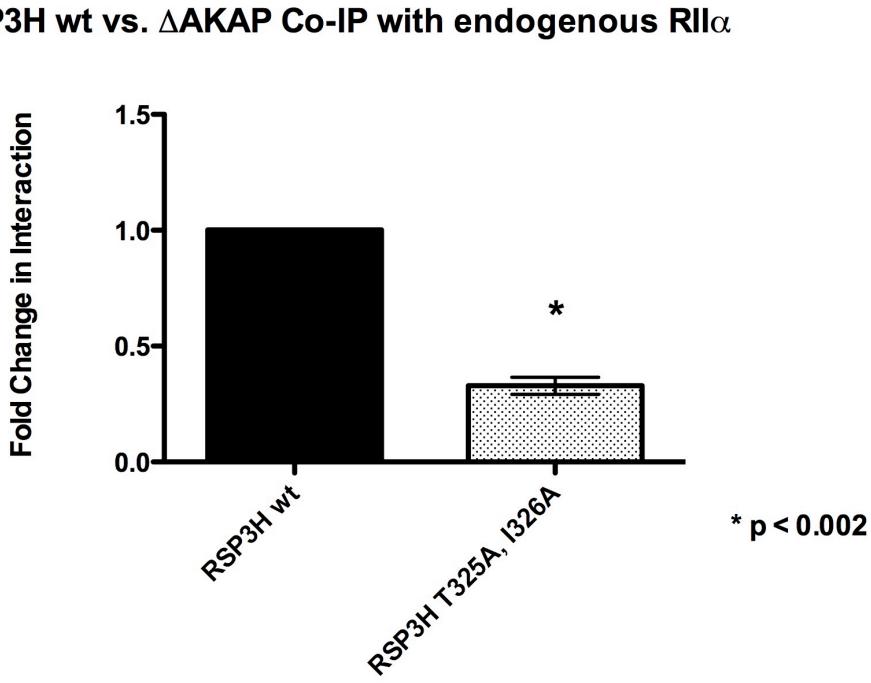

Figure 3.14. RSP3H is an A-kinase anchoring protein (continued).

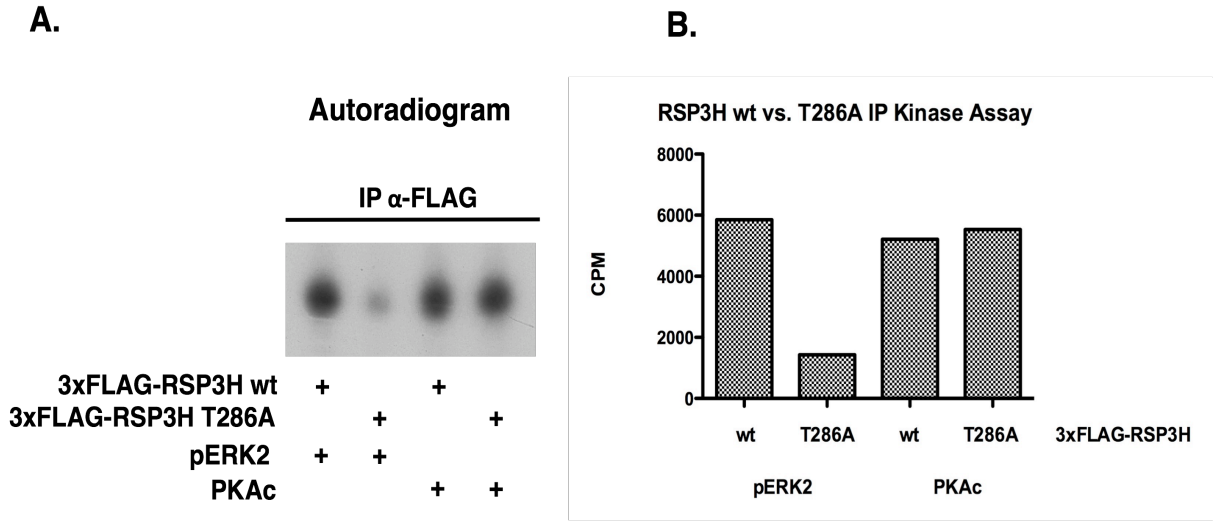

Figure 3.15. PKA phosphorylates RSP3H. Mutation of the major ERK1/2 phosphorylation site does not affect phosphorylation by PKA *in vitro*. **A.** Overexpressed 3xFLAG-RSP3H wt or T286A was immunoprecipitated from HEK293 cells and used as substrate for an *in vitro* IP kinase reaction with recombinant pERK2 (active ERK2) or purified catalytic subunit of PKA (PKAc) as the kinase. **B.** Quantification of ^{32}P-incorporation into RSP3H bands via scintillation counts.

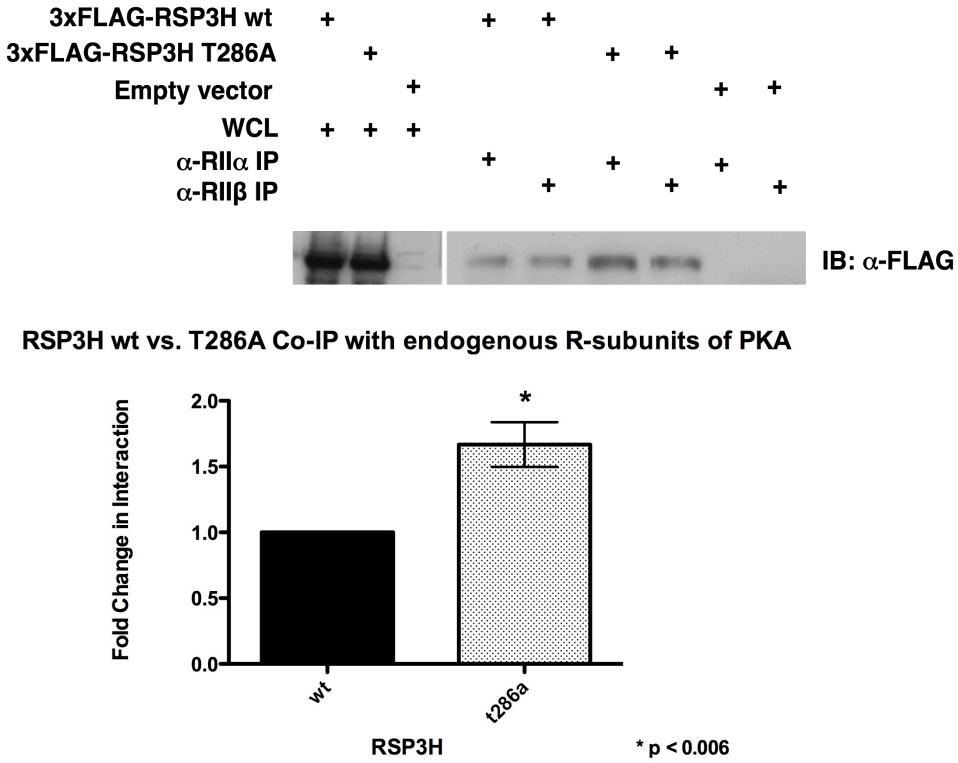

Figure 3.16. RSP3H wt versus T286A co-immunoprecipitation with RIIα. Mutating the major ERK1/2 phosphorylation site increases the amount of RSP3H that co-immunoprecipitates with the R-subunit of PKA. Endogenous RIIα was immunoprecipitated (IP) from the HEK293 cells expressing 3xFLAG-RSP3H wt, T286A, or empty vector as a negative control. Samples were immunoblotted (IB) with the indicated antibodies. WCL = whole cell lysates. Data represents mean ± SEM. n = 6. Fold change in interaction based on normalizing arbitrary units (AU) of intensity of the IP band to the WCL band intensity and measuring fold difference between wt and T286A RSP3H. T286A mean value = 1.8. Significance was determined using a one-tailed t-test with an obtained p-value = 0.0055.

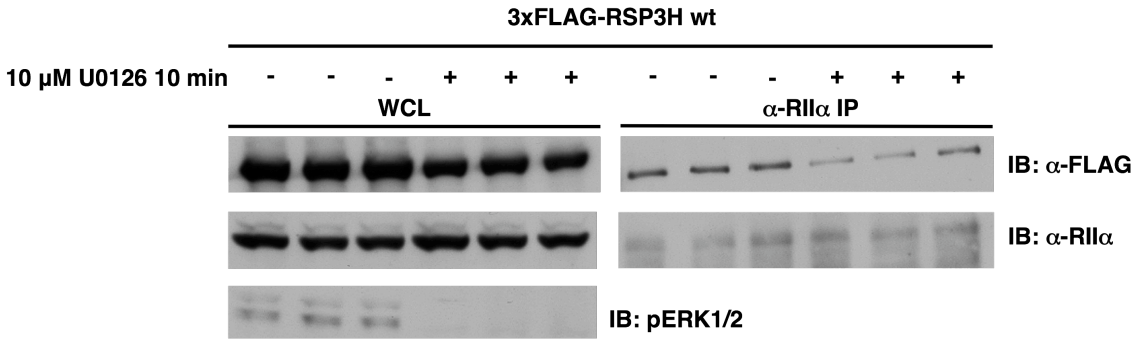

Figure 3.17. RSP3H co-immunoprecipitates with RIIα ± U0126. Inhibiting ERK activity with 10 μM U0126 for 10 minutes decreases the amount of RSP3H that co-immunoprecipitates with endogenous RIIα. Endogenous RIIα was immunoprecipitated (IP) from HEK293 cells expressing wild-type 3xFLAG-RSP3H. Samples were immunoblotted (IB) with the indicated antibodies. WCL = whole cell lysate. Data represents mean ± SEM. n = 3. Fold change in interaction based on the ratio of the intensity (AU) of α-FLAG IP band to the intensity of the WCL band, normalized to the RIIα IP band intensity and measuring fold difference between ± U0126. The mean value for U0126 = 0.325, which indicates a 67.5% reduction in interaction compared to the DMSO-treated control. Statistical significance was analyzed using a two-tailed t-test with an obtained p-value = 0.0139.

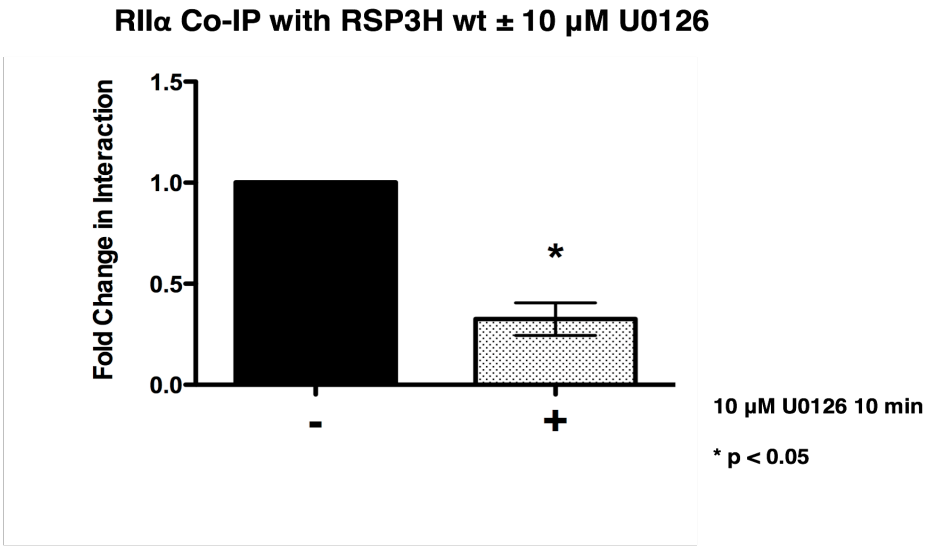

Figure 3.17. RSP3H co-immunoprecipitates with RIIα ± U0126 (continued).

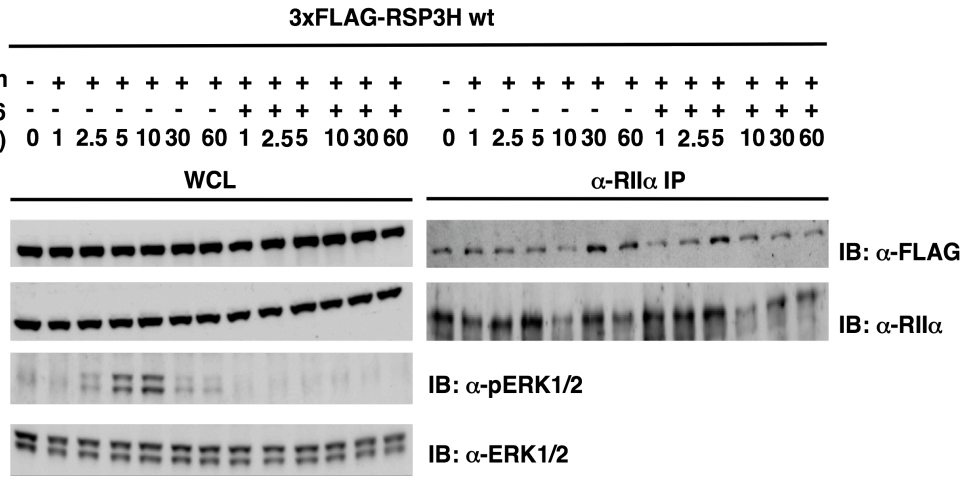

Figure 3.18. RSP3H co-immunoprecipitation with RIIα over a U0126 time course. Inhibiting ERK1/2 activity for 1-60 minutes with 10 μM U0126 diminishes the amount of RSP3H that co-immunoprecipitates with endogenous RIIα. **A.** HEK293 cells expressing 3xFLAG-RSP3H were stimulated with fresh serum-containing medium with 10 μM U0126 or DMSO as a control for the indicated times. RIIα was immunoprecipitated and probed for 3xFLAG-RSP3H in the pulldown. Whole cell lysate represents 5% of the total input used for the immunoprecipitation. Phospho and total ERK1/2 in the WCL were also immunoblotted. **B.** Fold change in interaction of RSP3H RIIα. Values were obtained via ratiometric analysis of the intensity (AU) of **α-**FLAG IP band to the intensity of the WCL band, normalized to the RII**α** IP band intensity and measuring fold difference between ± U0126 over time. Data represent mean ± SEM. n = 3. Statistical significance was analyzed using a two-tailed t-test with obtained p-values as indicated on the graph. **C.** Graph of the pERK1/2 over the given time course ± U0126.

B.

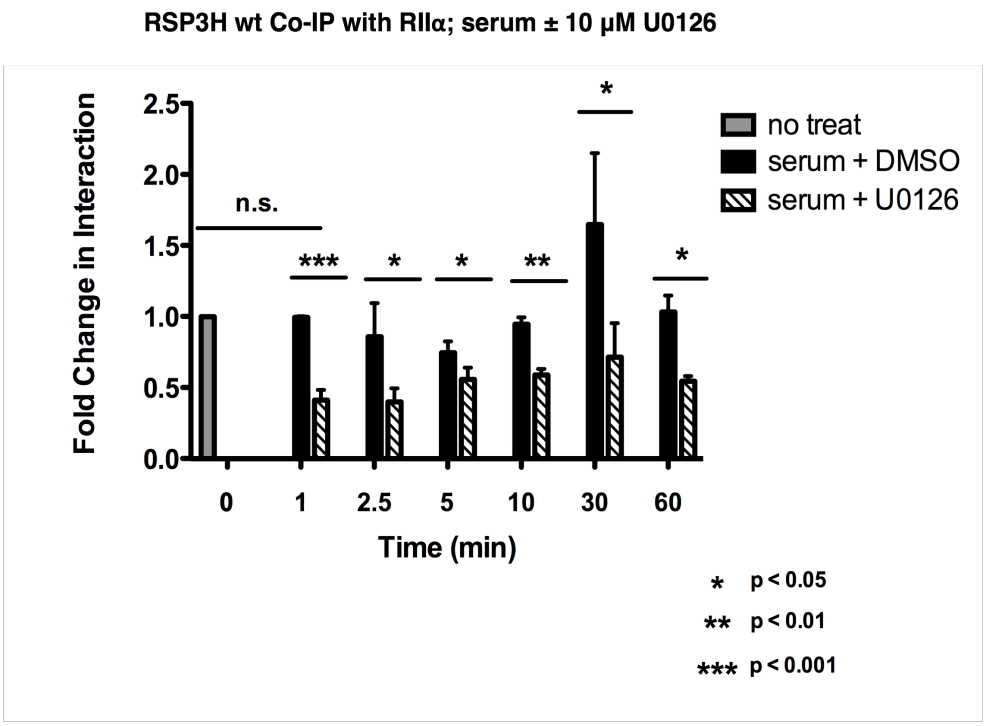

C.

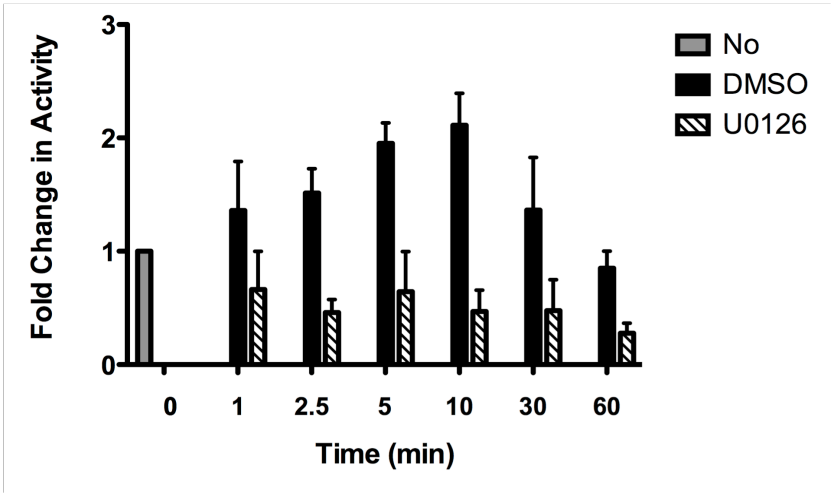

Figure 3.18. RSP3H co-immunoprecipitation with RIIα over a U0126 time course (continued).

Clone	pERK2	ERK2
KIF2A	0.140	-
Synapsin II	0.075	0.005
RSHL2	0.025	0.010

Bait = ERK2-MEK1R4F co-expression plasmid
Prey = mouse brain cDNA library
Controls = ERK2, MEK1R4F alone
MEK1R4F = Δ32-51, S118D, S222D

Liquid β-galactosidase assays of two-hybrid interactions between the hits and pERK2 or ERK2. Values are OD_{420}

Table 3.1. Initial identification of RSP3. A yeast two-hybrid screen was performed to identify interacting proteins that have a higher affinity for the phosphorylated, active form of ERK2 compared to the unphosphorylated, inactive form of ERK2. RSHL2 is the mouse ortholog of RSP3. MEK1R4F is a constitutively active form of MEK1. Other interacting proteins identified include: kinesin heavy chain member 2a (KIF2A), a subunit of the kinesin 2 motor protein and the synaptic vesicle-associated protein, synapsin II.

Time (min)	% Control (U0126/DMSO)	Fold decrease (DMSO/U0126)
1	42	2.4
2.5	47	2.1
5	75	1.3
10	62	1.6
30	43	2.3
60	53	1.9

Table 3.2. Quantification of RSP3H co-immunoprecipitation with RIIα over a U0126 time course.

CHAPTER 4. EXAMINING THE CELLULAR FUNCTIONS OF RSP3/RSP3H

I. Abstract

RSP3 is an established component of the *Chlamydomonas* flagellum and is required for motility (Luck et al, 1977; Piperno et al., 1981). Additionally, RSP3 is suggested to be present only in motile cilia and motile-ciliated cells (e.g. tracheal epithelial and bronchial epithelial cells) (Ostrowski et al., 2002; Wirschell et al., 2008). Primary cilia are immotile and lack the inner microtubule doublet and the radial spoke complexes that connect the outer microtubule ring to the inner pair, apparently obviating the need for RSP3. Interestingly, expression analysis of mRNA suggests RSP3/RSP3H is present in several different cell types that are thought to only contain a single primary cilium. Immunofluorescence staining of primary cilia-containing cells indicates that RSP3/RSP3H has a nuclear punctate distribution and localizes to promyelocytic leukemia (PML) bodies. These findings raise the possibility that RSP3/RSP3H may also have functions outside of cilia in both primary- and motile-ciliated cells.

II. Introduction

RSP3 is one of at least 23 identified radial spoke proteins of the radial spoke complex in the bi-flagellated, unicellular green-algae *Chlamydomonas reinhardtii* (Yang et al., 2006). The radial spoke complex is structurally conserved in motile-ciliated systems with the classical 9+2 axonemal structure – a ring of 9 outer microtubule pairs surrounding an inner pair of microtubules – and connects the outer and inner microtubule doublets analogous to bicycle wheel spokes (Figure 4.1). RSP3 has been shown to localize to motile cilia in mammals (see Figure 2.2) (Ostrowski et al., 2002; Wirschell et al., 2008). Interestingly, RSP3 has a fairly ubiquitous tissue distribution; expressed-sequence tag (EST) and Northern analysis indicates the presence of RSP3/RSP3H mRNA transcript in tissues not thought to contain specialized motile-ciliated cells (Koukoulas et al., 2004) (Table 4.1). Despite EST sequencing and evidence from Koukoulas and colleagues showing expression of RSP3/RSP3H in developing and adult mouse brain, a paucity of information exists regarding the expression (mRNA and/or protein) and function of RSP3 and RSP3H in other tissues and cell-types. Identifying the functional consequence of RSP3/RSP3H expression in cells that do not contain motile cilia will lead to identifying perhaps an evolutionarily conserved role for these proteins in both primary- and motile-ciliated cells, outside of its required function in mediating flagellar motility.

III. Materials and methods

Cell culture and transfection

Mouse inner-medullary collecting duct 3 (IMCD3) cells stably expressing GFP-tagged Somatostatin Receptor 3 were kindly provided by Winfield Sale (Emory University) and were maintained in DMEM:F12 containing 10% FBS and 1% L-glutamine. RPE1 and U2OS cells were cultured similarly to HEK293 cells. HEK293 cells were reverse-transfected with 2 μg of pCMV5 Myc-GFP-RSP3H plasmid using Fugene 6 according to manufacturer's protocol. RPE1 and U2OS cells were transfected with 2-4 μg of plasmid expressing Myc-GFP-RSP3H using Lipofectamine 2000 according to manufacturer's protocol. Cells were manipulated (i.e. fixed, permeabilized, and stained) 36-40 hours post-transfection.

Plasmids and antibodies

Human RSP3H was cloned into a pCMV5 N-terminal Myc-GFP vector for mammalian expression. Mouse monoclonal anti-SAM68 (1:500 dilution) and anti-PML (1:50 dilution; SC-966) were purchased from Santa Cruz Biotechnology (Santa Cruz, CA). Mouse monoclonal anti-splicing factor SC-35 (1:1000 dilution) and anti-acetylated tubulin (1:1000 dilution) were obtained from Sigma-Aldrich (St Louis, MO). Alexa-Fluor® 546 nm-conjugated secondary goat anti-mouse and 546 nm goat anti-rabbit antibodies (1:2000 dilution) were obtained from Invitrogen (Carlsbad, CA). Affinity purified rabbit anti-RSP3 antibody was kindly provided by Winfield Sale (Emory University School of Medicine, Atlanta, GA) and was generated as described in Wirschell et al., 2008.

RNA isolation/purification

RNA was isolated using TRI Reagent® Solution (Applied Biosystems Cat#AM9738) according to manufacturer's protocol. Following RNA isolation,

and prior to cDNA synthesis, total RNA was DNAse treated at 37° C for 15 minutes, and the enzyme was heat inactivated at 75°C for 5 minutes and 70° C for 5 minutes. 10 μg of cDNA was generated using Applied Biosystems High Capacity cDNA archive kit (catalog# 4322171) reverse transcription system and random hexamer oligonucleotides.

Q-PCR

Quantitative PCR was performed with BioRad iTaq SYBR® green supermix with ROX (catalog# 170-8851) on an ABI 7500 DNA Sequence Detection System using standard fluorescent chemistries and thermal cycling conditions specified by the manufacturer: 55° C for 2 minutes, 95° C for 10 minutes for one cycle, an additional 40 cycles at 95° C for 15 seconds, and 55° C for 1 minute. To determine specificity of primers and uniformity of product, a dissociation curve was generated with the following cycling conditions: 57° C for 2 minutes, 95° C for 15 seconds, 55° C for 1 minute, and 95° C for 15 seconds. SYBR green supermix with ROX was purchased from Bio-Rad. 18S rRNA was used as an internal expression control. Primers for human 18s are: forward 5'-GACACGGACAGGATTGACAGATTG-3' and reverse 5'-TGCCAGAGTCTCGTTCGTTATCG-3', generating a 122 bp product. 18s rRNA mouse primers are: forward 5'-TTGACGGAAGGGCACCACCAG-3' and reverse 5'-GCACCACCACCCACGGAATCG-3', generating a 130 bp product. The primers for RSP3/RSP3H include: RSP3H exon 1 (sequence conserved in human and mouse) forward 5'-CGGAACTGCCCGGAGTTC, reverse 5'-TGTAAGTAGTGCCAAGGGC, RSP3H gene intra-exon 1-2 boundary (human and mouse) forward 5'-GCAGCCAGATGAAGAACC, and intra-exon 3 (human and mouse) reverse 5'-CTTGTTTTCTGGCAAGAGCC. RSP3H exon 1 forward and reverse generates a 203 bp product in human and in mouse. Intra-exon 1-2 boundary forward and exon 3 reverse primers generate a 167 bp product. The

human and mouse gene both contain 8 exons. Human exonic sequences correspond to: 1-542 bp (exon 1), 543-630 bp (exon 2), 631-772 bp (exon 3), 773-918 bp (exon 4), 919-1122 bp (exon 5), 1123-1285 bp (exon 6), 1286-1372 bp (exon 7), and 1373-1683 bp (exon 8). Mouse exonic sequences correspond to: 1-494 bp (exon 1), 495-582 bp (exon 2), 583-724 bp (exon 3), 725-870 bp (exon 4), 871-1074 bp (exon 5), 1075-1237 bp (exon 6), 1238-1324 bp (exon 7), and 1324-1551 bp (exon 8).

Qualitative PCR was performed using an Eppendorf Mastercycler gradient PCR machine with the following cycling conditions: 95° C for 30 seconds followed by an additional 30 cycles at 95° C for 15 seconds, 55° C for 1 minute, and 68° C for 1 minute.

Immunofluorescence

IMCD3 cells stably expressing GFP-Somatostatin Receptor 3 were plated onto coverslips in 10cm dishes, grown to 70-80% confluency prior to serum withdrawal (if indicated). After 40 hours, the cells on coverslips were washed with PBS twice and fixed with 2% electron microscopy (EM) grade paraformaldehyde (PFA) (EM Sciences, Hatfield, PA) in PHEM (50 mM PIPES pH 6.9, 50 mM HEPES pH 7.4, 10 mM EGTA, 10 mM $MgCl_2$) for 15-30 minutes at room temperature. Cells were then permeabilized with 0.1% Triton X-100 in PHEM buffer containing 2% paraformaldehyde for 2 minutes at room temperature. The coverslips were subsequently washed with TBS containing 0.05% Tween-20 (TBST) twice, 5 minutes each time. HEK293, RPE1 and U2OS cells were plated onto coverslips and grown to 70-80% confluency prior to fixation. Cells were then washed twice with PBS, and fixed with 2-4% PFA in TBS for 5 minutes at room temperature. Coverslips were then washed twice with TBS for 10 minutes each followed by permeabilization in 0.1-0.5% Triton X-100

in TBS for 5 minutes at 4^{o} C. Coverslips were then washed in TBS twice for 10 minutes each. Prior to incubation with indicated primary antibodies, the cells were pre-hybridized in 1% bovine serum albumin (BSA) in TBS or TBST for 1 hour at room temperature. The primary antibodies in the same solution were incubated with cells overnight at 4^{o} C. On the following day, after washing three times in TBS for 10 minutes each, cells were incubated with Alexa-Fluor®-conjugated secondary antibodies (1:2000 dilution) and with DAPI (1:10000) for 1 hour at room temperature. Cells were then washed three times for 10 minutes each with TBS prior to mounting onto slides with Aqua Poly/Mount (Polysciences Inc., Warrington, PA).

Microscopy and colocalization statistics

Images were taken on a Zeiss LSM510 META LSM microscope with a Chameleon XR NIR laser at 63x magnification under oil immersion (n_a=1.518). Colocalization was determined using the Imaris x64 software colocalization module as described previously (Costes et al., 2004).

IV. Results

RSP3/RSP3H are expressed in primary-ciliated cells

Qualitative and quantitative reverse-transcriptase (RT)-PCR were performed to examine RSP3/RSP3H expression in several cell lines including: HEK293, RPE1, human osteosarcoma (U2OS), rat pheochromocytoma (PC12), and mouse inner-medullary collecting duct 3 (IMCD3) cells as well as primary human pancreatic islets. All of these cells, which are believed to contain a single primary cilium, express RSP3/RSP3H transcript. Products were derived from exon 1 of RSP3H or a shared region in RSP3 and RSP3H, corresponding to a fragment spanning the exon 1-2 boundary and exon 3 of RSP3H mRNA transcript (Figure 4.1). Quantitative analysis of RSP3/RSP3H mRNA indicated that RSP3 mRNA is approximately 250-300-fold more abundant than RSP3H in HEK293 and IMCD3 cells (Figure 4.2). We also generated an antibody against RSP3 to examine endogenous protein expression in the various cell lysates, and the antibody recognizes two prominent bands, most likely RSP3 and RSP3H, indicating that both are expressed (Figure 4.3). The anti-RSP3 antibody also detected two prominent bands, RSP3 and RSP3H, in HEK293 cells overexpressing 3xFLAG-RSP3H. Subsequent experiments with our antibody failed to detect endogenous RSP3/RSP3H protein in cell lysates; the antibody may be unstable or lacking sensitivity in detecting proteins of low abundance, despite being able to detect as little as 10 nanograms of purified His_6-RSP3 via immunoblot (Figure 4.4).

RSP3/RSP3H localize to the nucleus and PML bodies

As primary cilia lack the inner pair of microtubules and radial spoke complexes, we examined the intracellular localization of RSP3/RSP3H using an affinity-purified anti-RSP3 antibody as well as overexpressed Myc-GFP-RSP3H. IMCD3

cells stably expressing GFP-tagged Somatostatin Receptor 3, which is enriched in the primary cilium, displayed a punctate nuclear staining pattern of endogenous RSP3/RSP3H (Figure 4.5). Furthermore, overexpressed Myc-GFP-RSP3H localized to nuclear punctae in HEK293 cells. To visualize primary cilia, HEK293 cells were treated with 30μM nocodazole, a microtubule-depolymerizing agent, for 2.5 hours to disrupt the abundant cytosolic acetylated tubulin, leaving only the stabilized microtubule structures (e.g. primary cilia) intact (Figure 4.6). No RSP3/RSP3H signal was observed in the primary cilium. The ambiguity in whether the anti-RSP3 antibody recognizes RSP3 or RSP3H, or which species is predominantly expressed endogenously, necessitates that RSP3/RSP3H is referred to singularly.

Next, we sought to identify the nuclear sub-compartment to which RSP3/RSP3H localizes. RPE1 and U2OS cells expressing Myc-GFP-RSP3H were stained with antibodies against markers of various sub-nuclear structures including: splicing factor 35 (SC35; a nuclear speckle marker), Src-associated in mitosis (SAM68 bodies), and PML (PML bodies) (Figure 4.7; Figure 4.8). Localization of Myc-GFP was examined as a control against the potential artifact in the patterning of Myc-GFP-RSP3H. Vector-transfected and Alexa-Fluor® 546 nm goat anti-mouse secondary antibody stainings alone were also performed as negative controls. Myc-GFP-RSP3H punctae did not overlap with SC35-stained nuclear speckles or anti-SAM68 stained bodies in RPE1 cells. However, Myc-GFP-RSP3H displayed an apparent overlap in punctae with anti-PML-labeled PML bodies in U2OS cells (Figure 4.9). The Pearson's correlation coefficient of co-localization of Myc-GFP-RSP3H and PML was 0.40, indicating significantly positively correlated signals. In contrast, the correlation coefficient for Myc-GFP, which was diffuse throughout the cell, and PML was 0.089.

Identifying potential interacting partners for RSP3H

Concomitant mass-spectrometric analysis of proteins co-immunoprecipitated with 3xFLAG-RSP3H was performed to gain insight to potential interacting partners and towards the cellular function of RSP3H in cells with primary cilia. 3xFLAG-RSP3H was immunoprecipitated from three 100% confluent 10cm diameter plates of HEK293 cells (approximately $6x10^7$ cells). One milligram of total protein was used as input for each immunoprecipitation, and the subsequent fractions were pooled, loaded onto a 12% SDS-polyacrylamide gel and stained with colloidal Coomassie blue (Figure 4.10). Bands were compared between the 3xFLAG-RSP3H- and vector-transfected lanes, and the differential bands only present in the 3xFLAG-RSP3H sample were cut out of the gel, subjected to trypsin digest and analyzed for fragment composition using tandem MS/MS analysis and MASCOT database comparison/scoring. MASCOT gives a probability-based score, and hits with scores of 150 or higher are considered high confidence (Table 4.3). Certain hits of interest with lower scores, such as importin 7 and 8, exportin 1 (CRM-1), nucleolin, and transportin (karyopherin β2) were re-analyzed and verified as significant.

V. Discussion

These data indicate that RSP3/RSP3H, once thought to be simply a component of motile cilia, is also present in cells that only have a single primary cilium. Primary cilia are structurally distinct from motile cilia in that they lack the central microtubule pair and the radial spoke apparatuses that connect the outer doublet ring of microtubules to the inner pair. The lack of these components renders primary cilia immotile in the typical sense of flagellar beating, but they are still subject to shear and bending forces due to convective fluid flow in the extracellular space.

The presence of RSP3/RSP3H transcript in primary-ciliated cells is quite intriguing - suggestive of a novel function in these cells in addition to regulating motility of the cilium in motile-ciliated or flagellated cells. RSP3 appears to be more abundant than RSP3H at the message level, which could be due to stability or tighter regulation of RSP3H transcript in certain cellular contexts. Whether RSP3/RSP3H mRNA levels correlate with protein expression remains to be determined. The differential expression levels could lead to the identification of mechanisms that regulate RSP3H expression in response to some change in cell-state.

Generally, cilia components are upregulated at the transcript and protein levels during cilia formation, where cilia formation is coupled to centriolar duplication and cell cycle progression. The primary cilium emerges and elongates during G_1 and is maintained through S-phase as the centrioles duplicate (Sorokin, 1962; Pan and Snell, 2007). During G_2/M, the cilium begins to shorten, and components are resorbed and typically degraded (Rieder et al., 1979). Preliminary experiments examining the link between RSP3/RSP3H expression and cell cycle or confluency

state have been performed, and it appears, at least in HEK293 cells, that RSP3/RSP3H transcript levels increase as cells are induced into a quiescent state. We observe an increase in mRNA transcript of RSP3/RSP3H upon serum withdrawal, cellular quiescence and subsequent enrichment of ciliated cells in the population, but correlating ciliary emergence and RSP3/RSP3H levels as well as causality, if any, needs to be pursued further.

We have been hindered by an inability to detect endogenous protein via immunoblotting and can only ascertain, albeit indirectly, cellular effects based on measuring changes in mRNA transcript of RSP3/RSP3H or modulating RSP3/RSP3H protein through overexpression studies. We previously generated antisera against recombinant RSP3 and have tested it on several different cell lines. While the antibody recognizes as little as 10 nanograms of purified protein, definitive RSP3/RSP3H bands are not apparent in immunoblots. This is further obscured by an inability to get sufficient knockdown of RSP3/RSP3H with dsRNA oligonucleotides, at least by measuring total transcript. Moreover, dsRNA knockdown may cause translational repression of RSP3/RSP3H message rather than mRNA degradation and show change in RSP3/RSP3H message that under-represents the loss of protein. Additionally, the anti-RSP3 antibody used for immunofluorescence does not recognize a band via immunoblotting, and a non-affinity purified version of the antibody cross-reacts with a component in the serum that migrates at the same molecular weight as RSP3, thus obscuring any evident endogenous protein. We are currently exploring lentiviral-based short-hairpin RNA (shRNA)-mediated silencing, allowing stable integration of the shRNA into the genome and the ability to generate a stable RSP3/RSP3H knockdown cell line. We are also generating antibodies against peptides derived from the N-terminus of RSP3H and ones shared by both RSP3 and RSP3H.

Immunofluorescence staining with an antibody against endogenous RSP3/RSP3H indicated a nuclear punctate distribution in IMCD3 cells, and overexpressed GFP-tagged RSP3H localized to nuclear punctae in a similar fashion. A speckled pattern in the nucleus suggests possible localization to a diverse complement of sub-nuclear compartments, which include: splicing speckles, PML bodies, telomeric structures, Cajal bodies, and Gems, to name a few. These compartments are highly dynamic and are implicated in a multitude of processes such as pre-mRNA processing, splicing and mRNA export, RNA metabolism and DNA damage repair. Based on clues provided from the nature of the punctae and our mass-spectrometric analysis of putative interacting partners, we examined likely candidates of nuclear domains. SC35 is a pre-mRNA splicing factor that is a component of nuclear speckles - organizational sites of proteins involved in pre-mRNA splicing, transcriptional regulation and mRNA export (Spector, 2001). RSP3H punctae did not overlap with SC35 nuclear speckles. Although not much is known about their function, SAM68 nuclear bodies are thought to be involved in RNA metabolism (Spector, 2001). The SAM68 signal was diffuse throughout the nucleus; thus, it was difficult to discern whether there was any compartmental co-localization with GFP-RSP3H. However, we found Myc-GFP-RSP3H localized to PML bodies.

Mammalian nuclei typically contain 10-30 PML foci, which range in size from 0.2-1μm and are functionally and compositionally heterogeneous (Bernardi and Pandolfi, 2007). Although the capacity in which they affect diverse cellular processes is not clearly established, PML bodies have been implicated in a variety of tumor suppressive functions including: transcriptional regulation, telomere maintenance, inhibiting cell proliferation, induction of cellular senescence and/or apoptosis, DNA damage repair, and translational repression (Borden, 2002; Bernardi et al., 2006; Trotman et al., 2006; Bernardi and Pandolfi, 2007; Potts and

Yu, 2007). PML is modified post-translationally by the small ubiquitin-like modifier 1 (SUMO-1) protein, an 11kDa protein that generally regulates subcellular localization, protein stability, and activity of certain transcription factors, and is required for PML body formation (Ishov et al., 1999; Geiss-Friedlander and Melchior, 2007). Sumoylation also controls the recruitment of several transcriptional coactivators and repressors, such as the histone acetyltransferase CREB binding protein (CBP) and Daax respectively, to PML bodies (Doucas et al., 1999; Boisvert et al., 2001; Best et al., 2002). Nascent RNA has been shown to accumulate to the periphery of PML bodies, further supporting that these foci somehow modulate gene expression and may serve as sites of active transcription (Boisevert et al., 2000). PML bodies have also been suggested to be nuclear aggregation sites of overexpressed or foreign proteins or transient storage compartments for proteins, facilitating their post-translational modifications and localization to sites of action (Borden, 2002; Bernard and Pandolfi, 2007; Borden, 2008). Overexpressed Myc-GFP-RSP3H could localize to these structures as an artifact of exogenous manipulation, however staining of endogenous RSP3/RSP3H and mass-spectrometric identification of several nuclear proteins is highly suggestive that RSP3/RSP3H reside and possibly function in the nucleus. ERK1/2 are known to phosphorylate PML at least *in vitro*, influence PML sumoylation and mediate arsenic trioxide (As_2O_3)-induced apoptosis in cells (Hayakawa and Privalsky, 2004). With the potential roles of ERK1/2 and PKA at PML bodies, it is not inconceivable to hypothesize that RSP3/RSP3H may scaffold and regulate ERK1/2 and/or PKA function at these nuclear domains.

Mass-spectrometric analysis of co-precipitated bands in the 3xFLAG-RSP3H pull-down yielded several interesting putative interacting partners and potential modifiers. Of interest are those that have defined nuclear roles or are involved in

modulating gene expression at any level. Figure 4.11 lists these proteins grouped by function, which include: proteins within the RNA helicase family, RNA-binding proteins, those involved in pre-mRNA splicing, mRNA export, DNA maintenance and repair, epigenetic regulation of transcription, structural nuclear proteins, translational-regulatory proteins, and proteins that mediate nuclear import and export.

One of the proteins identified, importin 7, participates in nuclear import of ERK (James et al., 2007). Another, transportin (karyopherin β2) is a nuclear import factor that recognizes P-Y motifs within substrates, although the requirement for tyrosine is not strictly conserved (Suel et al., 2008). Characterizing RSP3/RSP3H nuclear import will be enabled with the recent development of a specific inhibitor of karyopherin β2. ADAR1, a double-stranded RNA-binding protein, is imported into the nucleus by karyopherin β2 (Fritz et al., 2009). Also identified was exportin 1. Also known as CRM-1, exportin 1 mediates the nuclear export of proteins. RSP3/RSP3H contains several basic residue-rich regions consistent with monopartite or bipartite nuclear localization signals (NLSs). Additionally, the presence of a leucine-rich, hydrophobic repeat suggests the possibility of a nuclear export signal (NES). The presence of such sequences in RSP3/RSP3H needs to be analyzed through mutagenesis, *in vitro* binding and cell-imaging studies.

All three bands contained RSP3H, suggesting possible, multiple post-translational modifications. Indeed, SUMO-1 and ubiquitin peptides were identified in the samples. Poly-ubiquitin chains typically represent a signal for proteasomal degradation of modified substrates (covalently ubiquitylated on a lysine within the substrate). Mono-, multi-mono-ubiquitylation, or differently conjugated poly-ubiquitin can regulate cellular processes (e.g. transcription, DNA repair, cell-

cycle progression, and receptor trafficking) independently of proteolytic degradation, through modulating protein-protein interactions, enzymatic activity or localization of certain proteins (Haglund and Dikic, 2005). Sumoylation typically occurs on lysines within a ϕ-K-X-E consensus motif, where ϕ denotes a hydrophobic residue, however this motif is fairly degenerate except for the invariant, covalently modified lysine (Rodriguez et al., 2001). RSP3/RSP3H do not contain such a consensus sequence, but this does not necessarily eliminate the possibility of sumoylation. Identifying whether RSP3/RSP3H are sumoylated and/or ubiquitylated, the site(s) on which they are modified, and the consequence of these modifications may provide clues to the functional cellular regulation and roles of RSP3/RSP3H.

While some of the mass-spectrometrically identified proteins are typically considered co-immunoprecipitating artifacts in a pull-down of overexpressed protein (e.g. heat shock protein 70 (HSP70) and the DEAD-box helicases), the confluence in function of many of the identified proteins lends credence towards a possible role for RSP3/RSP3H in these cellular processes. Accordingly, all of the potential interacting partners need to be individually verified through co-immunoprecipitation and *in vitro* binding studies.

Localization of RSP3/RSP3H to compartments other than cilia in motile-ciliated cells requires more extensive examination. Preliminary fluorescent staining with anti-RSP3 antibody on mouse lung histological sections has not provided sufficient enough resolution to examine localization outside of the motile cilia of the airway epithelia. These and continual experiments in cells containing primary cilia will elucidate potential non-canonical functions for RSP3/RSP3H beyond the motile cilium. Examining localization of RSP3/RSP3H by ERK1/2 has proved difficult, as fluorescent protein-tagged constructs (e.g. N- and C-terminal GFP,

dsRed, CFP) of the ERK1/2 phosphorylation-dead mutant, RSP3H T286A, do not express in the cell. Phosphorylation by ERK1/2 may regulate protein stability and/or localization of RSP3/RSP3H. As RSP3 transcript is more abundant than RSP3H, perhaps RSP3 protein is similarly more abundantly translated or has a longer half-life than RSP3H, which could be produced in relatively low quantities and/or turned over rapidly. GFP-RSP3 and subsequent mutants will be studied to overcome this possibility; once the necessary reagents are available, as will endogenous RSP3/RSP3H.

Finally, recent evidence has linked PKA and ERK1/2 to post-transcriptional mRNA events including pre-mRNA splicing and processing, thus leading to the question of how these kinases are coordinated at these sites of action (Kvissel et al., 2007; Fujita et al., 2008). RSP3/RSP3H may scaffold ERK1/2 to nuclear sub-domains and serve as a node of convergence facilitating cAMP-dependent and PKA-mediated influence upon ERK1/2 downstream signaling and vice versa. Alternatively, RSP3/RSP3H may coordinate ERK1/2- and PKA-dependent regulation of nuclear processes from transcription to mRNA processing and/or export.

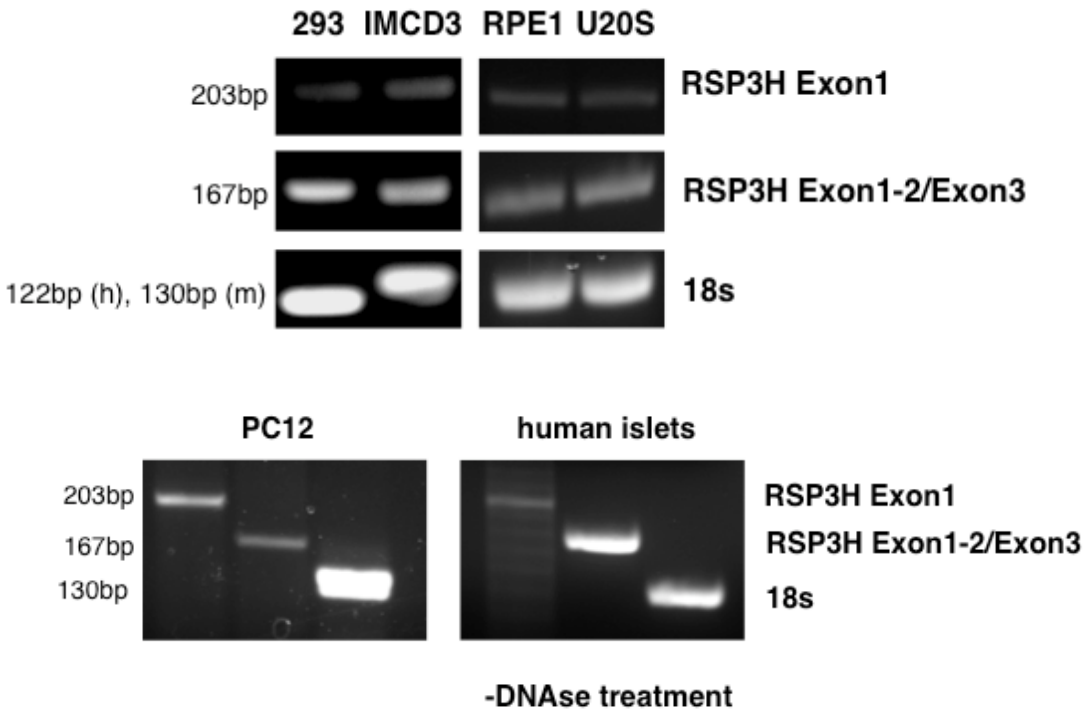

Figure 4.1. RSP3/RSP3H mRNA is present in non-motile-ciliated cells. Qualitative RT-PCR indicates the presence of RSP3/RSP3H transcript in primary-ciliated cells (i.e. those not thought to contain motile cilia). Products were generated using primers designed to the 5' extension of exon 1 in RSP3H (not conserved in RSP3) as well as intra-RSP3/RSP3H with the forward primer spanning the exon 1-2 boundary to ensure product was derived from mRNA and not genomic sequence. Harvested total RNA was also treated with DNAse prior to cDNA generation except for the primary human islet sample. As a result, the exon 1 product (lane 1 in the human islet panel) shows laddering indicative of genomic DNA contamination.

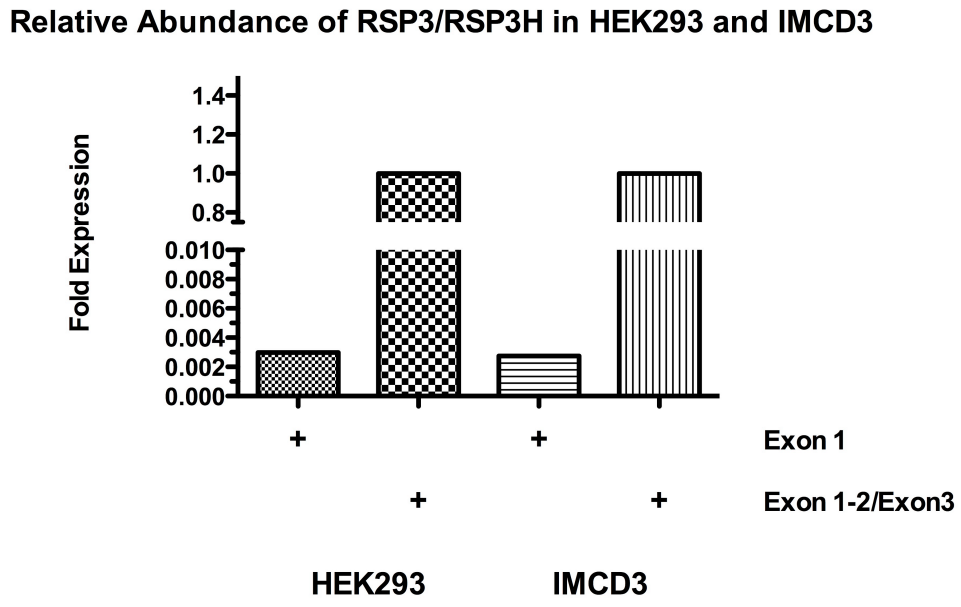

Figure 4.2. RSP3 mRNA is more abundant than RSP3H in HEK293 and IMCD3 cells. Q-PCR was performed on cells grown to 70-80% confluent prior to total RNA harvest. Product generated from primers to RSP3/RSP3H shared sequence is 250-300 fold more abundant than product generated from the 5' end of RSP3H.

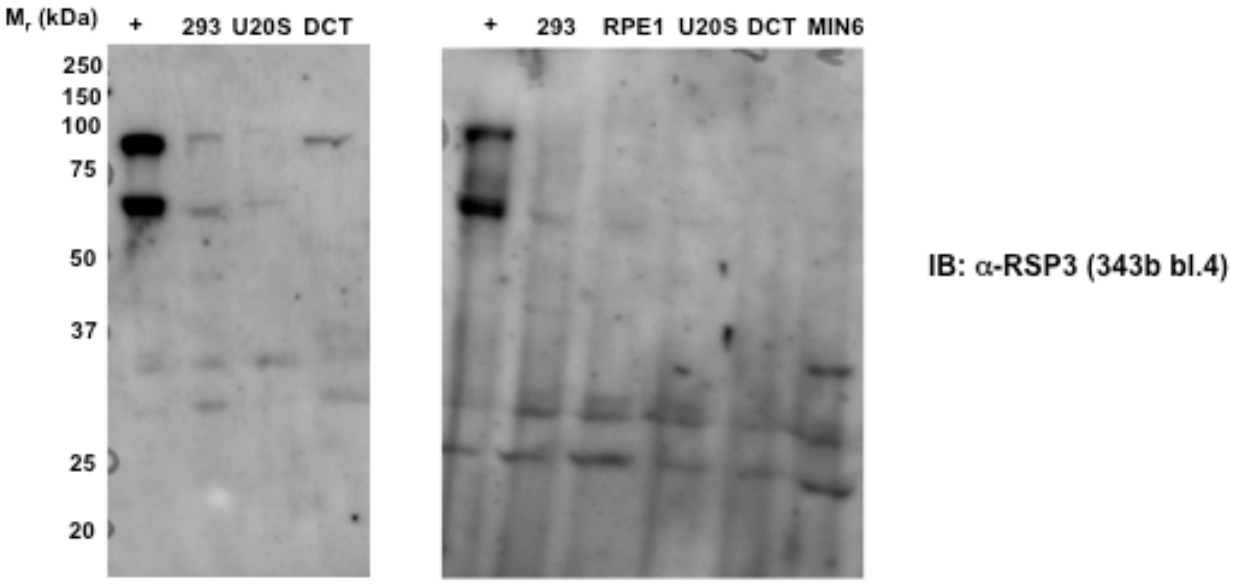

Figure 4.3.a. Endogenous RSP3/RSP3H protein is present in several primary-ciliated cell lines. Immunoblot of various cell lysates using rabbit antiserum against RSP3 to visualize endogenous protein. HEK293 cells overexpressing 3xFLAG-RSP3H was used as a positive control (+). DCT = mouse distal convoluted tubule cells; MIN6 = mouse insulinoma β cells. 343b bleed (bl) 4 indicates the provenance of the antiserum.

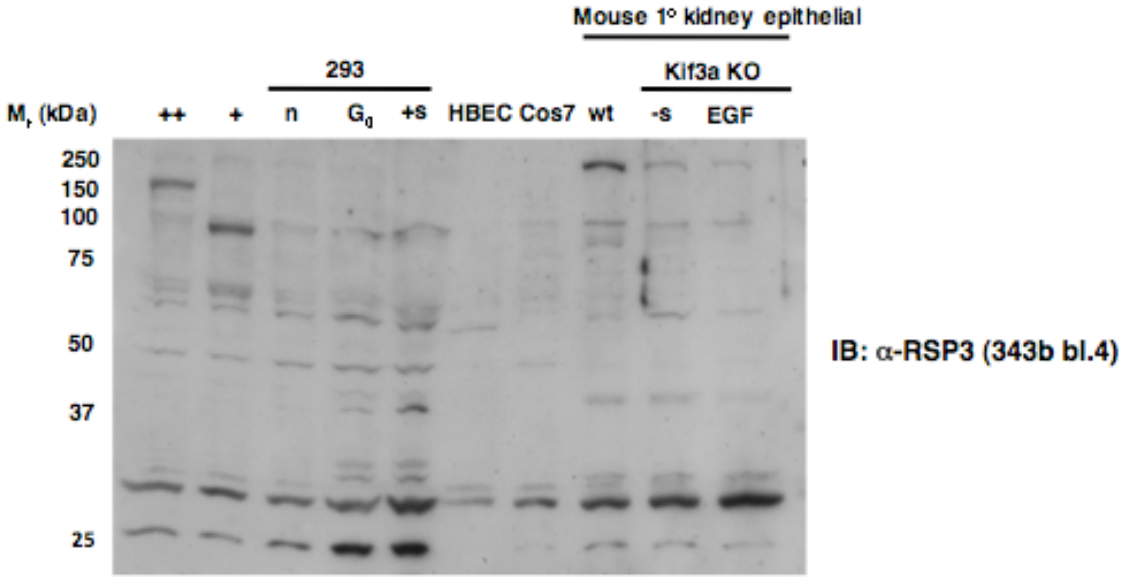

Figure 4.3.b. Endogenous RSP3/RSP3H protein is present in several primary-ciliated cell lines (continued). Immunoblot of various cell lysates using rabbit antiserum against RSP3 to visualize endogenous protein. Positive controls include: HEK293 overexpressing Myc-GFP-RSP3H (++) and HEK293 overexpressing 3xFLAG-RSP3H (+). HEK293 cells were also cultured in normal medium (n), serum starved for 48 hours to induce cell-growth arrest (G_0), or supplemented with serum (s). HBEC = human bronchial epithelial cells. Cos7 = African green monkey kidney fibroblast cells. Wild-type (wt) and Kif3A knockout (KO) primary mouse kidney epithelial cells were obtained from the Igarashi laboratory. Knockout cells were either grown in serum-free medium or stimulated with 10 ng/mL EGF for 10 minutes.

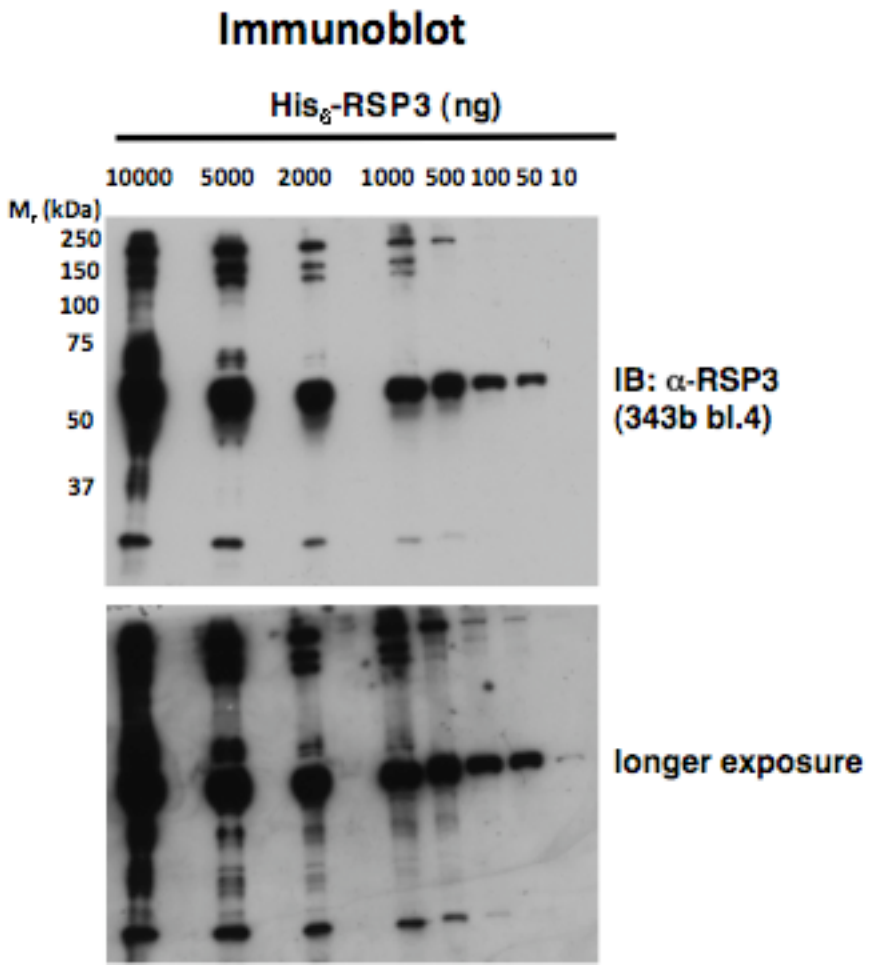

Figure 4.4. . Immunoblot of titrated amounts of purified His_6-RSP3 using rabbit antiserum against RSP3.

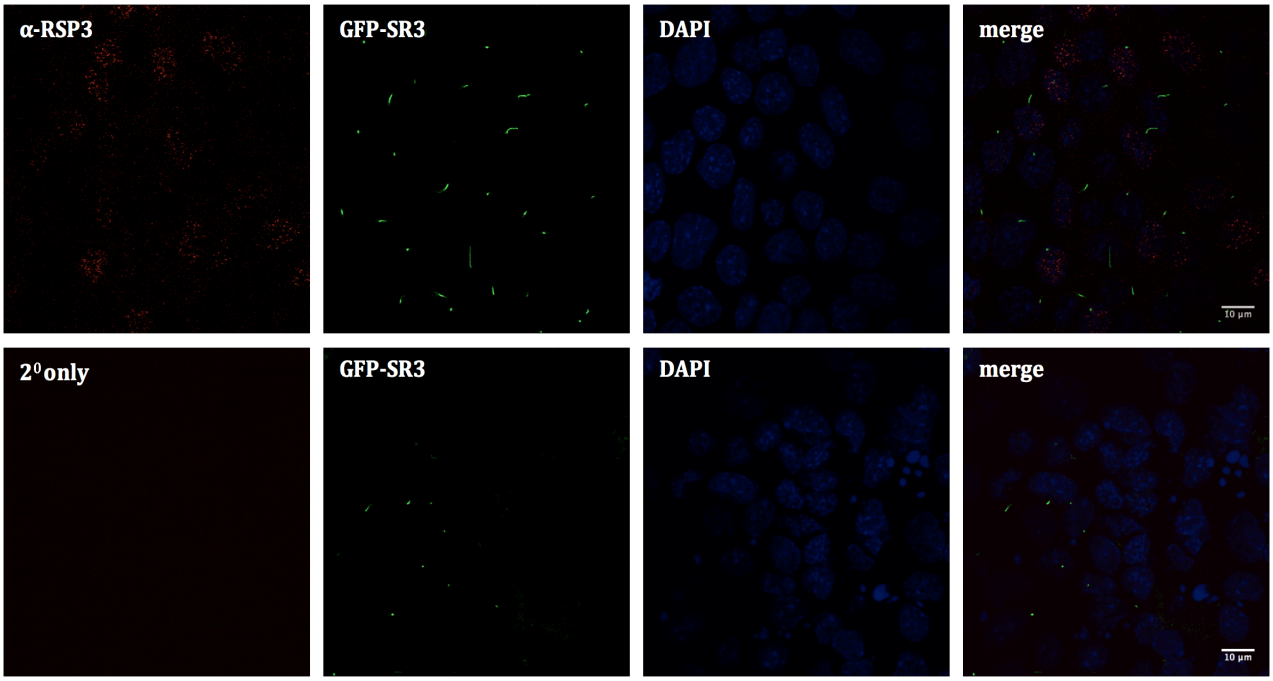

Figure 4.5.a. Endogenous RSP3/RSP3H localizes to the nucleus in GFP-SR3 IMCD3 cells. IMCD3 cells stably expressing GFP-Somatostatin Receptor 3 (SR3) were stained with anti-RSP3 antibody (red). GFP-SR3 (green) localizes to the primary cilium, whereas RSP3/RSP3H displayed a punctate nuclear pattern (red). Nuclei were visualized with the DNA-dye, DAPI (blue). 2^{o} only = cells stained with Alexa-Fluor® 546 nm goat anti-rabbit alone as a negative control. Images were taken at 63x under oil immersion on a Zeiss LSM510 confocal microscope. Scale bar = 10 μm.

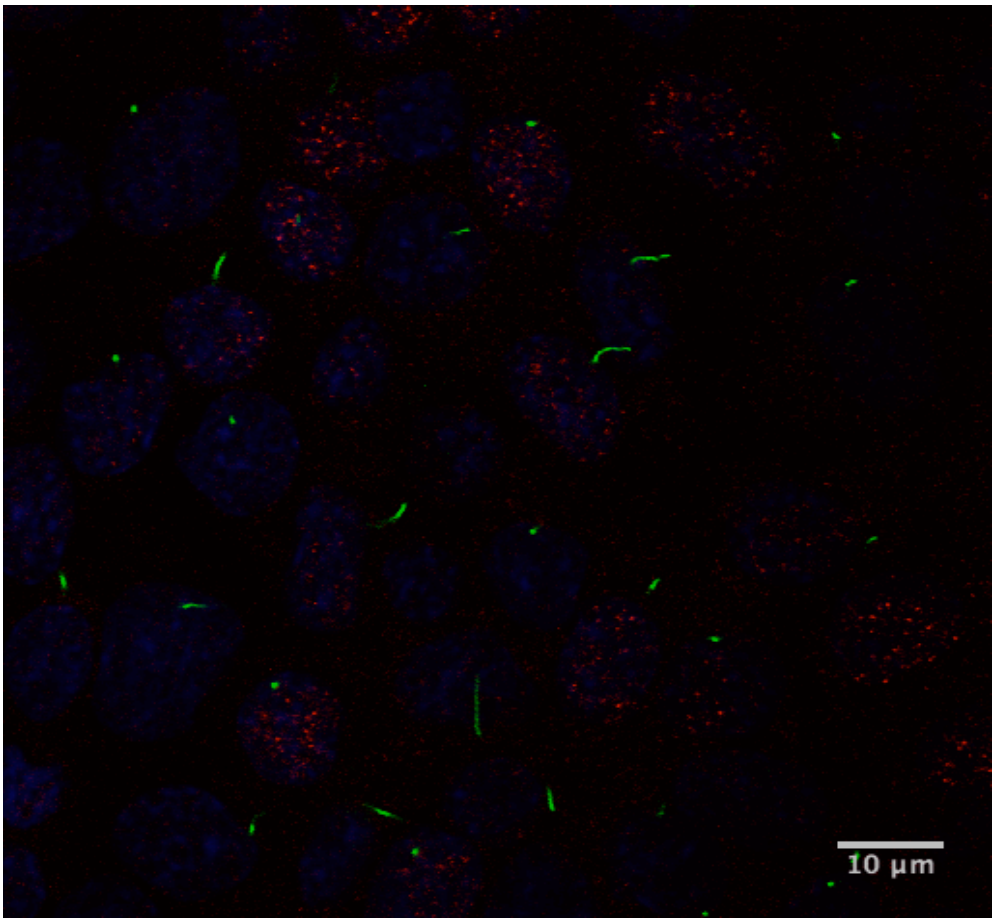

Figure 4.5.b. Endogenous RSP3/RSP3H localizes to the nucleus in GFP-SR3 IMCD3 cells (continued). Enlarged merged image of red, green and blue channels displaying anti-RSP3 staining, GFP-SR3, and DAPI respectively.

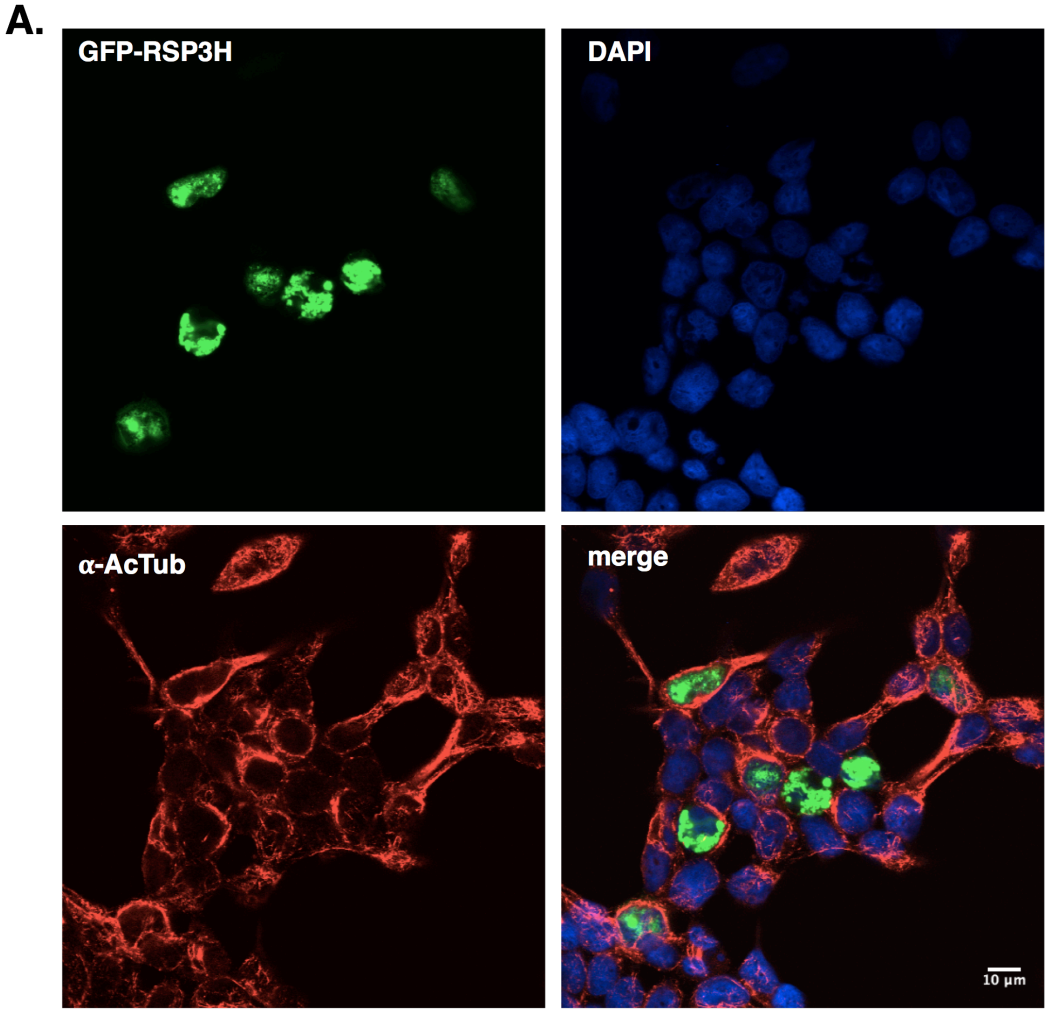

Figure 4.6.a. Myc-GFP-RSP3H localizes to the nucleus in HEK293 cells. HEK293 cells expressing Myc-GFP-RSP3H were grown on collagen-coated coverslips prior to fixation and staining **A.** Untreated cells. **B.** Cells were treated with 30 μM nocodazole for 2.5 hours to disrupt cytosolic microtubule structures, leaving stabilized microtubules intact (e.g. primary cilia). Cells were then fixed in 2% paraformaldehyde, permeabilized with 0.1% Triton X-100 and stained with anti-acetylated tubulin (red), which is enriched in the primary cilium. Scale bar = 10 μm.

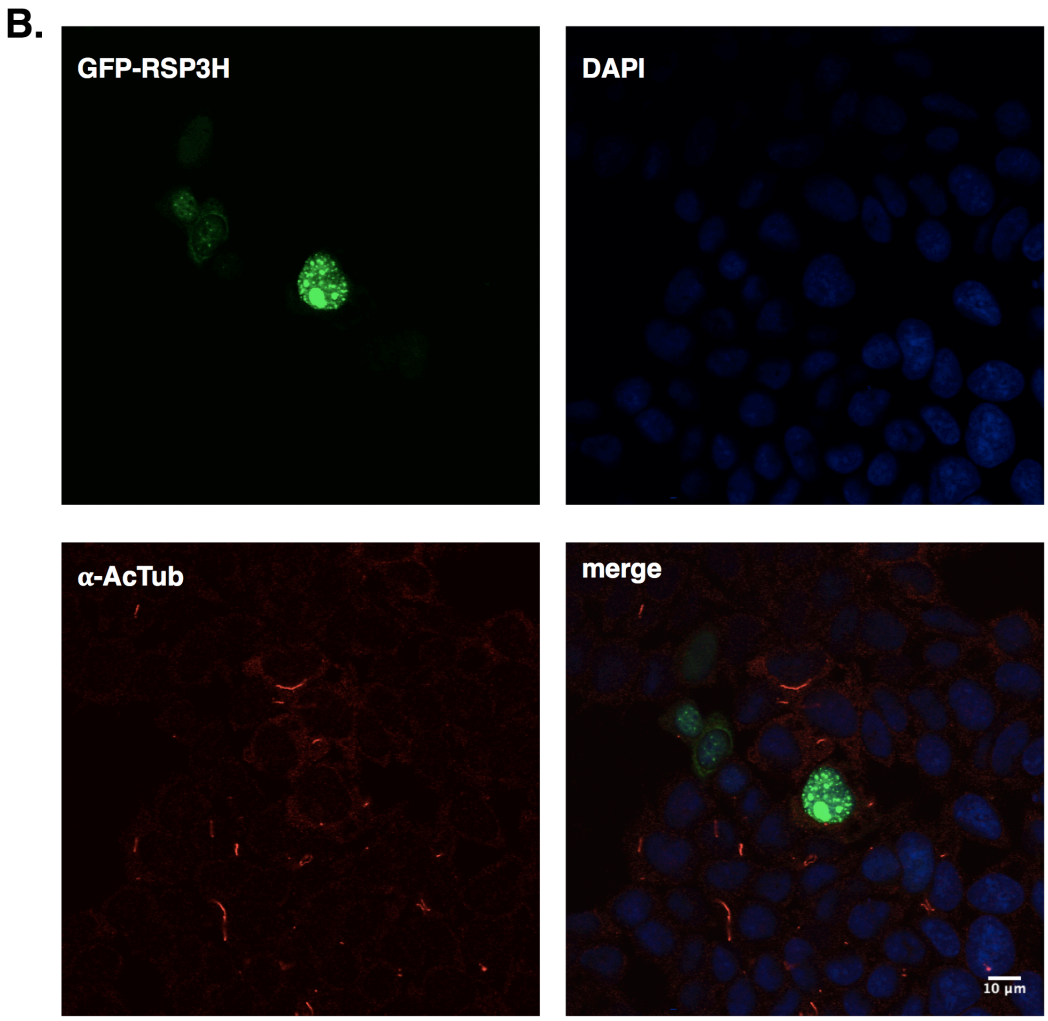

Figure 4.6.b. Myc-GFP-RSP3H localizes to the nucleus in HEK293 cells (continued). Nocodazole-treated cells. Scale bar = 10 μm.

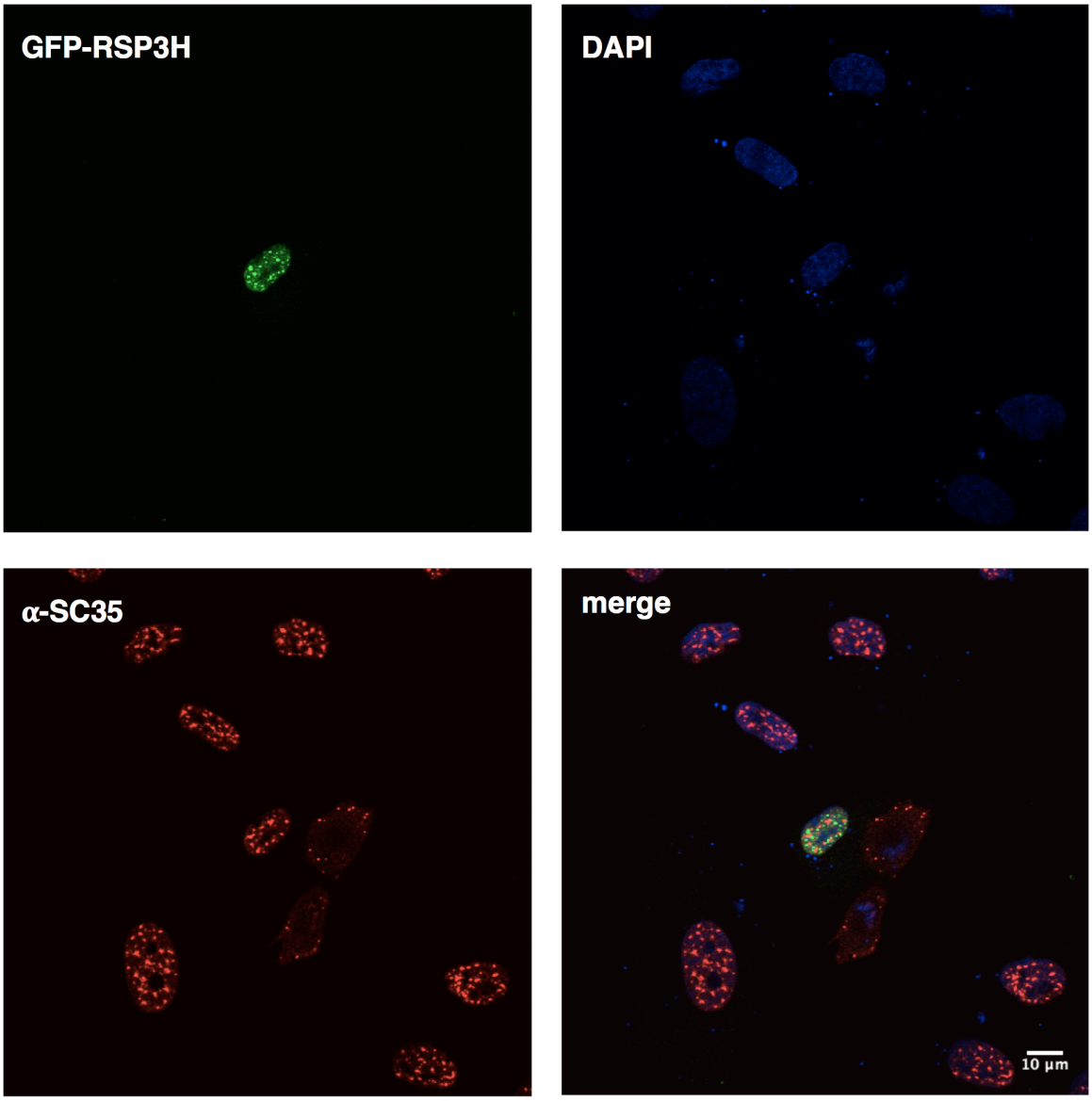

Figure 4.7.a. Myc-GFP-RSP3H has a nuclear punctate distribution in RPE1 cells. RPE1 cells expressing Myc-GFP-RSP3H were grown to 70-80% confluency and then fixed with 4% paraformaldehyde, followed by permeabilization with 0.5% Triton X-100. Cells were stained with mouse anti-SC35, a pre-mRNA splicing factor enriched in nuclear speckles, Alexa-Fluor® 546 nm goat anti-mouse (red), and DAPI (blue). Scale bar = 10 μm.

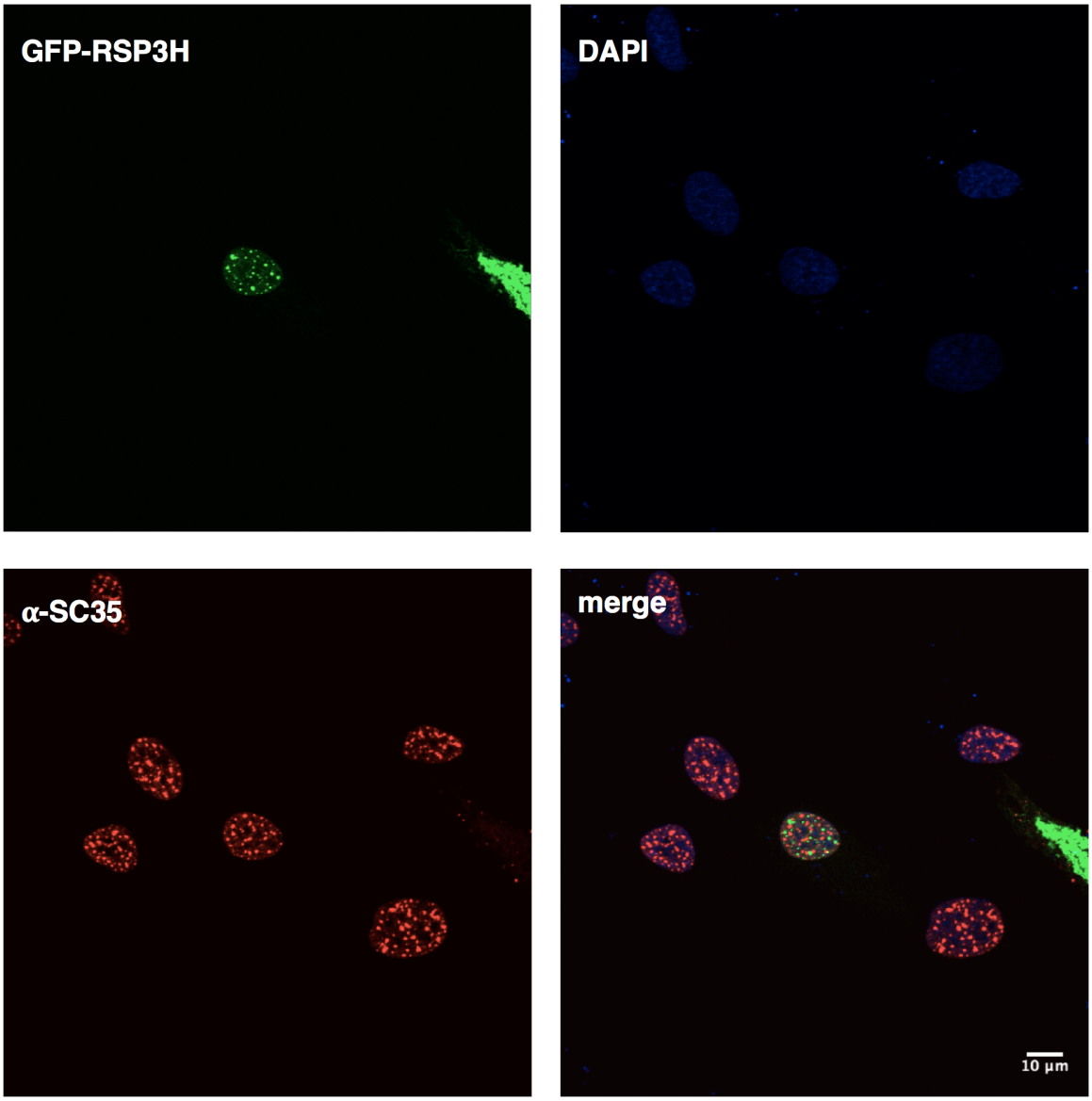

Figure 4.7.b. Myc-GFP-RSP3H has a nuclear punctate distribution in RPE1 cells (continued). Image of another cell expressing Myc-GFP-RSP3H stained with α-SC35 and DAPI.

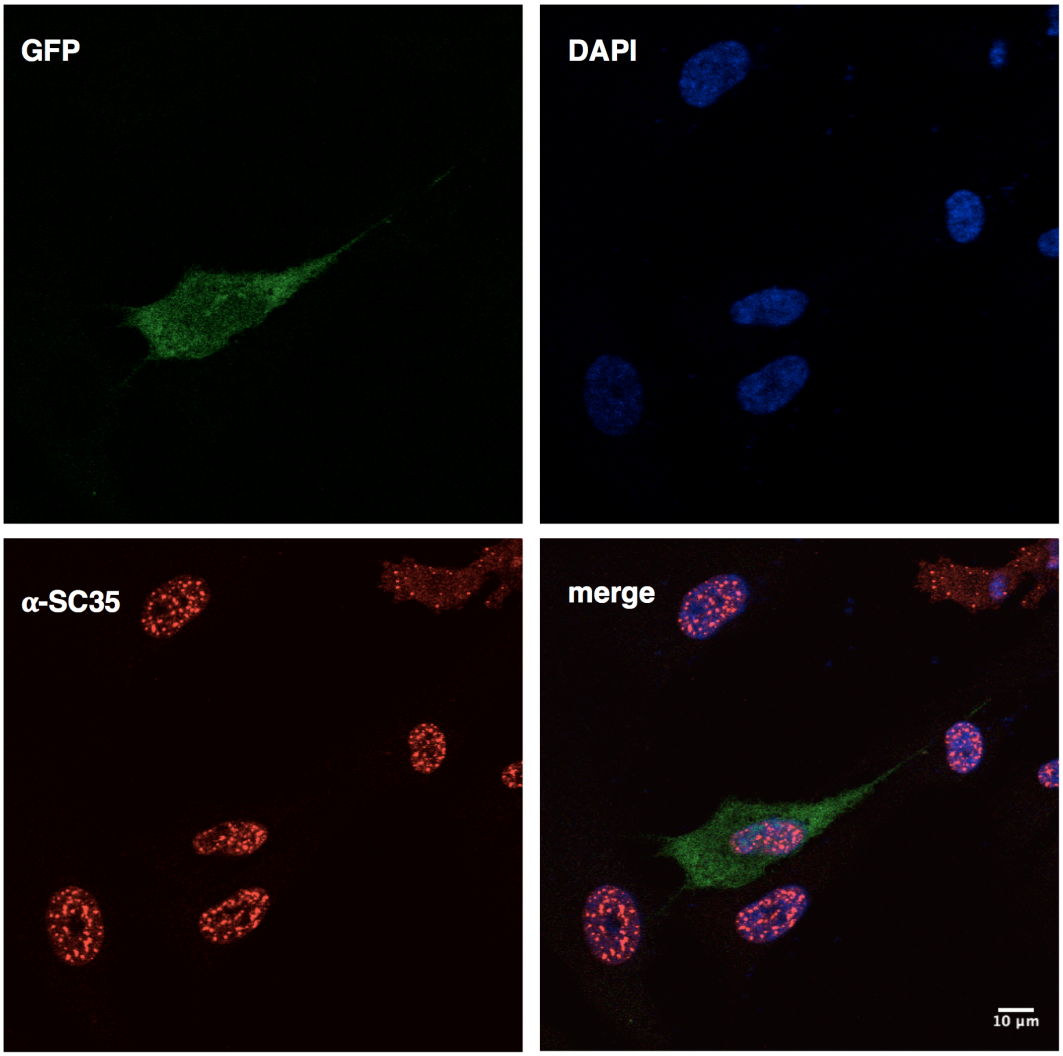

Figure 4.7.c. Myc-GFP is diffuse throughout RPE1 cells. RPE1 transfected with Myc-GFP were fixed, permeabilized and stained as previously described. Scale bar = 10 µm.

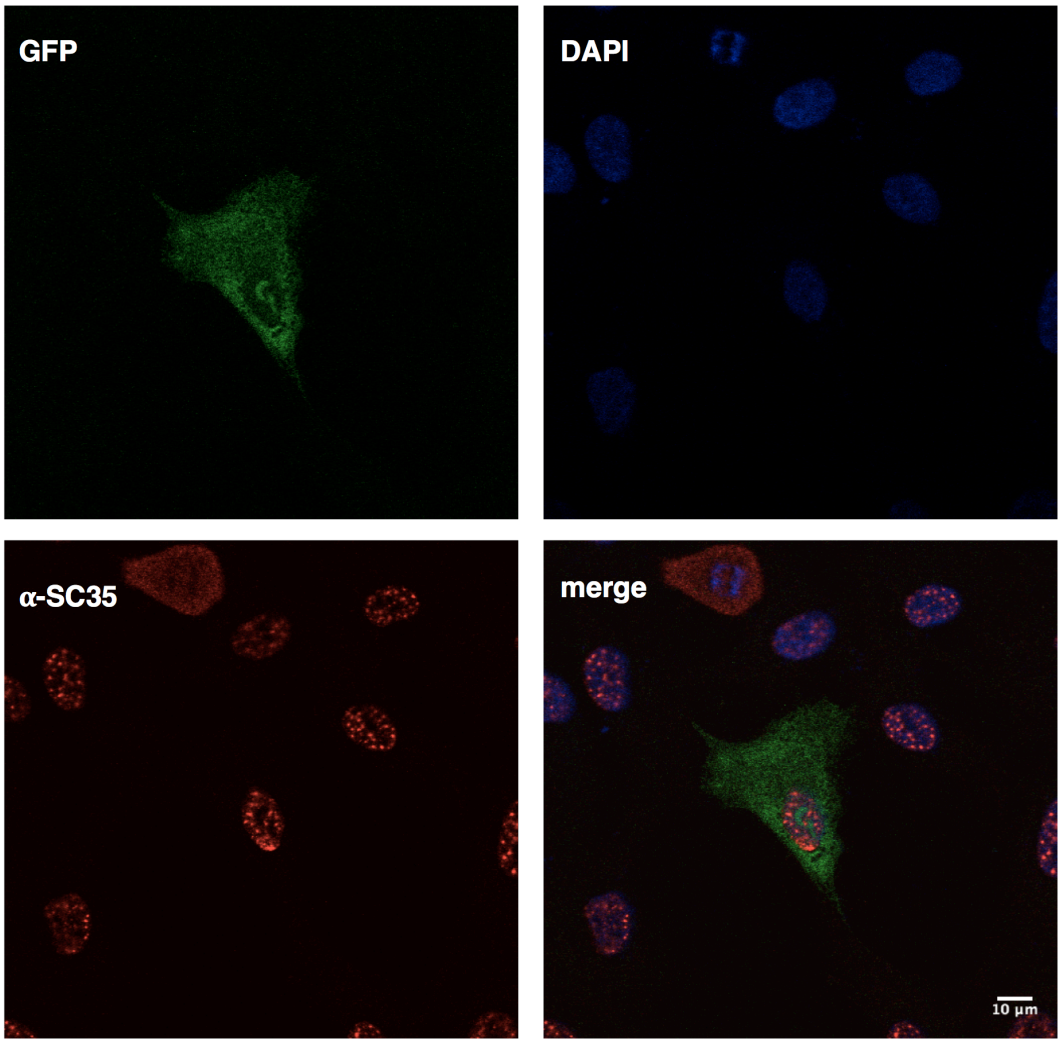

Figure 4.7.d. Myc-GFP is diffuse throughout RPE1 cells (continued). Image of another cell expressing Myc-GFP.

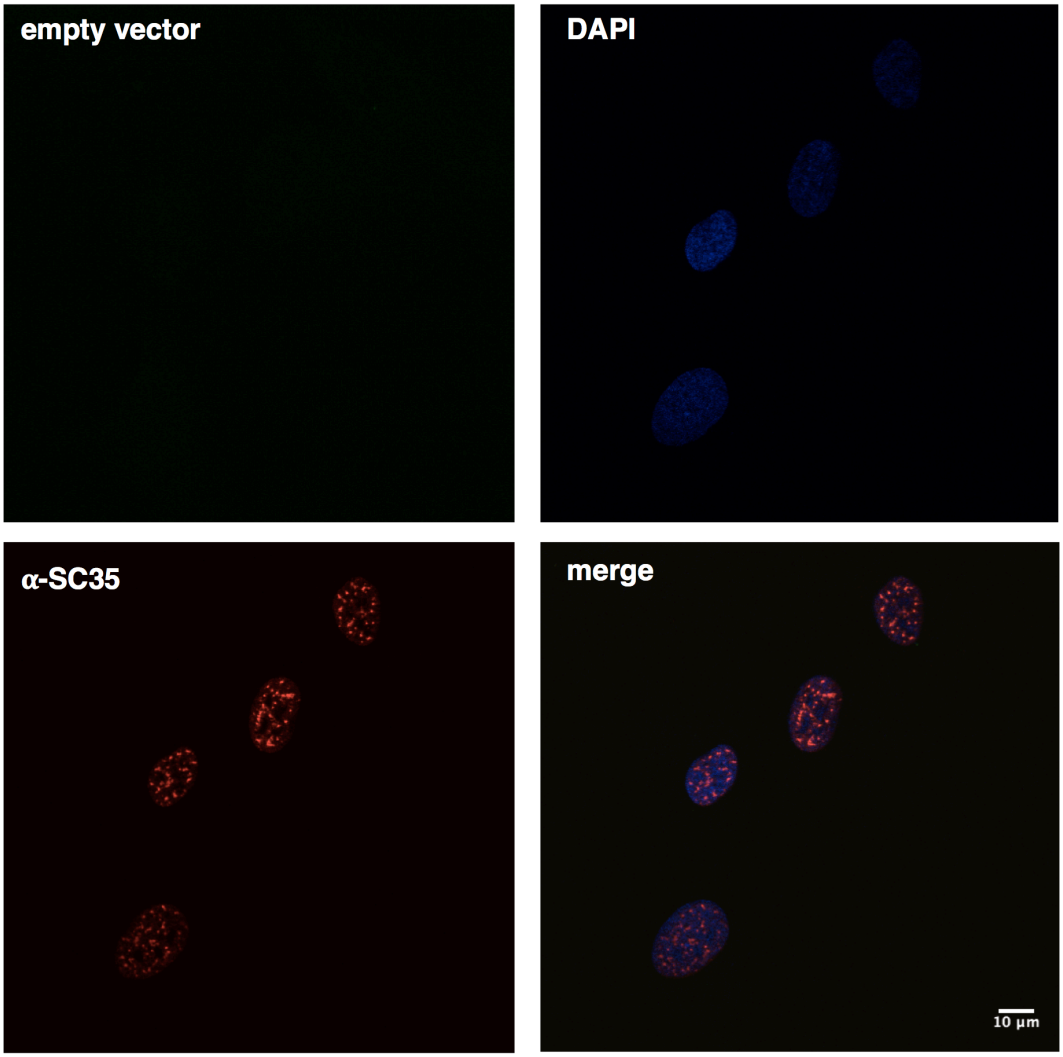

Figure 4.7.e. Empty vector transfected RPE1 cells. RPE1 cells were transfected with empty vector as a negative control. No background green fluorescence was observed. Scale bar = 10 μm.

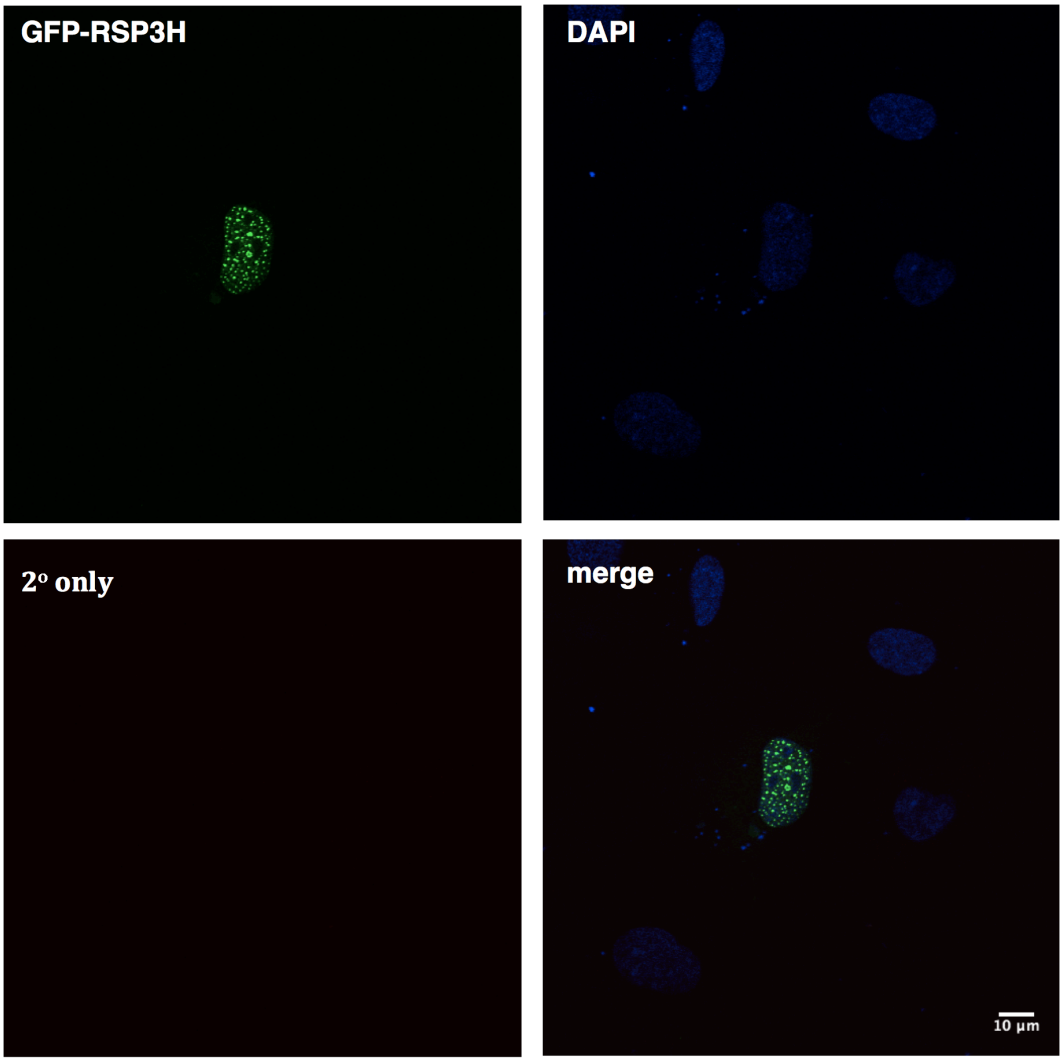

Figure 4.7.f. Secondary only treated RPE1 cells. RPE1 cells were stained with Alexa-Fluor® 546 nm-conjugated goat anti-mouse secondary alone as a negative control. No background red fluorescence was observed. Secondary alone-treated U2OS cells had little to no background as well (data not shown). Scale bar = 10 µm.

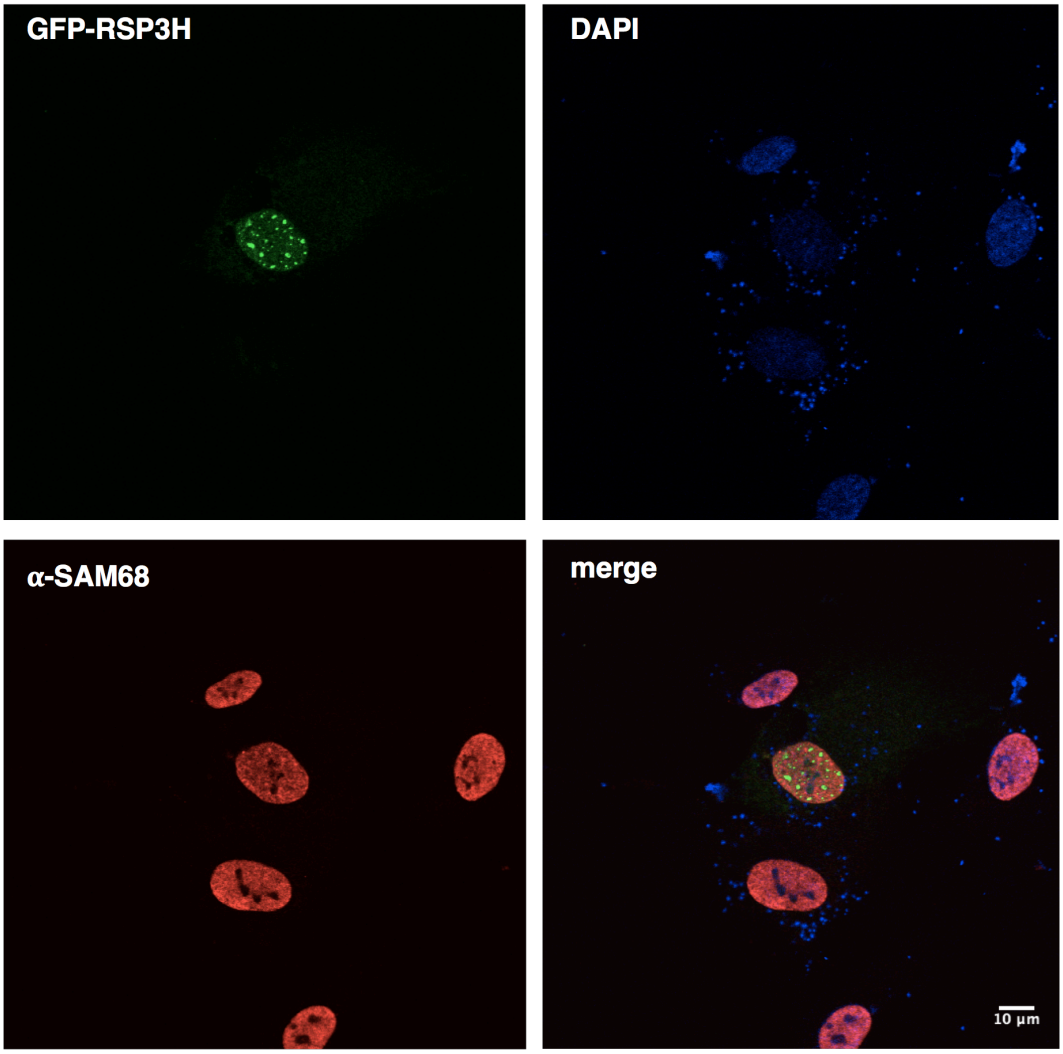

Figure 4.8. RPE1 cells expressing Myc-GFP-RSP3H stained with anti-SAM68. RPE1 cells expressing Myc-GFP-RSP3H were stained with an antibody against SAM68. SAM68 staining was diffuse throughout the nucleus, making visualization of distinct sub-domains difficult. Scale bar = 10 µm.

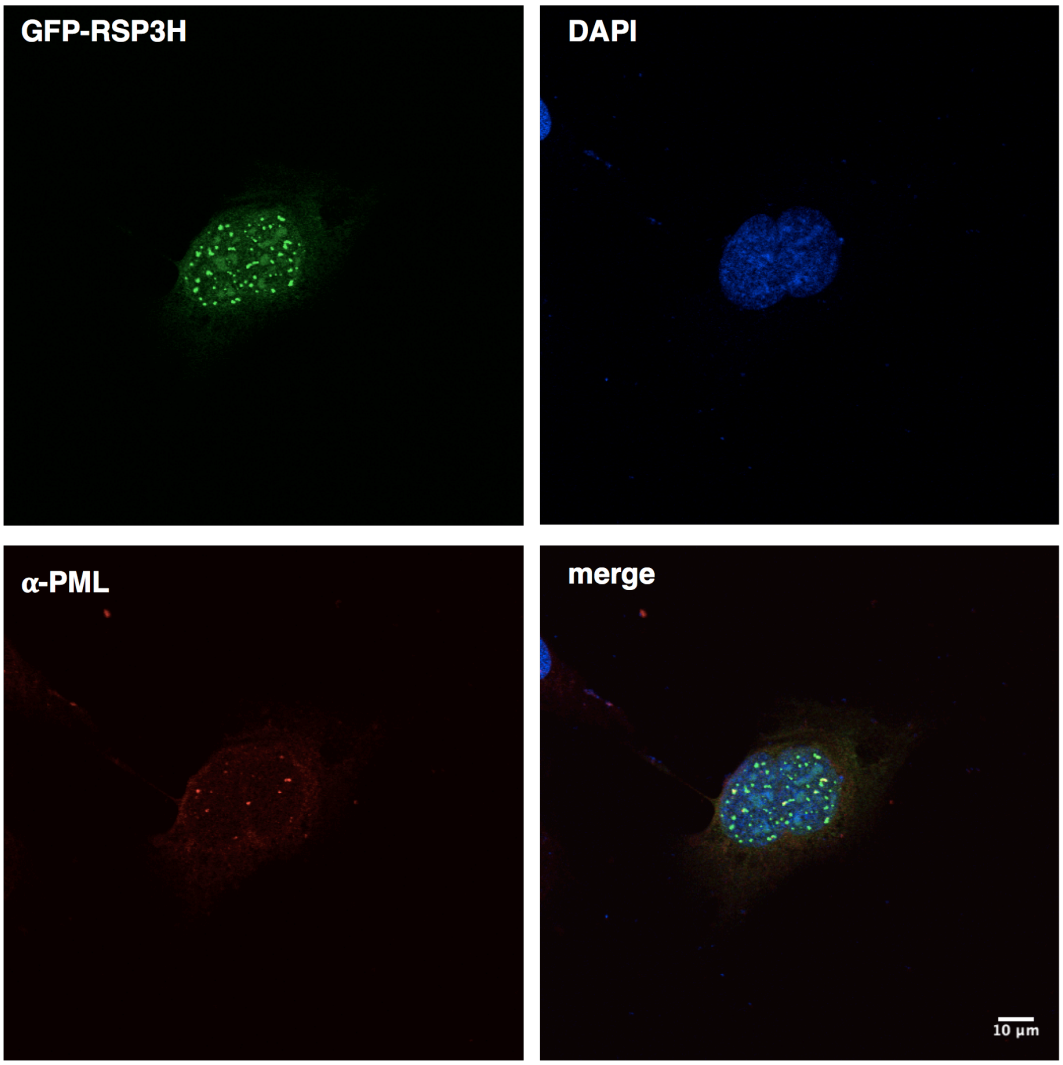

Figure 4.9.a. Myc-GFP-RSP3H co-localizes with PML in U2OS cells. U2OS cells were grown to 70-80% confluency, prior to fixation in 4% paraformaldehyde, permeabilization in 0.5% Triton X-100, and staining with anti-PML (red). Myc-GFP-RSP3H displayed significant co-localization with anti-PML staining, although not all Myc-GFP-RSP3H punctae overlapped with PML. Scale bar = 10 μm.

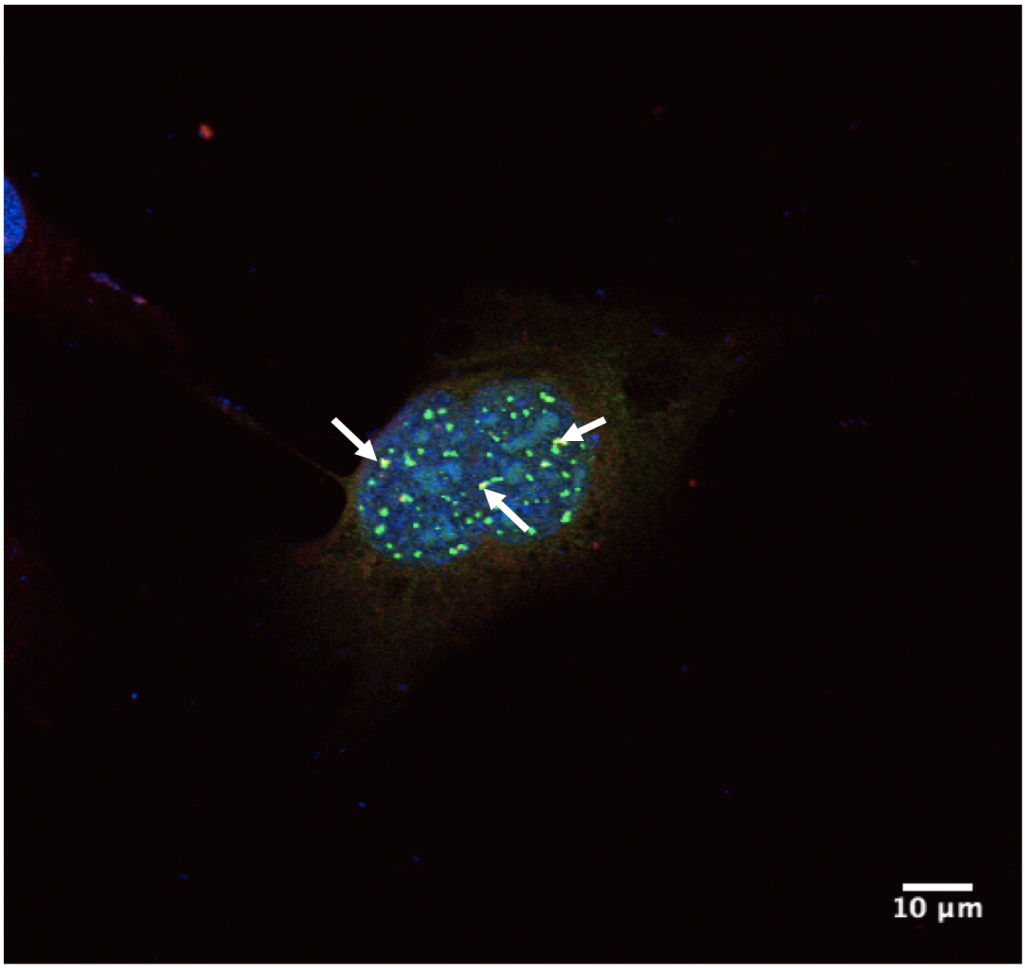

Figure 4.9.b. Myc-GFP-RSP3H co-localizes with PML in U2OS cells (continued). Enlarged merged image of red, green and blue channels displaying α-PML staining, Myc-GFP-RSP3H, and DAPI respectively. Arrows indicate representative areas of co-localization of GFP-RSP3H and PML.

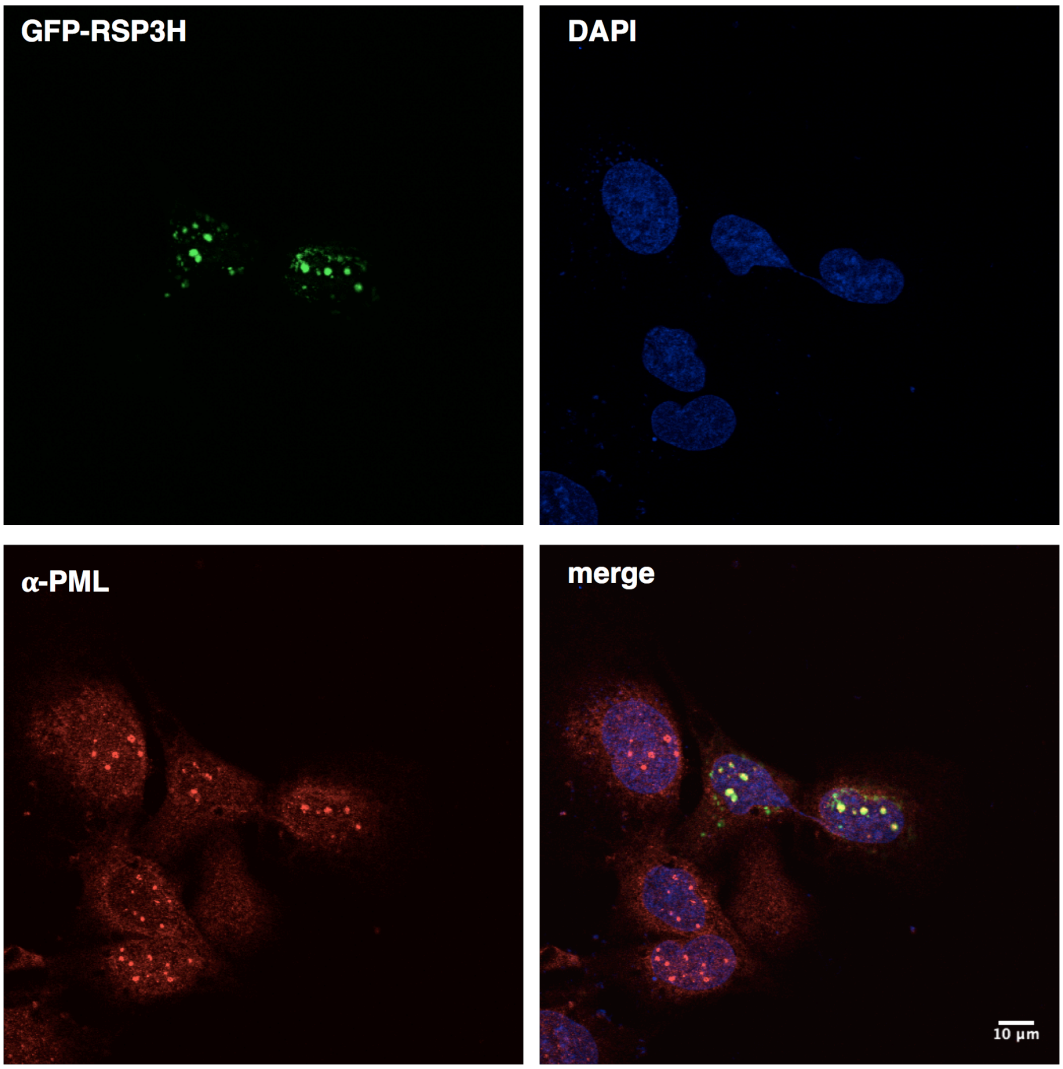

Figure 4.9.c. Myc-GFP-RSP3H co-localizes with PML in U2OS cells (continued). Image of another cell expressing Myc-GFP-RSP3H stained with α-PML and DAPI. Scale bar = 10 μm.

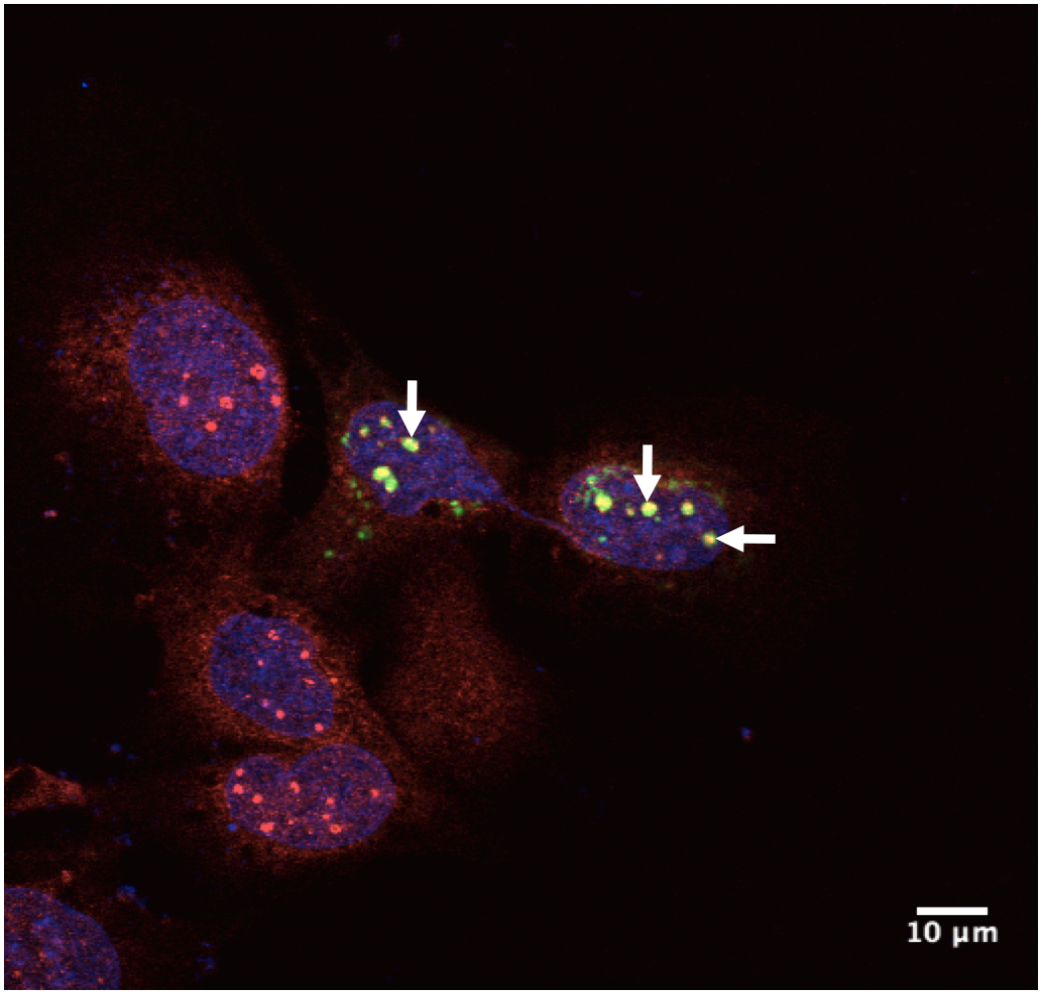

Figure 4.9.d. Myc-GFP-RSP3H co-localizes with PML in U2OS cells (continued). Enlarged merged image of red, green and blue channels displaying α-PML staining, Myc-GFP-RSP3H, and DAPI respectively. Arrows indicate representative areas of co-localization of GFP-RSP3H and PML.

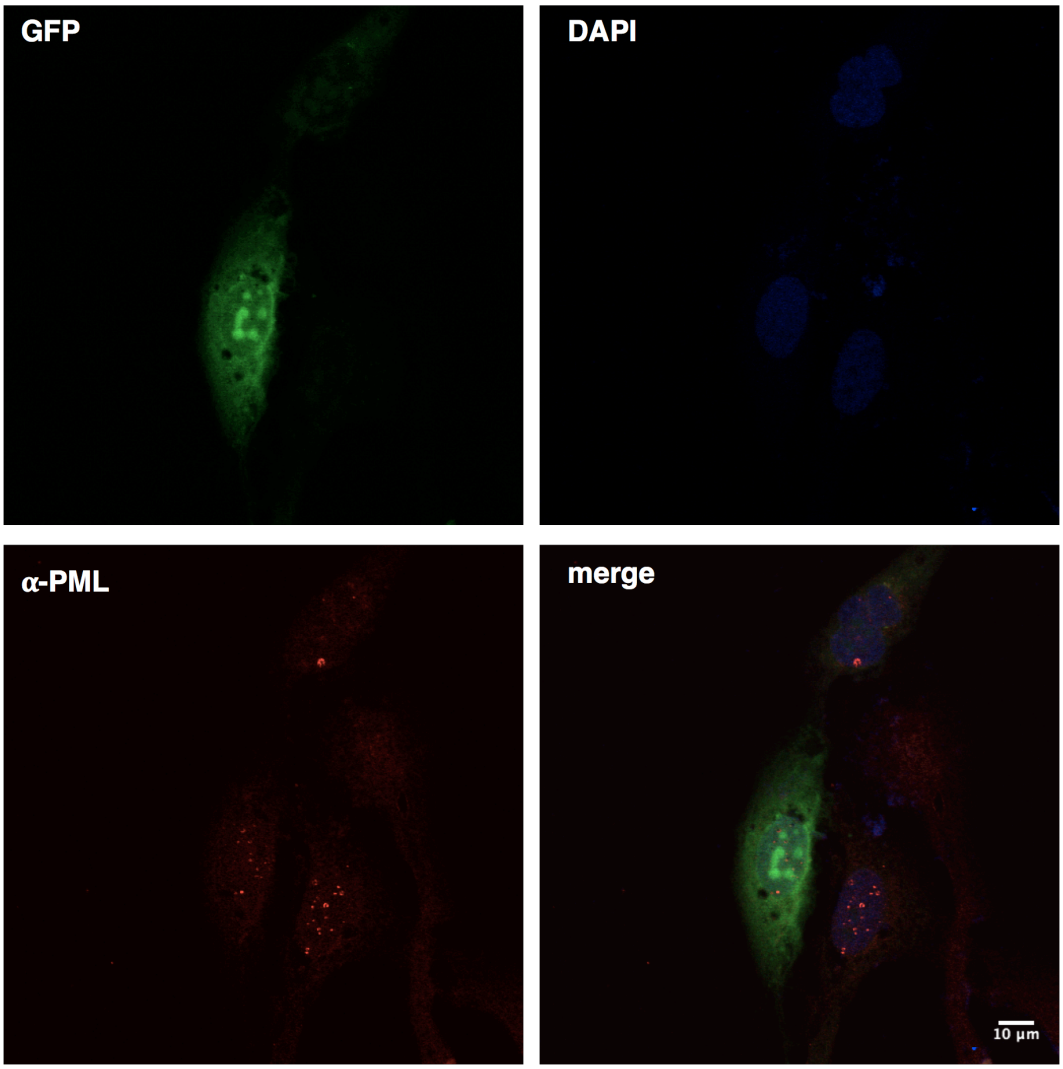

Figure 4.9.e. Myc-GFP is diffuse throughout U2OS cells. U2OS transfected with Myc-GFP were fixed, permeabilized and stained as previously described.

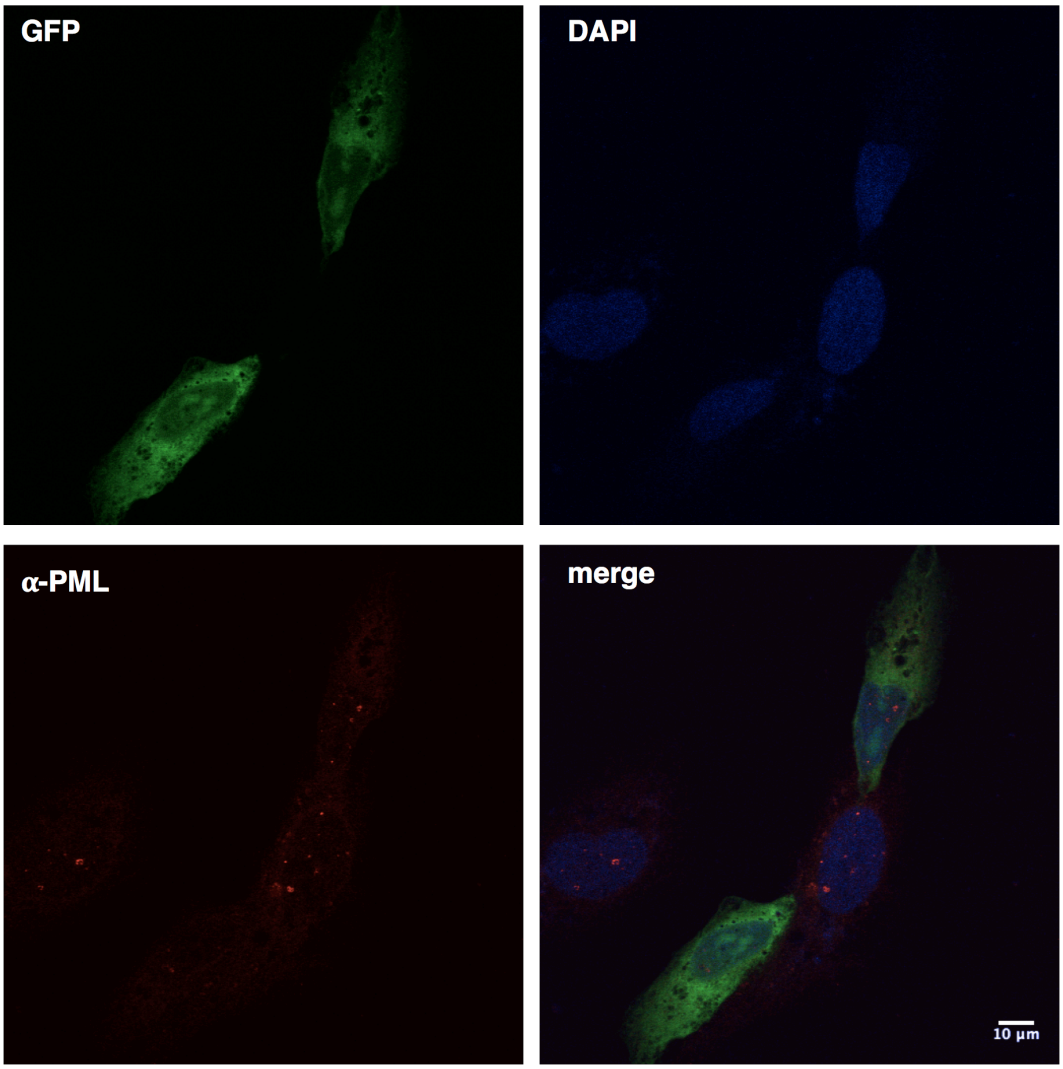

Figure 4.9.f. Myc-GFP is diffuse throughout U2OS cells (continued). Another image of U2OS transfected with Myc-GFP.

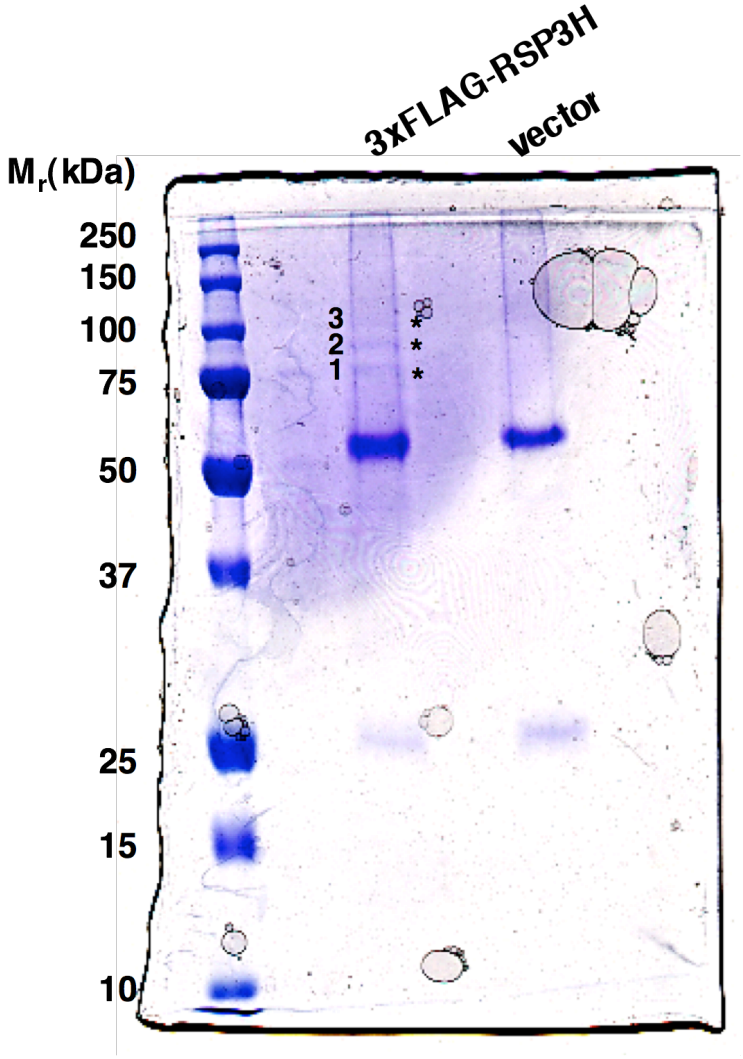

Figure 4.10. Mass-spectrometric analysis of potential RSP3H-interacting proteins. Tryptic peptide tandem MS/MS was used to identify co-immunoprecipitated proteins in a 3xFLAG-RSP3H pull-down. Asterisks indicate bands cut out for trypsin digest and analysis. Samples 1-3 in Table 4.3 correspond to bands numbered 1-3 on the colloidal Coomassie blue-stained gel. 3mg of HEK293 total cell lysate from 3xFLAG-RSP3H- or empty vector-transfected cells was used as input for α-FLAG immunoprecipitation.

RNA helicase
growth regulated nuclear 68 protein
DEAD box polypeptide 17 isoform 1
DEAD box, X isoform
Gu protein (nucleolar RNA Helicase II)

RNA-binding, pre-mRNA splicing, mRNA export
A-kinase anchor protein 8-like (AKAP8-like protein) (Neighbor of A-kinase-anchoring protein 95; HA95)
hnRNP U
hnRNP M (heterogeneous nuclear ribonucleoprotein M isoform 10)
heterogeneous nuclear ribonucleoprotein M, isoform CRA_c
polyadenylate binding protein II
PABPC4 protein: poly(A) binding protein C4
KSRP: K-homology splicing regulatory protein
Ribonucleoprotein PTB-binding 1 (Protein raver-1)

Translation
EIF3S8 (translation initiation factor)
eukaryotic translation elongation factor 2

Nuclear import/export
Importin 7
Exportin 1 (aka CRM1)
Importin-8 (aka RanBP8)
Transportin (Karyopherin beta 2)

DNA damage, telomeric maintenance
ATP-dependent DNA helicase II, 70 kDa subunit (Ku70)
nuclear corepressor KAP-1

Chromosomal architecture, epigenetic regulation of transcription
Histone 2A
Myosin-Ic (Myosin I beta)

Other nuclear proteins
Nucleolin
Tubulin, alpha 6
SUMO1/sentrin/SMT3 specific protease 3
Lamin B1

Figure 4.11. Interesting MS/MS hits grouped by known cellular function.
Relevant hits based on nuclear localization of RSP3/RSP3H.

Expression profile suggested by analysis of EST counts.
Hs.154628- RSHL2: Radial spokehead-like 2

See Legend
Note: Please mouseover the Tissue criterion to view complete details

Breakdown by Tissue

	Hs.154628	
adipose tissue	0	0 / 12777
adrenal gland	0	0 / 32215
ascites	24	1 / 40022
bladder	0	0 / 29175
blood	8	1 / 119874
bone	27	2 / 71667
bone marrow	0	0 / 47392
brain	11	10 / 890811
cervix	0	0 / 47558
cochlea	124	2 / 16098
colon	11	2 / 181250
connective tissue	6	1 / 145437
cranial nerve	55	1 / 18109
embryonic tissue	0	0 / 194985
esophagus	0	0 / 18916
eye	10	2 / 199696
heart	0	0 / 87149
kidney	19	4 / 206123
larynx	0	0 / 24256
liver	5	1 / 197800
lung	8	3 / 333931
lymph	0	0 / 44428
lymph node	33	3 / 90609
mammary gland	0	0 / 151863
mouth	15	1 / 62897
muscle	0	0 / 106514
nerve	0	0 / 15645
ovary	0	0 / 101128
pancreas	18	4 / 214089
parathyroid	0	0 / 20554
pharynx	0	0 / 41803
pituitary gland	60	1 / 16586
placenta	0	0 / 281155
prostate	0	0 / 189548
salivary gland	0	0 / 20254
skin	10	2 / 186159
small intestine	0	0 / 43311
spleen	0	0 / 50510
stomach	0	0 / 95320
testis	50	17 / 337730
thymus	13	1 / 74105

Table 4.1. EST analysis of human RSP3 (RSHL2) tissue distribution.

Reprinted from NCBI UniGene Hs.154628:
http://www.ncbi.nlm.nih.gov/UniGene/ESTProfileViewer.cgi?uglist=Hs.154628

thyroid	0		0 / 47348
tonsil	0		0 / 17026
trachea	63		3 / 46887
umbilical cord	0		0 / 13515
uterus	8		2 / 228444
vascular	0		0 / 49597
whole body	23		1 / 43023
whole brain	22		3 / 133484

Breakdown by Health State

	Hs.154628		
adrenal tumor	0		0 / 12703
bone tumor	20		2 / 99675
breast (mammary gland) cancer	0		0 / 93020
cervical tumor	0		0 / 33938
colorectal cancer	8		1 / 112359
esophageal tumor	0		0 / 16386
gastrointestinal tumor	33		4 / 119030
germ cell tumor	31		8 / 254527
glioma	0		0 / 106450
head and neck tumor	0		0 / 133267
kidney tumor	0		0 / 67205
leukemia	0		0 / 93575
liver tumor	0		0 / 88101
lymphoma	0		0 / 72121
non-glioma	23		3 / 128043
non-neoplasia	22		2 / 90133
normal	13		45 / 3231433
ovarian tumor	0		0 / 76097
pancreatic tumor	0		0 / 104989
prostate tumor	0		0 / 111050
respiratory tract tumor	0		0 / 103597
retinoblastoma	0		0 / 46485
skin tumor	8		1 / 124880
soft tissue/muscle tissue tumor	15		2 / 125478
urinary bladder tumor	0		0 / 26381
uterine tumor	0		0 / 90251

Breakdown by Developmental Stage

	Hs.154628		
embryo	11		2 / 179566
embryoid body	0		0 / 70535
fetus	10		6 / 553710
neonate (less than 4 weeks old)	0		0 / 26593
infant (less than 3 years old)	45		1 / 21845
juvenile (less than 17 years old)	0		0 / 53891
adult (17 years old and older)	9		18 / 1909841

Table 4.1. EST analysis of human RSP3 (RSHL2) tissue distribution (continued). Expressed-sequence tag sequencing of cDNA from various tissues identifying transcribed, spliced nucleotide sequence (mRNA) representing expressed *RSP3* (also known as RSHL2) gene product.

EXON NUMBER	SEQUENCE (BP)
1	1-542
2	543-640
3	631-772
4	773-918
5	919-1122
6	1123-1285
7	1286-1372
8	1373-1680

Table 4.2. Exon structure of the coding sequence of RSP3/RSP3H.

Protein ID for Three Samples from Dr. Melanie Cobb

Sample from: Arif Jivan
Principle Investigator: Melanie Cobb
Sample Received: June 24, 2008
Sample Type: Colloidial Coomassie Blue samples

Operator: Junmei Zhang
Report Date: July 10, 2008
Database: NCBI-nr human
Program: Mascot
Modifications: Methionine Oxidation (Variable)
Note:

1. The proteins identified for a sample are listed in the order of high confidence to low confidence. The higher the protein score, the higher th protein identification confidence is.

2. For all the samples, the proteins are listed below without manual verification unless requested. For the proteins requested for manual verification, all the good-matching peptides are listed in the last column.

3. Database search reference : Electrophoresis, 20(18) 3551-67 (1999). Its website is http://www.matrixscience.com.

Sample Name	Hit	Protein Name	GI Number	Score	MW (kDa)	Peptide Sequence
Arif1	4~1	heat shock 70kDa protein 8 isoform 1 [Homo sapiens]	gi|5729877	1136	70.9 kDa	
	6~2	heat shock 70kDa protein 1A [Homo sapiens]	gi|5123454	787	70.0 kDa	
	8~3	MTHSP75	gi|292059	491	73.7 kDa	
	9~4	myristoylated alanine-rich C-kinase substrate	gi|187387	433	31.9 kDa	
	11~5	alkyldihydroxyacetone phosphate synthase precursor [Homo sapiens]	gi|4501993	288	72.9 kDa	
	12~6	anti-colorectal carcinoma heavy chain [Homo sapiens]	gi|425518	275	50.6 kDa	
	13~7	growth regulated nuclear 68 protein	gi|226021	202	66.9 kDa	
	16~8	aralar2 [Homo sapiens]	gi|6523256	153	74.1 kDa	
	18~9	TNF receptor-associated protein 1 variant [Homo sapiens]	gi|62897971	137	80.0 kDa	
	19~10	ORF [Homo sapiens]	gi|1200089	130	59.9 kDa	
	20~11	unnamed protein product [Homo sapiens]	gi|16553914	109	63.6 kDa	
	21~12	lamin B1, isoform CRA_a [Homo sapiens]	gi|119569230	103	37.6 kDa	
	22~13	90kDa heat shock protein	gi|306891	96	83.2 kDa	
	23~14	Desmoglein-1 precursor (Desmosomal glycoprotein 1) (DG1) (DGI) (Pemphigus foliaceus antigen)	gi|416917	89	113.6 kDa	
	24~15	immunoglobulin kappa light chain variable region [Homo sapiens]	gi|4323920	81	10.8 kDa	
	26~16	albumin, isoform CRA_t [Homo sapiens]	gi|119626083	66	58.6 kDa	
	27~17	75 kDa subunit NADH dehydrogenase precursor [Homo sapiens]	gi|38079	63	79.5 kDa	
	29~18	PREDICTED: similar to filaggrin 2 [Homo sapiens]	gi|113412360	56	186.5 kDa	
	30~19	ATP-dependent DNA helicase II, 70 kDa subunit [Homo sapiens]	gi|4503841	53	69.8 kDa	
	31~20	ubiquitin	gi|229532	52	8.4 kDa	
	32~21	SUMO1/sentrin/SMT3 specific protease 3 [Homo sapiens]	gi|21361499	52	65.0 kDa	
	33~22	unnamed protein product [Homo sapiens]	gi|32111	51	14.2 kDa	
	35~23	tubulin alpha 6 [Homo sapiens]	gi|14389309	49	49.9 kDa	
	36~24	KIAA0719 protein [Homo sapiens]	gi|40788338	46	69.5 kDa	

Table 4.3. MS/MS hits from 3xFLAG-RSP3H pull-down. Samples correspond to bands indicated in Figure 4.10. Proteins with MASCOT scores of 150 and higher represent high confidence hits. Samples with peptide sequences in red are manually verified as significant.

Sample Name	Hit	Protein Name	GI Number	Score	MW (kDa)	
Arif2	1~1	unnamed protein product [Homo sapiens]	gi|16553914	1242	63.6 kDa	
	5~2	heat shock 70kDa protein 5 [Homo sapiens]	gi|16507237	587	72.3 kDa	
	7~3	anti-colorectal carcinoma heavy chain [Homo sapiens]	gi|425518	525	50.6 kDa	
	8~4	heterogeneous nuclear ribonucleoprotein M, isoform CRA_c [Homo sapiens]	gi|119589327	436	77.6 kDa	
	9~5	heat shock 70kDa protein 8 isoform 1 [Homo sapiens]	gi|5729877	360	70.9 kDa	
	10~6	polyadenylate binding protein II [Homo sapiens]	gi|693937	346	58.5 kDa	
	11~7	hepatocellular carcinoma associated protein [Homo sapiens]	gi|4099969	304	64.9 kDa	
	12~8	DEAD box polypeptide 17 isoform 1 [Homo sapiens]	gi|38201710	300	80.2 kDa	
	14~9	Chain A, Heat-Shock 70kd Protein 42kd Atpase N-Terminal Domain	gi|6729803	205	41.8 kDa	
	15~10	enoyl-CoA hydratase/3-hydroxyacyl-CoA dehydrogenase alpha-subunit of trifunctional protein [Homo sa	gi|862457	190	82.9 kDa	
	17~11	dead box, X isoform [Homo sapiens]	gi|2580550	179	73.2 kDa	
	18~12	PABPC4 protein [Homo sapiens]	gi|41388837	166	69.6 kDa	
	19~13	unnamed protein product [Homo sapiens]	gi|21752190	155	66.0 kDa	
	20~14	4F2 heavy chain antigen	gi|177216	146	58.0 kDa	
	22~15	KSRP [Homo sapiens]	gi|2055427	142	73.1 kDa	
	23~16	Chain L, Crystal Structure Of Fab Fragment Complexed With Gibberellin A4	gi|24158782	137	23.7 kDa	
	24~17	90kDa heat shock protein	gi|306891	136	83.2 kDa	
	25~18	myristoylated alanine-rich C-kinase substrate	gi|187387	133	31.9 kDa	
	28~19	pyrroline 5-carboxylate synthetase [Homo sapiens]	gi|1304314	125	87.2 kDa	
	29~20	hypothetical protein [Homo sapiens]	gi|31874069	121	70.2 kDa	
	30~21	phosphofructokinase, platelet [Homo sapiens]	gi|11321601	118	85.5 kDa	
	31~22	hypothetical protein [Homo sapiens]	gi|31873242	114	82.6 kDa	
	33~23	leucine zipper-EF-hand containing transmembrane protein 1, isoform CRA_a [Homo sapiens]	gi|119602966	104	63.5 kDa	
	34~24	MTHSP75	gi|292059	102	73.7 kDa	
	35~25	JUP protein [Homo sapiens]	gi|33875446	94	85.6 kDa	
	36~26	TRPP [Homo sapiens]	gi|913174	93	57.6 kDa	
	37~27	alpha-tubulin [Homo sapiens]	gi|37492	87	50.1 kDa	
	38~28	NRAGE [Homo sapiens]	gi|9963810	82	86.1 kDa	
	39~29	immunoglobulin kappa light chain VJ region [Homo sapiens]	gi|186016	78	12.6 kDa	
	40~30	immunoglobulin kappa light chain variable region [Homo sapiens]	gi|4323920	78	10.8 kDa	
	41~31	neutral amino acid transporter B	gi|1478281	74	56.6 kDa	
	42~32	80K-H protein	gi|182855	71	59.3 kDa	
	43~33	NADH dehydrogenase (ubiquinone) Fe-S protein 1, 75kDa (NADH-coenzyme Q reductase), isoform CRA_a [H	gi|119590785	68	80.9 kDa	
	44~34	metadherin [Homo sapiens]	gi|30520310	68	63.8 kDa	
	46~35	unnamed protein product [Homo sapiens]	gi|31283	64	69.4 kDa	
	47~36	Ribonucleoprotein PTB-binding 1 (Protein raver-1)	gi|74759693	63	63.8 kDa	
	48~37	FLJ00158 protein [Homo sapiens]	gi|18676522	61	34.9 kDa	
	49~38	novel protein [Homo sapiens]	gi|5578958	58	81.2 kDa	
	50~39	acyl-CoA synthetase-like protein [Homo sapiens]	gi|2960069	57	74.3 kDa	
	51~40	unnamed protein product [Homo sapiens]	gi|10433479	57	77.2 kDa	
	52~41	Vesicle-fusing ATPase (Vesicular-fusion protein NSF) (N-ethylmaleimide sensitive fusion protein) (N	gi|119364624	55	82.5 kDa	VLDDGELLVQQTK
	53~42	TLS protein	gi|448295	54	27.2 kDa	
	54~43	phosphoinositide-3-kinase, regulatory subunit, polypeptide 1 isoform 1 [Homo sapiens]	gi|32455248	52	83.5 kDa	TAIEAFNETIK
	55~44	hnRNP U protein [Homo sapiens]	gi|32358	52	88.9 kDa	
	56~45	insulin receptor substrate 4 [Homo sapiens]	gi|4504733	50	133.7 kDa	AIGDGEDEMLFTR
	57~46	unnamed protein product [Homo sapiens]	gi|32111	49	14.2 kDa	
	58~47	ubiquitin	gi|229532	48	8.4 kDa	
	59~48	calnexin	gi|179832	48	67.5 kDa	
	60~49	protein inhibitor of activated STAT protein PIAS1 [Homo sapiens]	gi|3643107	47	71.7 kDa	
	61~50	hCG1654256 [Homo sapiens]	gi|119622632	45	24.9 kDa	

Table 4.3. MS/MS hits from 3xFLAG-RSP3H pull-down (continued). Sample 2.

Sample Name	Hit	Protein Name	GI Number	Score	MW (kDa)
Arif3	5~1	Na+/K+ -ATPase alpha 1 subunit isoform a proprotein [Homo sapiens]	gi|21361181	538	112.8 kDa
	6~2	anti-colorectal carcinoma heavy chain [Homo sapiens]	gi|425518	528	50.6 kDa
	7~3	90kDa heat shock protein	gi|306891	453	83.2 kDa
	8~4	HSP90AA1 protein [Homo sapiens]	gi|83318444	433	68.3 kDa
	9~5	Chain L, Crystal Structure Of Fab Fragment Complexed With Gibberellin A4	gi|24158782	315	23.7 kDa
	10~6	Na+, K+ -ATPase catalytic subunit	gi|497763	307	111.6 kDa
	11~7	radial spokehead-like 2, isoform CRA_a [Homo sapiens]	gi|119568026	296	52.7 kDa
	13~8	CAS	gi|951338	267	110.2 kDa
	14~9	coiled-coil domain containing 8 [Homo sapiens]	gi|14042972	250	59.4 kDa

Table 4.3. MS/MS hits from 3xFLAG-RSP3H pull-down (continued). Sample 3.

	15~10	Chain L, Crystal Structure Of The Fab Fragment Of The Monoclonal Antibody Mak33	gi|10835838	221	23.4 kDa	
	16~11	Chain A, Structure Of Importin Beta Bound To The Ibb Domain Of Importin Alpha	gi|5107666	216	97.2 kDa	
	18~12	NRAGE [Homo sapiens]	gi|9963810	179	86.1 kDa	
	20~13	calnexin	gi|179832	169	67.5 kDa	
	21~14	Myosin-Ic (Myosin I beta) (MMI-beta) (MMIb)	gi|13431674	161	118.0 kDa	YMDVQFDFK DGTIDFTPGSELLITK
	23~15	insulin receptor substrate 4 [Homo sapiens]	gi|4504733	153	133.7 kDa	
	24~16	poly(ADP-ribose) synthetase	gi|337424	136	113.1 kDa	
	25~17	nuclear corepressor KAP-1 [Homo sapiens]	gi|1699027	135	88.5 kDa	
	26~18	immunoglobulin kappa light chain VJ region [Homo sapiens]	gi|186016	135	12.6 kDa	
	27~19	tumor rejection antigen (gp96) 1 variant [Homo sapiens]	gi|62088648	130	65.9 kDa	
	28~20	importin7 [Homo sapiens]	gi|11544639	108	116.3 kDa	AFAVGVQQVLLK
	29~21	transferrin receptor [Homo sapiens]	gi|4507457	107	84.8 kDa	
	30~22	exportin 1 [Homo sapiens]	gi|4507943	106	123.3 kDa	NVDILKDPETVK IYLDMLNVYK EFAGEDTSDLFLEER
	31~23	nucleolin	gi|189306	104	76.3 kDa	GFGFVDFNSEEDAK
	32~24	Ewing sarcoma breakpoint region 1 isoform EWS [Homo sapiens]	gi|4885225	92	68.4 kDa	
	33~25	Xeroderma Pigmentosum Group E Complementing protein [Homo sapiens]	gi|2632123	91	126.8 kDa	
	34~26	eukaryotic translation elongation factor 2 [Homo sapiens]	gi|4503483	88	95.3 kDa	
	36~27	gastric H(+)-K(+)-ATPase alpha-subunit [Xenopus laevis]	gi|147899270	86	115.0 kDa	
	37~28	albumin, isoform CRA_t [Homo sapiens]	gi|119626083	85	58.6 kDa	
	38~29	human 26S proteasome subunit p97 [Homo sapiens]	gi|1060888	85	100.1 kDa	
	39~30	EIF3S8 protein [Homo sapiens]	gi|12653523	84	37.7 kDa	
	40~31	motor protein [Homo sapiens]	gi|516766	84	18.2 kDa	
	41~32	tubulin alpha 6 [Homo sapiens]	gi|14389309	79	49.9 kDa	
	42~33	HT019 [Homo sapiens]	gi|9963851	79	29.6 kDa	
	43~34	A-kinase anchor protein 8-like (AKAP8-like protein) (Neighbor of A-kinase-anchoring protein 95) (Ne	gi|21431604	78	71.6 kDa	
	44~35	hypothetical protein [Homo sapiens]	gi|52545599	77	98.0 kDa	
	45~36	immunoglobulin kappa light chain variable region [Homo sapiens]	gi|98956399	77	12.3 kDa	
	46~37	hnRNP U protein [Homo sapiens]	gi|32358	71	88.9 kDa	
	47~38	C-1-tetrahydrofolate synthase, cytoplasmic (C1-THF synthase) [Includes: Methylenetetrahydrofolate d	gi|115206	67	101.5 kDa	
	48~39	beta-cop homolog [Homo sapiens]	gi|5257007	63	107.1 kDa	
	49~40	hypothetical protein [Homo sapiens]	gi|31873730	58	65.1 kDa	
	50~41	unnamed protein product [Homo sapiens]	gi|10434578	58	53.9 kDa	
	51~42	unnamed protein product [Homo sapiens]	gi|10434688	58	76.8 kDa	
	52~43	kinesin family member 5B [Homo sapiens]	gi|4758648	57	109.6 kDa	No good peptide
	54~44	unnamed protein product [Homo sapiens]	gi|32111	56	14.2 kDa	
	55~45	Gu protein	gi|1230564	55	89.2 kDa	
	56~46	protein-serine/threonine kinase [Homo sapiens]	gi|405737	55	7.5 kDa	
	57~47	alpha2(E)-catenin	gi|414982	54	102.7 kDa	
	58~48	G protein-coupled receptor associated sorting protein 2 [Homo sapiens]	gi|19923967	53	93.7 kDa	
	59~49	unknown [Homo sapiens]	gi|62630113	52	60.6 kDa	
	60~50	beta-tubulin [Homo sapiens]	gi|1297274	52	50.5 kDa	
	61~51	WD repeat domain 6 protein [Homo sapiens]	gi|11072093	51	121.6 kDa	
	62~52	KIAA0088 [Homo sapiens]	gi|577295	51	106.7 kDa	
	63~53	Chain A, Karyopherin Beta2TRANSPORTIN-Hnrnpm Nls Complex	gi|146387644	49	96.5 kDa	
	64~54	ubiquitin activating enzyme E1 [Homo sapiens]	gi|35830	49	117.7 kDa	
	65~55	transportin [Homo sapiens]	gi|1613834	49	101.2 kDa	FSDQFPLPLK
	66~56	beta-catenin [Homo sapiens]	gi|20384898	49	34.3 kDa	
	67~57	Importin-8 (Imp8) (Ran-binding protein 8) (RanBP8)	gi|45477008	47	119.9 kDa	TYAVGIQQVLLK

Table 4.3. MS/MS hits from 3xFLAG-RSP3H pull-down (continued). Sample 3.

CHAPTER 5. FUTURE DIRECTIONS

RSP3H is a novel ERK1/2-interacting A-kinase anchoring protein. Through yeast two-hybrid analysis, ERK directly binds to RSP3H. RSP3/RSP3H are also substrates for ERK1/2, and phosphorylation by these protein kinases affects the ability of RSP3H to interact with PKA. Additionally, RSP3/RSP3H are expressed in cells that are not thought to contain motile cilia, implying a possible atypical role for these proteins in cells that only have a single primary cilium. Alternatively, this could be evidence of other cellular actions of RSP3/RSP3H, beyond the motile cilium, conserved in both primary- and motile-ciliated cells. Further biochemical and cell-biological studies will be employed to examine the functions of RSP3/RSP3H in a variety of cell types. I have outlined some of these specific experiments in the Discussion sections of the previous two chapters. In this chapter, I will briefly reiterate several of the most critical directions and speculate on the potential cellular role(s) and regulation of RSP3/RSP3H. Furthermore, I will provide a long-term prospectus on what we hope to achieve in elucidating how RSP3/RSP3H is potentially governed by ERK1/2 and PKA as well as how RSP3/RSP3H may coordinate ERK1/2 and PKA activity in certain cellular processes.

Three overarching questions define the direction of our studies. Firstly, how do RSP3/RSP3H coordinate ERK and PKA activity? Do RSP3/RSP3H scaffold signaling through these protein kinases at specific subcellular locales and in certain cellular processes? Secondly, what are the functions, if any, of RSP3/RSP3H in cells with primary cilia? Are these activities conserved in motile-ciliated cells as well? Finally, what are the nuclear roles of RSP3/RSP3H? More specifically, what function(s) do RSP3/RSP3H have in PML bodies?

Much of the biochemical characterization of RSP3/RSP3H will be performed using *in vitro* binding studies and exogenous overexpression in cultured cells. Further analysis will be performed to identify the ERK1/2-binding domains within RSP3/RSP3H. Individually mutating the putative FXF motifs within RSP3H did not disrupt the association with ERK. RSP3H containing mutations to all three motifs will be tested for the ability to interact with ERK. RSP3H containing a deletion of a putative N-terminal D motif will also be tested to see whether it co-immunoprecipitates with endogenous ERK. Furthermore, co-immunoprecipitation experiments and pair-wise yeast two-hybrid interaction studies utilizing various mutants of ERK2, including mutations within the MAP kinase insert (Y261N) and the CD motif (D316A, D319A, E320A), will be performed to test for interaction with RSP3H.

Other potential ERK1/2 phosphorylation sites are currently being examined. The RSP3H T243V, T286A double mutant will be used as a substrate in immunoprecipitation kinase reactions and ^{32}P-cell labeling experiments. Cell labeling will also be utilized to determine other stimuli (e.g. PDGF and prostaglandin E2) and protein kinases (e.g. PKA) that could result in RSP3H phosphorylation. Phosphoamino acid analysis and site-directed mutagenesis will be performed to determine the PKA phosphorylation sites in RSP3/RSP3H.

RSP3/RSP3H also contains putative nuclear localization and nuclear export signal sequences. Mapping the NLS and NES as well as determining the import factor(s) with which RSP/RSP3H bind will provide more clues to the intracellular localization of RSP3/RSP3H. Karyopherin β2, importin 7 and 8 are all potential interacting partners identified from the mass-spectrometric analysis of the RSP3H pull-down. Confirming the interaction of RSP3H with other co-precipitating

proteins through individual co-immunoprecipitation studies will also provide suggestions towards cellular function.

Both SUMO-1 and ubiquitin were identified as potential covalent modifiers for RSP3H. Overexpression and mutagenesis studies will be employed to identify whether RSP3H is sumoylated or ubiquitylated and the site(s) on which it is modified. Sumoylation may affect the nuclear translocation of RSP3/RSP3H or perhaps its incorporation and function at PML bodies, where many components are sumoylated. Ubiquitylation most likely mediates proteasomal degradation of RSP3/RSP3H. Mass-spectrometry will also be employed to identify other post-translational modifications of RSP3H purified from Sf9 insect cells.

ERK1/2 and PKA could regulate the ability of RSP3/RSP3H to scaffold other proteins or modulate the activity of other scaffolded proteins. The finding that ERK1/2 activity affects the ability of RSP3H to interact with the regulatory subunits of PKA raises the question of whether this regulation by phosphorylation is applicable to any other known AKAPs such as MAP2. MAP2 is a substrate for PKA and ERK (Theurkauf and Vallee, 1983; Ray and Sturgill, 1987; Silliman and Sturgill, 1989; Boulton et al., 1990). The ability of MAP2 to interact with PKA upon changes in ERK1/2 activity has not been explored. As discussed in Chapter 3, ERK1/2 activity could also affect the localization of PKA to certain sites of action. Additionally, several AKAPs are known to coordinate a phosphodiesterase to rapidly decrease localized cAMP (Dodge-Kafka et al., 2005; Houslay and Baillie, 2005). ERK1/2 and/or PKA activity could contribute to cAMP concentration through phosphorylating associated PDEs (Hoffmann et al., 1999). Phosphorylation of RSP3/RSP3H by ERK1/2 and PKA could also affect localization or precede/facilitate other post-translational modifications on RSP3/RSP3H. One can envision the various mutants of RSP3/RSP3H that can be

generated from these biochemical analyses; these will be examined in their capacity to disrupt endogenous RSP3/RSP3H function.

Ultimately, as one of our goals is to examine the cellular functions of RSP3/RSP3H, we must first be able to observe and manipulate endogenous RSP3/RSP3H protein and message. Such cell biological approaches are predicated upon generating a highly specific and sensitive antibody against endogenous protein. Lentiviral shRNA RNA interference directed against RSP3/RSP3H will also be employed for more stable knockdowns of message and protein. With the development of these specific tools, we can examine whether RSP3/RSP3H may affect a variety of cellular processes including primary cilia formation, cell cycle progression, and gene expression (e.g. transcription, pre-mRNA processing/splicing, mRNA export, and translation). As mentioned in Chapter 4, preliminary experiments suggest that RSP3/RSP3H mRNA expression correlates with the induction of G_0 arrest and primary cilia emergence. More experiments will be pursued to determine the relationship between RSP3/RSP3H expression and primary cilia formation. RSP3H wild-type, a mutant lacking the major ERK1/2 phosphorylation site (T286A) and a phosphomimetic mutant (T286D) were overexpressed in HEK293 cells, which were then examined for any changes in cell cycle distribution of the asynchronous population. These cells were stained with the DNA dye, propidium iodide, to measure DNA content and subsequently sorted using fluorescence activated cell-sorting (FACS) analysis to examine percentages of cells in the different cell cycle stages. Overexpression of wild-type and mutant RSP3H had no apparent effects on this distribution. Once we are able measure and manipulate endogenous protein, RSP3/RSP3H protein and message levels will be examined during cell cycle progression in synchronized cell populations. Furthermore, perturbations to cell cycle distribution and primary cilia emergence will be measured in the context of

RSP3/RSP3H knockdown. IMCD3 cells stably expressing GFP-SR3 will be monitored for primary cilia regulation – length, emergence relative to the cell cycle, copy number, and other aberrations to primary cilia formation – after knockdown of RSP3/RSP3H or overexpressing wild-type and mutant RSP3 (the short form). While studies up to this point have utilized GFP-RSP3H (long form), we will use fluorescently-tagged (e.g. dsRed and GFP) RSP3 (short form) in subsequent experiments because of the relative abundance in mRNA levels and to overcome perceived challenges with protein stability. In a given cell population, GFP-RSP3H expresses at either low levels, giving a punctate nuclear distribution or at significantly high enough levels to display an aggresomal-like pattern indicating that high expression is not tolerated by the cell. N- and C-terminal dsRed- as well as N-terminal-cyan fluorescent protein (CFP)-RSP3H do not express at all. The dynamic localization of dsRed-RSP3 during cell cycle progression will be monitored in live-cell imaging experiments.

To further examine whether RSP3/RSP3H mRNA and protein levels are related to primary cilia formation, we will utilize primary kidney epithelial cells from wild-type and kidney-specific KIF3A knockout mice, where cells fail to form or have shortened cilia. If differences in RSP3/RSP3H expression are evident between wild-type and KIF3A knockout cells, we can correlate the presence of primary cilia and the necessity of the cell to express RSP3/RSP3H.

More experiments examining endogenous protein expression will lend clues to functionally separating RSP3 and RSP3H. As seen with mRNA expression, RSP3 message is 250-300-fold more abundant than RSP3H, indicating that perhaps RSP3H expression is tightly controlled and may be upregulated under some cell-context or state. It would be also be worthwhile to compare protein stability of RSP3 and RSP3H through ^{35}S-labeling pulse-chase experiments. Targeted

knockdown of the long form, RSP3H, could also distinguish functionality from RSP3.

One hypothesis based on the mass-spectrometric identification of putative interacting partners and nuclear localization is that RSP3/RSP3H may play a role in gene expression – through transcriptional or translation control or through pre-mRNA processing and/or export. Preliminary bulk mRNA distribution did not appear affected when overexpressing wild-type RSP3H. Nuclear versus cytosolic distribution of total, cellular mature mRNA was measured fluorescently using Cy3-fluorophore-conjugated streptavidin and biotinylated oligo-dT hybridization to poly-A-tail processed mRNA (Chakraborty et al., 2006). Gene expression, as measured by firefly luciferase activity also did not seem to be affected when overexpressing wild-type or T286A mutant RSP3H. If RSP3/RSP3H participates in regulating gene expression at any step, the protein(s) most likely control a subset of ERK1/2- and/or PKA-dependent genes. Quantitative PCR of ERK1/2- and PKA-modulated transcripts (such as c-Fos or E1A) will be performed when modulating RSP3/RSP3H level (either overexpressing or knockdown) to measure a transcriptional regulatory role for RSP3/RSP3H. If RSP3/RSP3H participates in mRNA export from the nucleus, mRNA can be isolated from nuclear and cytosolic extracts and Q-PCR can measure levels of transcripts in each compartment. Ideally, changes in global transcript levels as well as nuclear- versus cytosolic-distributed transcripts levels upon RSP3/RSP3H knockdown can be measured using microarray.

Based on the localization to PML bodies, RSP3/RSP3H could have an effect in mediating ERK1/2 and PKA signaling at these nuclear sub-domains. Any number of cellular events connected to PML bodies can be assayed in the context of modulating RSP3/RSP3H protein level. These include: cell viability studies, PML

body formation and number, as well as the transcription and mRNA processing experiments as described.

The directions presented here and in previous chapters will contribute to a greater understanding of how scaffolding proteins serve as signaling loci and their role in the interconnectivity between the ERK1/2 and PKA signaling pathways. Additionally, the suggested experiments will provide a framework to pursue studying RSP3/RSP3H in this context for years to come.

BIBLIOGRAPHY

Afzelius BA. (2004). Cilia-related disease. *J Pathol* **204**: 470-477.

Aouadi M, Binetruy B, Caron L, Le Marchand-Brustel Y, Bost F. (2006). Role of MAPKs in development and differentiation: lessons from knockout mice. *Biochimie* **88**: 1091-1098.

Bauman AL, Soughayer J, Nguyen BT, Willoughby D, Carnegie GK, Wong W, Hoshi N, Langeberg LK, Cooper DM, Dessauer CW, Scott JD. (2006). Dynamic regulation of cAMP synthesis through anchored PKA-adenylyl cyclase V/VI complexes. *Mol Cell* **23**: 925-931.

Belibi FA, Reif G, Wallace DP, Yamaguchi T, Olsen L, Li H, Helmkamp GM Jr, Grantham JJ. (2004). Cyclic AMP promotes growth and secretion in human polycystic kidney epithelial cells. *Kidney Int* **66**: 1283-1285.

Berman DE, Hazvi S, Rosenblum K, Seger R, Dudai Y. (1998). Specific and differential activation of mitogen-activated protein kinase cascades by unfamiliar taste in the insular cortex of the behaving rat. *J Neurosci* **18**:10037-10044.

Bernardi R, Guernah I, Jin D, Grisendi S, Alimonti A, Teruya-Feldstein J, Cordon-Cardo C, Simon MC, Rafii S, Pandolfi PP. (2006). PML inhibits HIF-1alpha translation and neoangiogenesis through repression of mTOR. *Nature* **442**: 779-785.

Bernardi R, Pandolfi PP. (2007). Structure, dynamics and functions of promyelocytic leukaemia nuclear bodies. *Nat Rev Mol Cell Biol* **8**: 1006-1016.

Berthet J, Rall TW, Sutherland EW. (1957). The relationship of epinephrine and glucagon to liver phosphorylase. IV. Effect of epinephrine and glucagon on the reactivation of phosphorylase in liver homogenates. *J Biol Chem* **224**: 463-475.

Best JL, Ganiatsas S, Agarwal S, Changou A, Salomoni P, Shirihai O, Meluh PB, Pandolfi PP, Zon LI. (2002). SUMO-1 protease-1 regulates gene transcription through PML. *Mol Cell* **10**: 843-855.

Boisvert FM, Hendzel MJ, Bazett-Jones DP. (2000). Promyelocytic leukemia (PML) nuclear bodies are protein structures that do no accumulate RNA. *J Cell Biol* **148**: 283-292.

Boisvert FM, Kruhlak MJ, Box AK, Hendzel MJ, Bazett-Jones DP. (2001). The transcription coactivator CBP is a dynamic component of the promyelocytic leukemia nuclear body. *J Cell Biol* **152**: 1099-1106.

Borden KL. (2002). Pondering the Promyelocytic Leukemia Protein (PML) Puzzle: Possible Functions for PML Nuclear Bodies. *Mol Cell Biol* **15:** 5259-5269.

Borden KL. (2008). Pondering the puzzle of PML (promyelocytic leukemia) nuclear bodies: can we fit the pieces together using an RNA regulon? *Biochim Biophys Acta* **1783**: 2145-2154.

Boulton TG, Cobb MH. (1991). Identification of multiple extracellular signal-regulated kinases (ERKs) with antipeptide antibodies. *Cell Regul* **2**: 357-371.

Boulton TG, Yancopoulos GD, Gregory JS, Slaughter C, Moomaw C, Hsu J, Cobb MH. (1990). An insulin-stimulated protein kinase similar to yeast kinases involved in cell cycle control. *Science* **249**: 64-67.

Burnett G, Kennedy EP. (1954). The enzymatic phosphorylation of proteins. *J Biol Chem* **211**: 969-980.

Burns-Hamuro LL, Ma Y, Kammerer S, Reineke U, Self C, Cook C, Olson GL, Cantor CR, Braun A, Taylor SS. (2003). Designing isoform-specific peptide disruptors of protein kinase A localization. *Proc Natl Acad Sci U S A* **100**: 4072-4077.

Burton KA, Johnson BD, Hausken ZE, Westenbroek RE, Idzerda RL, Scheuer T, Scott JD, Catterall WA, McKnight GS. (1997). Type II regulatory subunits are not required for the anchoring-dependent modulation of Ca2+ channel activity by cAMP-dependent protein kinase. *Proc Natl Acad Sci U S A* **94**: 11067-11072.

Cano DA, Sekine S, Hebrok M. (2006). Primary cilia deletion in pancreatic epithelial cells results in cyst formation and pancreatitis. *Gastroenterology* **131**: 1856-1869.

Carnegie GK, Smith FD, McConnachie G, Langeberg LK, Scott JD. (2004). AKAP-Lbc nucleates a protein kinase D activation scaffold. *Mol Cell* **15**: 889-899.

Carr DW, Stofko-Hahn RE, Fraser ID, Bishop SM, Acott TS, Brennan RG, Scott JD. (1991). Interaction of the regulatory subunit (RII) of cAMP-dependent protein kinase with RII-anchoring proteins occurs through an amphipathic helix binding

motif. *J Biol Chem* **266**: 14188-14192.

Casar B, Sanz-Moreno V, Yazicioglu MN, Rodríguez J, Berciano MT, Lafarga M, Cobb MH, Crespo P. (2007). Mxi2 promotes stimulus-independent ERK nuclear translocation. *EMBO J* **26**: 635-646.

Chakraborty P, Satterly N, Fontoura BM. (2006). Nuclear export assays for poly(A) RNAs. *Methods* **39**: 363-369.

Christensen ST, Pedersen LB, Schneider L, Satir P. (2007). Sensory cilia and integration of signal transduction in human health and disease. *Traffic* **8**: 97-109.

Citterio C, Jones HD, Pacheco-Rodriguez G, Islam A, Moss J, Vaughan M. (2006). Effect of protein kinase A on accumulation of brefeldin A-inhibited guanine nucleotide-exchange protein 1 (BIG1) in HepG2 cell nuclei. *Proc Natl Acad Sci U S A* **103**: 2683-2688.

Clegg CH, Cadd GG, McKnight GS. (1988). Genetic characterization of a brain-specific form of the type I regulatory subunit of cAMP-dependent protein kinase. *Proc Natl Acad Sci U S A* **85**: 3703-3707.

Coghlan VM, Perrino BA, Howard M, Langeberg LK, Hicks JB, Gallatin WM, Scott JD. (1995). Association of protein kinase A and protein phosphatase 2B with a common anchoring protein. *Science* **267**: 108-111.

Collas P, Le Guellec K, Taskén K. (1999). The A-kinase-anchoring protein AKAP95 is a multivalent protein with a key role in chromatin condensation at mitosis. *J Cell Biol* **147**: 1167-1180.

Colledge M, Scott JD. (1999). AKAPs: from structure to function. *Trends Cell Biol* **9**: 216-221.

Condorelli G, Vigliotta G, Iavarone C, Caruso M, Tocchetti CG, Andreozzi F, Cafieri A, Tecce MF, Formisano P, Beguinot L, Beguinot F. (1998). PED/PEA-15 gene controls glucose transport and is overexpressed in type 2 diabetes mellitus. *EMBO J* **17**: 3858-3866.

Corbin JD, Keely SL. (1977). Characterization and regulation of heart adenosine 3':5'-monophosphate-dependent protein kinase isozymes. *J Biol Chem* **252**: 910-918.

Corbin JD, Keely SL, Soderling TR, Park CR. (1977). Hormonal regulation of adenosine 3',5'-monophosphate-dependent protein kinase. *Adv Cyclic Nucleotide Res* **5**: 265-279.

Corbin JD, Sugden PH, Lincoln TM, Keely SL. (1977). Compartmentalization of adenosine 3':5'-monophosphate and adenosine 3':5'-monophosphate-dependent protein kinase in heart tissue. *J Biol Chem* **11**: 3854-3861.

Corbin JD, Sugden PH, West L, Flockhart DA, Lincoln TM, McCarthy D. (1978). Studies on the properties and mode of action of the purified regulatory subunit of bovine heart adenosine 3':5'-monophosphate-dependent protein kinase. *J Biol Chem* **253**: 3997-4003.

Costes SV, Daelemans D., Cho EH, Dobbin Z, Pavlakis G, Lockett S. (2004). Automatic and quantitative measurement of protein-protein colocalization in live

cells. *Biophys J* **86**: 3993-4003.

Cowley BD Jr. (2008). Calcium, cyclic AMP, and MAP kinases: dysregulation in polycystic kidney disease. *Kidney Int* **73**: 251-253.

Daaka Y, Luttrell LM, Lefkowitz RJ. (1997). Switching of the coupling of the beta2-adrenergic receptor to different G proteins by protein kinase A. *Nature* **390**: 88-91.

Dawe HR, Farr H, Gull K. (2007). Centriole/basal body morphogenesis and migration during ciliogenesis in animal cells**.** *J Cell Sci* **120**: 7-15.

Diviani D, Abuin L, Cotecchia S, Pansier L. (2004). Anchoring of both PKA and 14-3-3 inhibits the Rho-GEF activity of the AKAP-Lbc signaling complex. *EMBO J* **23**: 2811-2820.

Dodge-Kafka KL, Kapiloff MS. (2006). The mAKAP signaling complex: integration of cAMP, calcium, and MAP kinase signaling pathways. *Eur J Cell Biol* **85**: 593-602.

Dodge-Kafka KL, Soughayer J, Pare GC, Carlisle Michel JJ, Langeberg LK, Kapiloff MS, Scott JD. (2005). The protein kinase A anchoring protein mAKAP coordinates two integrated cAMP effector pathways. *Nature* **437**: 574-578.

Doucas V, Tini M, Egan DA, Evans RM. (1999). Modulation of CREB binding protein function by the promyelocytic (PML) oncoprotein suggests a role for nuclear bodies in hormone signaling. *Proc Natl Acad Sci U S A* **96**: 2627-2632.

Dugan LL, Kim JS, Zhang Y, Bart RD, Sun Y, Holtzman DM, Gutmann DH. (1999). Differential effects of cAMP in neurons and astrocytes. Role of B-Raf. *J Biol Chem* **274**: 25842-25848.

Eide T, Coghlan V, Orstavik S, Holsve C, Solberg R, Skålhegg BS, Lamb NJ, Langeberg L, Fernandez A, Scott JD, Jahnsen T, Taskén K. (1998). Molecular cloning, chromosomal localization, and cell cycle-dependent subcellular distribution of the A-kinase anchoring protein, AKAP95. *Exp Cell Res* **238**: 305-316.

Elion EA. (2001). The Ste5p scaffold. *J Cell Sci* **114**: 3967-3978.

Elion EA, Brill JA, Fink GR. (1991). FUS3 represses CLN1 and CLN2 and in concert with KSS1 promotes signal transduction. *Proc Natl Acad Sci U S A* **88**: 3967-3978.

Fantozzi DA, Harootunian AT, Wen W, Taylor SS, Feramisco JR, Tsien RY, Meinkoth JL. (1994). Thermostable inhibitor of cAMP-dependent protein kinase enhances the rate of export of the kinase catalytic subunit from the nucleus. *J Biol Chem* **269**: 2676-2686.

Faux MC, Scott JD. (1997). Regulation of the AKAP79-protein kinase C interaction by Ca2+/Calmodulin. *J Biol Chem* **272**: 17038-17044.

Fleischer N, Sarkar D, Rubin C, Erlichman J. (1981). Radioimmunoassay of bovine type II cAMP-dependent kinase. *Methods Enzymol* **74**: 310-320.

Flotho A, Simpson DM, Qi M, Elion EA. (2004). Localized feedback phosphorylation of Ste5p scaffold by associated MAPK cascade. *J Biol Chem* **279**: 47391-47401.

Francis SH, Corbin JD (1994). Structure and function of cyclic nucleotide-dependent protein kinases. *Annu Rev Physiol* **56**: 237-272.

Formstecher E, Ramos JW, Fauquet M, Calderwood DA, Hsieh JC, Canton B, Nguyen XT, Barnier JV, Camonis J, Ginsberg MH, Chneiweiss H. (2001). PEA-15 mediates cytoplasmic sequestration of ERK MAP kinase. *Dev Cell* **1**:239-250.

Fritz J, Strehblow A, Taschner A, Schopoff S, Pasierbek P, Jantsch MF. (2009). RNA-regulated interaction of transportin-1 and exportin-5 with the double-stranded RNA-binding domain regulates nucleocytoplasmic shuttling of ADAR1. *Mol Cell Biol* **29**: 1487-1497.

Gaillard AR, Diener DR, Rosenbaum JL, Sale WS. (2001). Flagellar radial spoke protein 3 is an A-kinase anchoring protein (AKAP). *J Cell Biol* **153**: 443-448.

Gaillard AR, Fox LA, Rhea JM, Craige B, Sale WS. (2006). Disruption of the A-kinase anchoring domain in flagellar radial spoke protein 3 results in unregulated axonemal cAMP-dependent protein kinase activity and abnormal flagellar motility. *Mol Biol Cell* **17**: 2626-2635

Geiss-Friedlander R, Melchior F. (2007). Concepts in sumoylation: a decade on. *Nat Rev Mol Cell Biol* **8**: 947-956.

Gold MG, Lygren B, Dokurno P, Hoshi N, McConnachie G, Taskén K, Carlson CR, Scott JD, Barford D. (2006). Molecular basis of AKAP specificity for PKA regulatory subunits. *Mol Cell* **24**: 383-395.

Goodman DB, Rasmussen H, DiBella F, Guthrow CE Jr. (1970). Cyclic adenosine 3':5'-monophosphate-stimulated phosphorylation of isolated neurotubule subunits. *Proc Natl Acad Sci U S A* **67**: 652-659.

Haglund K, Dikic I. (2005). Ubiquitylation and cell signaling *EMBO J* **24**: 3353–3359.

Hatano N, Mori Y, Oh-hora M, Kosugi A, Fujikawa T, Nakai N, Niwa H, Miyazaki J, Hamaoka T, Ogata M. (2003). Essential role for ERK2 mitogen-activated protein kinase in placental development. *Genes Cells* **8**: 847-856.

Hayakawa F, Privalsky ML. (2004). Phosphorylation of PML by mitogen-activated protein kinases plays a key role in arsenic trioxide-mediated apoptosis. *Cancer Cell* **5**: 389-401.

Hoffmann R, Baillie GS, MacKenzie SJ, Yarwood SJ, Houslay MD. (1999). The MAP kinase ERK2 inhibits the cyclic AMP-specific phosphodiesterase HSPDE4D3 by phosphorylating it at Ser579. *EMBO J* **18**: 893-903.

Houslay MD, Baillie GS. (2005). Beta-arrestin-recruited phosphodiesterase-4 desensitizes the AKAP79/PKA-mediated switching of beta2-adrenoceptor signalling to activation of ERK. *Biochem Soc Trans* **33**: 1333-1336.

Hu Y, Yu H, Pask AJ, O'Brien DA, Shaw G, Renfree MB. (2009). A-kinase anchoring protein 4 has a conserved role in mammalian spermatogenesis. *Reproduction* [Epub ahead of print]

Huang LJ, Durick K, Weiner JA, Chun J, Taylor SS. (1997). Identification of a novel protein kinase A anchoring protein that binds both type I and type II regulatory subunits. *J Biol Chem* **272**: 8057-8064.

Igarashi P, Somlo S. (2002). Genetics and pathogenesis of polycystic kidney disease. *J Am Soc Nephrol* **13**: 2384-2398.

Hunter T, Sefton BM. (1980). Transforming gene product of Rous sarcoma virus phosphorylates tyrosine. *Proc Natl Acad Sci U S A* **77**: 1311-1315.

Ishibe S, Joly D, Zhu X, Cantley LG. (2003). Phosphorylation-dependent paxillin-ERK association mediates hepatocyto growth factor stimulated epithelial morphogenesis. *Mol Cell* **5**: 1275-1285.

Ishibe S, Joly D, Liu ZX, Cantley LG. (2004). Paxillin serves as an ERK-regulated scaffold for coordinating FAK and Rac activation in epithelial morphogenesis. *Mol Cell* **16**: 257-267.

Ishov AM, Sotnikov AG, Negorev D, Vladimirova OV, Neff N, Kamitani T, Yeh ET, Strauss JF, Maul GG. (1999). PML is critical for ND10 formation and recruits the PML-interacting protein daxx to this nuclear structure when modified by SUMO-1. *J Cell Biol* **147**: 221-234.

Jacobs D, Glossip D, Xing H, Muslin AJ, Kornfeld K. (1999). Multiple docking sites on substrate proteins form a modular system that mediates recognition by ERK MAP kinase. *Genes Dev* **13**: 163-175.

Jahnsen T, Hedin L, Kidd VJ, Beattie WG, Lohmann SM, Walter U, Durica J, Schulz TZ, Schiltz E, Browner M, Lawrence CB, Goldman D, Ratoosh SL, Richards JS. (1986). *J Biol Chem* **261**: 12352-12361.

Jones HD, Moss J, Vaughan M. (2005). BIG1 and BIG2, brefeldin A-inhibited guanine nucleotide-exchange factors for ADP-ribosylation factors. *Methods Enzymol* **404**: 174-184.

Kamps MP, Sefton BM. (1989). Acid and base hydrolysis of phosphoproteins bound to immobilon facilitates analysis of phosphoamino acids in gel-fractionated proteins. *Anal Biochem* **176**: 22-27.

Kapiloff MS, Schillace RV, Westphal AM, Scott JD. (1999). mAKAP: an A-kinase anchoring protein targeted to the nuclear membrane of differentiated myocytes. *J Cell Sci* **112**: 2725–2736.

Kinderman FS, Kim C, von Daake S, Ma Y, Pham BQ, Spraggon G, Xuong NH, Jennings PA, Taylor SS. (2006). A dynamic mechanism for AKAP binding to RII isoforms of cAMP-dependent protein kinase. *Mol Cell* **24**: 397-403.

Khoo S, Cobb MH. (1997). Activation of mitogen-activating protein kinase by glucose is not required for insulin secretion. *Proc Natl Acad Sci U S A* **94**: 5599-5604.

Khoo S, Griffen SC, Xia Y, Baer RJ, German MS, Cobb MH. (2003). Regulation of insulin gene transcription by ERK1 and ERK2 in pancreatic beta cells. *J Biol Chem* **278**: 32969-32977.

Klauck TM, Faux MC, Labudda K, Langeberg LK, Jaken S, Scott JD. (1996). Coordination of three signaling enzymes by AKAP79, a mammalian scaffold protein. *Science* **271**: 1589–1592.

Kolch W. (2005). Coordinating ERK/MAPK signaling through scaffolds and inhibitors. *Nat Rev Mol Cell Biol* **6**: 827-837.

Kornfeld K, Hom DB, Horvitz HR. (1995). The ksr-1 gene encodes a novel protein kinase involved in Ras-mediated signaling in C. elegans. *Cell* **83**: 879-888.

Krebs EG, Fischer EH. (1956). The phosphorylase *b* to *a* converting enzyme of rabbit skeletal muscle. *Biochimica et Biophysica Acta* **20**: 150-157.

Krebs EG, Graves DJ, Fischer EH. (1959). Factors Affecting the Activity of Muscle Phosphorylase *b* Kinase. *J Biol Chem* **234**: 2867-2873.

Koukoulas I, Augustine C, Silkenbeumer N, Gunnersen JM, Scott HS, Tan SS. (2004). Genomic organisation and nervous system expression of radial spoke protein 3. *Gene* **336**: 15-23.

Kuettel MR, Squinto SP, Kwast-Welfeld J, Schwoch G, Schweppe JS, Jungmann RA. (1985). Localization of nuclear subunits of cyclic AMP-dependent protein kinase by the immunocolloidal gold method. *J Cell Biol* **101**: 965-975.

Kultgen PL, Byrd SK, Ostrowski LE, Milgram SL. (2002). Characterization of an A-kinase anchoring protein in human ciliary axonemes. *Mol Biol Cell* **13**: 4156-4166.

Kvissel AK, Ørstavik S, Eikvar S, Brede G, Jahnsen T, Collas P, Akusjärvi G, Skålhegg BS. (2007). Involvement of the catalytic subunit of protein kinase A and of HA95 in pre-mRNA splicing. *Exp Cell Res* **313**: 2795-2809.

Lawrence MC, Jivan A, Shao C, Duan L, Goad D, Zaganjor E, Osborne J, McGlynn K, Stippec S, Earnest S, Chen W, Cobb MH. (2008). The roles of MAPKs in disease. *Cell Res* **18**: 436-442.

Lawrence MC, McGlynn K, Park BH, Cobb MH. (2005). ERK1/2-dependent activation of transcription factors required for acute and chronic effects of glucose on the insulin gene promoter. *J Biol Chem* **280**: 26751-26759.

Lee DC, Carmichael DF, Krebs EG, McKnight GS. (1983). Isolation of a cDNA clone for the type I regulatory subunit of bovine cAMP-dependent protein kinase. *Proc Natl Acad Sci U S A* **80**: 3608-3612.

Leon DA, Herberg FW, Banky P, Taylor SS (1997). A stable α-helical domain at the N terminus of the RIα subunit of cAMP-dependent protein kinase is a novel dimerization/docking motif. *J Biol Chem* **272**: 28431-28437.

Lester LB, Coghlan VM, Nauert B, Scott JD. (1996). Cloning and characterization of a novel A-kinase anchoring protein, AKAP220, association with testicular peroxisomes. *J Biol Chem* **271**: 9460-9465.

Levene PA, Alsberg CL. (1906). The cleavage products of vitellin. *J Biol Chem* **2**: 127-133.

Lienhard GE. (2008). Non-functional phosphorylations? *Trends Biochem Sci* **33**: 351-352.

Lin F, Hiesberger T, Cordes K, Sinclair AM, Goldstein LS, Somlo S, Igarashi P. (2003). Kidney-specific inactivation of the KIF3A subunit of kinesin-II inhibits renal ciliogenesis and produces polycystic kidney disease. *Proc Natl Acad Sci U S A* **100**: 5286-5291

Lipmann FA, Levene PA. (1932). Serinephosphoric acid obtained on hydrolysis of vitellinic acid. *J Biol Chem* **98**: 109-114.

Lohmann SM, DeCamilli P, Einig I, Walter U. (1984). High-affinity binding of the regulatory subunit (RII) of cAMP-dependent protein kinase to microtubule-associated and other cellular proteins. *Proc Natl Acad Sci U S A* **81**: 6723-6727.

Loktev AV, Zhang Q, Beck JS, Searby CC, Scheetz TE, Bazan JF, Slusarski DC, Sheffield VC, Jackson PK, Nachury MV. (2008). A BBSome subunit links ciliogenesis, microtubule stability, and acetylation. *Dev Cell* **15**: 854-865.

Lynch MJ, Baillie GS, Mohamed A, Li X, Maisonneuve C, Klussmann E, van Heeke G, Houslay MD. (2005). RNA silencing identifies PDE4D5 as the functionally relevant cAMP phosphodiesterase interacting with beta arrestin to control the protein kinase A/AKAP79-mediated switching of the beta2-adrenergic

receptor to activation of ERK in HEK293B2 cells. *J Biol Chem* **280**: 33178-33189.

Mahanty SK, Wang Y, Farley FW, Elion EA. (1999). Nuclear shuttling of yeast scaffold Ste5 is required for its recruitment to the plasma membrane and activation of the mating MAPK cascade. *Cell* **98**: 501-512.

Makman MH, Sutherland EW. (1964). Use of liver adenyl cyclase for assay of glucagon in human gastro-intestinal tract and pancreas. *Endocrinology*. **75** 127-134.

Mazzucchelli C, Vantaggiato C, Ciamei A, Fasano S, Pakhotin P, Krezel W, Welzl H, Wolfer DP, Pagès G, Valverde O, Marowsky A, Porrazzo A, Orban PC, Maldonado R, Ehrengruber MU, Cestari V, Lipp HP, Chapman PF, Pouysségur J, Brambilla R. (2002). Knockout of ERK1 MAP kinase enhances synaptic plasticity in the striatum and facilitates striatal-mediated learning and memory. *Neuron* **34**: 807-820.

McKnight GS (1991). Cyclic AMP second messenger systems. *Curr Opin Cell Biol* **3**: 213-217.

Meinkoth JL, Ji Y, Taylor SS, Feramisco JR. (19990). Dynamics of the distribution of cyclic AMP-dependent protein kinase in living cells. *Proc Natl Acad Sci U S A* **87**: 9595-9599.

Miki K, Eddy EM. (1999). Single amino acids determine specificity of binding of protein kinase A regulatory subunits by protein kinase A anchoring proteins. *J Biol Chem* **274**: 29057-29062.

Morrison DK, Davis RJ. (2003). Regulation of MAP kinase signaling modules by scaffolding proteins in mammals. *Annu Rev Cell Dev Biol* **19**: 91-118.

Nachury MV, Loktev AV, Zhang Q, Westlake CJ, Peränen J, Merdes A, Slusarski DC, Scheller RH, Bazan JF, Sheffield VC, Jackson PK. (2007). A core complex of BBS proteins cooperates with the GTPase Rab8 to promote ciliary membrane biogenesis. *Cell* **129**: 1201-1213.

Nagao S, Nishii K, Yoshihara D, Kurahashi H, Nagaoka K, Yamashita T, Takahashi H, Yamaguchi T, Calvet JP, Wallace DP. (2008). Calcium channel inhibition accelerates polycystic kidney disease progression in the Cy/+ rat. *Kidney Int* **73**: 269-277.

Nagao S, Yamaguchi T, Kusaka M, Maser RL, Takahashi H, Cowley BD, Grantham JJ. (2003). Renal activation of extracellular signal-regulated kinase in rats with autosomal-dominant polycystic kidney disease. *Kidney Int* **63**: 427-437.

Nauert JB, Rigas JD, Lester LB. (2003). Identification of an IQGAP1/AKAP79 complex in beta-cells. *J Cell Biochem* **90**: 97-108.

Newbern J, Zhong J, Wickramasinghe RS, Li X, Wu Y, Samuels I, Cherosky N, Karlo JC, O'Loughlin B, Wikenheiser J, Gargesha M, Doughman YQ, Charron J, Ginty DD, Watanabe M, Saitta SC, Snider WD, Landreth GE. (2008). Mouse and human phenotypes indicate a critical conserved role for ERK2 signaling in neural crest development. *Proc Natl Acad Sci* **105**: 17115-171120.

Nigg EA, Schäfer G, Hilz H, Eppenberger HM. (1985). Cyclic-AMP-dependent

protein kinase type II is associated with the Golgi complex and with centrosomes. *Cell* **41**: 1039-1051.

Obenauer JC, Cantley LC, Yaffe MB. (2003). Scansite 2.0: Proteome-wide prediction of cell signaling interactions using short sequence motifs. *Nucleic Acids Res* **31**: 3635-3641.

Omori S, Hida M, Fujita H, Takahashi H, Tanimura S, Kohno M, Awazu M. (2006). Extracellular signal-regulated kinase inhibition slows disease progression in mice with polycystic kidney disease. *J Am Soc Nephrol* **17**:1604-1614.

Ostrowski LE, Blackburn K, Radde KM, Moyer MB, Schlatzer DM, Moseley A, Boucher RC. (2002). A proteomic analysis of human cilia: identification of novel components. *Mol Cell Proteomics* **1**: 451-465.

Øyen O, Myklebust F, Scott JD, Hansson V, Jahnsen T (1989). Human testis cDNA for the regulatory subunit RIIα of cAMP-dependent protein kinase encodes an alternate amino-terminal region. *FEBS Lett* **246**: 57-64.

Padilla PI, Chang MJ, Pacheco-Rodriguez G, Adamik R, Moss J, Vaughan M. (2003). Interaction of FK506-binding protein 13 with brefeldin A-inhibited guanine nucleotide-exchange protein 1 (BIG1): effects of FK506. *Proc Natl Acad Sci U S A* **100**: 2322-2327.

Padilla PI, Uhart M, Pacheco-Rodriguez G, Peculis BA, Moss J, Vaughan M. (2008). Association of guanine nucleotide-exchange protein BIG1 in HepG2 cell nuclei with nucleolin, U3 snoRNA, and fibrillarin. *Proc Natl Acad Sci U S A* **105**: 3357-3361.

Pagès G, Guérin S, Grall D, Bonino F, Smith A, Anjuere F, Auberger P,

Pouysségur J. (1999). Defective thymocyte maturation in p44 MAP kinase (Erk 1) knockout mice. *Science* **286**: 1374-1377.

Pan J, Snell W. (2007). The primary cilium: keeper of the key to cell division. *Cell* **129**: 1255-57.

Pare GC, Bauman AL, McHenry M, Michel JJ, Dodge-Kafka KL, Kapiloff MS. (2005). The mAKAP complex participates in the induction of cardiac myocyte hypertrophy by adrenergic receptor signaling. *J Cell Sci* **118**: 5637-5646.

Pearson GW, Earnest S, Cobb MH. (2006). Cyclic AMP selectively uncouples mitogen-activated protein kinase cascades from activating signals. *Mol Cell Biol* **26**: 3039-3047.

Piperno G, Mead K, Shestak W. (1992). The inner dynein arms I2 interact with a "dynein regulatory complex" in Ch/amydomonas flagella. *J. Cell Biol* **118**:1455-1463.

Potts PR, Yu H. (2007). The SMC5/6 complex maintains telomere length in ALT cancer cells through SUMOylation of telomere-binding proteins. *Nat Struct Mol Biol* **14**: 581-590.

Printen JA, Sprague GF Jr. (1994). Protein-protein interactions in the yeast pheromone response pathway: Ste5p interacts with all members of the MAP kinase cascade. *Genetics* **138**: 609-619.

Pugacheva EN, Jablonski SA, Hartman TR, Henske EP, Golemis EA. HEF1-dependent Aurora A activation induces disassembly of the primary cilium. (2007). *Cell* **129**: 1351-1363.

Pullikuth A, McKinnon E, Schaeffer HJ, Catling AD. (2005). The MEK1 scaffolding protein MP1 regulates cell spreading by integrating PAK1 and Rho signals. *Mol Cell Biol* **25**: 5119-5133.

Qin H, Wang Z, Diener D, Rosenbaum J. (2007). Intraflagellar transport protein 27 is a small G protein involved in cell-cycle control. *Curr Biol* **17**: 193-202.

Rall TW, Sutherland EW, Wosilait WD. (1956). The relationship of epinephrine and glucagon to liver phosphorylase. III. Reactivation of liver phosphorylase in slices and in extracts. *J Biol Chem* **218**: 483-495.

Rall TW, Sutherland EW. (1957). Formation of a cyclic adenine ribonucleotide by tissue particles. *J Biol Chem* **232**: 1065-1076.

Ranganathan A, Yazicioglu MN, Cobb MH. (2006). The nuclear localization of ERK2 occurs by mechanisms both independent of and dependent on energy. *J Biol Chem* **281**: 15645-15652.

Ray LB, Sturgill TW. (1987). Rapid stimulation by insulin of a serine/threonine kinase in 3T3-L1 adipocytes that phosphorylates microtubule-associated protein 2 in vitro. *Proc Natl Acad Sci U S A* **84**: 1502-1506.

Rieder CL, Jensen CG, Jensen LC. (1979). The resorption of primary cilia during

mitosis in a vertebrate (PtK1) cell line. *J Ultrastruct Res* **68**: 173-185.

Reimann EM, Brostrom CO, Corbin JD, King CA, Krebs EG. (1971). Separation of regulatory and catalytic subunits of the cyclic 3',5'-adenosine monophosphate-dependent protein kinase(s) of rabbit skeletal muscle. *Biochem Biophys Res Commun* **42**: 187-194.

Reinton N, Orstavik S, Haugen TB, Jahnsen T, Taskén K, Skålhegg BS. (2000). A novel isoform of human cyclic 3',5'-adenosine monophosphate-dependent protein kinase, c alpha-s, localizes to sperm midpiece. *Biol Reprod* **63**: 607-611.

Roberts PJ, Der CJ. (2007). Targeting the Raf-MEK-ERK mitogen-activated protein kinase cascade for the treatment of cancer. *Oncogene* **26**:3291-3310.

Rodriguez, MS, Dargemont C, Hay RT. (2001). SUMO-1 conjugation in vivo requires both a consensus modification motif and nuclear targeting. *J Biol Chem* **276**: 12654–12659.

Rubin CS, Erlichman J, Rosen OM. (1972). Cyclic adenosine 3',5'-monophosphate-dependent protein kinase of human erythrocyte membranes. *J Biol Chem* **247**: 6135-6139.

Saba-El-Leil MK, Vella FD, Vernay B, Voisin L, Chen L, Labrecque N, Ang SL, Meloche S. (2003). An essential function of the mitogen-activated protein kinase Erk2 in mouse trophoblast development. *EMBO Rep* **4**: 964-968.

Saeki N, Tokuo H, Ikebe M. (2005). BIG1 is a binding partner of myosin IXb and regulates its Rho-GTPase activating protein activity. *J Biol Chem* **280**: 10128-10134.

Samuels IS, Karlo JC, Faruzzi AN, Pickering K, Herrup K, Sweatt JD, Saitta SC, Landreth GE. (2008). Deletion of ERK2 mitogen-activated protein kinase identifies its key roles in cortical neurogenesis and cognitive function. *J Neurosci* **28**: 6983-6985

San Agustin JT, Leszyk JD, Nuwaysir LM, Witman GB. (1998). The catalytic subunit of the cAMP-dependent protein kinase of ovine sperm flagella has a unique amino-terminal sequence. *J Biol Chem* **273**: 24874-24883.

Sandberg M, Taskén K, Øyen O, Hansson V, Jahnsen T. (1987). Molecular cloning, cDNA structure and deduced amino acid sequence for a type I regulatory subunit of cAMP-dependent protein kinase from human testis. *Biochem Biophys Res Commun* **149**: 939-945.

Sanz-Moreno V, Casar B, Crespo P. (2003). p38alpha isoform Mxi2 binds to extracellular signal-regulated kinase 1 and 2 mitogen-activated protein kinase and regulates its nuclear activity by sustaining its phosphorylation levels. *Mol Cell Biol* **23**: 3079-3090.

Sastri M, Barraclough DM, Carmichael PT, Taylor SS. (2005). A-kinase-interacting protein localizes protein kinase A in the nucleus. *Proc Natl Acad Sci U S A* **102**: 349-354.

Satir P, Christensen ST. Overview of structure and function of mammalian cilia.

(2007). *Annu Rev Physiol* **69**: 377-400.

Schneider L, Clement CA, Teilmann SC, Pazour GJ, Hoffmann EK, Satir P, Christensen ST. (2005). PDGFRαα signaling is regulated through the primary cilium in fibroblasts. *Curr Biol* **15**: 1861-1866.

Scott JD, Glaccum MB, Zoller MJ, Uhler MD, Helfman DM, McKnight GS, Krebs EG. (1987). The molecular cloning of a type II regulatory subunit of the cAMP-dependent protein kinase from rat skeletal muscle and mouse brain. *Proc Natl Acad Sci U S A* **84**: 5192-5196 (1987).

Scott JD, Stofko RE, McDonald JR, Comer JD, Vitalis EA, Mangili JA. (1990). Type II regulatory subunit dimerization determines the subcellular localization of the cAMP-dependent protein kinase. *J Biol Chem* **265**: 21561-21566.

Seidel JJ, Graves BJ. (2002). An ERK2 docking site in the Pointed domain distinguishes a subset of ETS transcription factors. *Genes Dev* **16**: 127-137.

Sette C, Conti M. (1996). Phosphorylation and activation of a cAMP-specific phosphodiesterase by the cAMP-dependent protein kinase. Involvement of serine 54 in the enzyme activation. *J Biol Chem* **271**: 16526-16534.

Sharrocks AD, Yang SH, Galanis A. (2000). Docking domains and substrate-specificity determination for MAP kinases. *Trends Biochem Sci* **25**: 448-453.

Shibazaki S, Yu Z, Nishio S, Tian X, Thomson RB, Mitobe M, Louvi A, Velazquez H, Ishibe S, Cantley LG, Igarashi P, Somlo S. (2008). Cyst formation and activation of the extracellular regulated kinase pathway after kidney specific

inactivation of Pkd1. *Hum Mol Genet* **17**: 1505-1516.

Silliman CC, Sturgill TW. (1989). Phosphorylation of microtubule-associated protein 2 by MAP kinase primarily involves the projection domain. *Biochem Biophys Res Commun* **160**: 993-998.

Solberg R, Taskén K, Keiserud A, Jahnsen T (1991). Molecular cloning, cDNA structure and tissue-specific expression of the human regulatory subunit RIb of cAMP-dependent protein kinases. *Biochem Biophys Res Commun* **176**: 166-172.

Solberg R, Sandberg M, Natarajan V, Torjesen PA, Hansson V, Jahnsen T, Taskén K. (1997). The human gene for the regulatory subunit RIa of cAMP-dependent protein kinase - Two distinct promoters provide differential regulation of alternately spliced mRNAs. *Endocrinology* **138**: 169-181.

Sorokin S. (1962). Centrioles and the formation of rudimentary cilia by fibroblasts and smooth muscle cells. *J Cell Biol* **15**: 363-377.

Spector D. (2001). Nuclear domains. *J Cell Sci* **114**: 2891-2893.

Stewart S, Sundaram M, Zhang Y, Lee J, Han M, Guan KL. (1999). Kinase suppressor of Ras forms a multiprotein signaling complex and modulates MEK localization. *Mol Cell Biol* **19**: 5523-5534.

Süel KE, Gu H, Chook YM. (2008). Modular organization and combinatorial energetics of proline-tyrosine nuclear localization signals. *PLoS Biol* **6**: 1253-1267.

Sundaram M, Han M. (1995). The C. elegans ksr-1 gene encodes a novel Raf-related kinase involved in Ras-mediated signal transduction. *Cell* **83**: 879-888.

Takeda S, Yonekawa Y, Tanaka Y, Okada Y, Nonaka S, Hirokawa N. (1999). Left-right asymmetry and kinesin superfamily protein KIF3A: new insights in determination of laterality and mesoderm induction by kif3A-/- mice analysis. *J Cell Biol* **145**: 825-836.

Takio K, Smith SB, Krebs EG, Walsh KA, Titani K. (1984). Amino acid sequence of the regulatory subunit of bovine type II adenosine 3',5'-phosphate dependent protein kinase. *Biochemistry* **23**: 4200-4206.

Tanoue T, Adachi M, Moriguchi T, Nishida E. (2000). A conserved docking motif in MAP kinases common to substrates, activators and regulators. *Nat Cell Biol* **2**: 110-116.

Tanoue T, Maeda R, Adachi M, Nishida E. (2001). Identification of a docking groove on ERK and p38 MAP kinases that regulates the specificity of docking interactions. *EMBO J* **20**: 466-479.

Teis D, Taub N, Kurzbauer R, Hilber D, de Araujo ME, Erlacher M, Offterdinger M, Villunger A, Geley S, Bohn G, Klein C, Hess MW, Huber LA. (2006). p14-MP1-MEK1 signaling regulates endosomal traffic and cellular proliferation during tissue homeostasis. *J Cell Biol* **175**: 861-868.

Teis D, Wunderlich W, Huber LA. (2002). Localization of the MP1-MAPK scaffold complex to endosomes is mediated by p14 and required for signal transduction. *Dev Cell* **3**: 803-814.

Theurkauf WE, Vallee RB. (1982). Molecular characterization of the cAMP-dependent protein kinase bound to microtubule-associated protein 2. *J Biol Chem* **257**: 3284-3290.

Theurkauf WE, Vallee RB. (1983). Extensive cAMP-dependent and cAMP-independent phosphorylation of microtubule-associated protein 2. *J Biol Chem* **258**: 7883-7886.

Therrien M, Chang HC, Solomon NM, Karim FD, Wassarman DA, Rubin GM. (1995). KSR, a novel protein kinase required for RAS signal transduction. *Cell* **83**: 879-888.

Therrien M, Michaud NR, Rubin GM, Morrison DK. (1996). KSR modulates signal propagation within the MAPK cascade. *Genes Dev* **10**: 2684-2685.

Titani K, Sasagawa T, Ericsson LH, Kumar S, Smith SB, Krebs EG, Walsh KA (1984). Protein sequence of the rabbit Type I regulator subunit of the cAMP-dependent kinase. *Biochemistry* **23**: 4193-4199.

Trotman LC, Alimonti A, Scaglioni PP, Koutcher JA, Cordon-Cardo C, Pandolfi PP. (2006). Identification of a tumour suppressor network opposing nuclear Akt function. *Nature* **441**: 523-527.

Tu H, Tang TS, Wang Z, Bezprozvanny I. (2004). Association of type 1 inositol 1,4,5-trisphosphate receptor with AKAP9 (Yotiao) and protein kinase A. *J Biol Chem* **279**: 19375-19382.

Tucker RW, Pardee AB, Fujiwara K. (1979). Centriole ciliation is related to quiescence and DNA synthesis in 3T3 cells. *Cell* **17**: 527-535.

Uhler MD, Carmichael DF, Lee DC, Chrivia JC, Krebs EG, McKnight GS. (1986). Isolation of cDNA clones for the catalytic subunit of mouse cAMP-dependent protein kinase. *Proc Natl Acad Sci U S A* **83**: 1300-1304.

Uhler MD, Chrivia JC, McKnight GS. (1986). Evidence for a second isoform of the catalytic subunit of cAMP-dependent protein kinase. *J Biol Chem* **261**: 15360-15363.

Vigliotta G, Miele C, Santopietro S, Portella G, Perfetti A, Maitan MA, Cassese A, Oriente F, Trencia A, Fiory F, Romano C, Tiveron C, Tatangelo L, Troncone G, Formisano P, Beguinot F. (2004). Overexpression of the ped/pea-15 gene causes diabetes by impairing glucose-stimulated insulin secretion in addition to insulin action. *Mol Cell Biol* **24**:5005-5015.

Walsh DA, Ashby CD, Gonzalez C, Calkins D, Fischer EH, Krebs EG. (1971). Purification and characterization of a protein inhibitor of adenosine 3',5'-monophosphate-dependent protein kinases. *J Biol Chem* **246**: 1977-1985.

Walsh DA, Perkins JP, Krebs EG. (1968). An Adenosine 3',5'-Monophosphate-dependent Protein Kinase from Rabbit Skeletal Muscle. *J Biol Chem* **243**: 3763-3774.

Wen W, Harootunian AT, Adams SR, Feramisco J, Tsien RY, Meinkoth JL, Taylor SS. (1994). Heat-stable inhibitors of cAMP-dependent protein kinase carry a nuclear export signal. *J Biol Chem* **269**: 32214-32220.

Wetzker R, Bohmer FD (2003). Transactivation joins multiple tracks to the ERK/MAPK cascade. *Nat Rev Mol Cell Biol* **4**: 651-657.

Whitehurst AW, Robinson FL, Moore MS, Cobb MH. (2004). The death effector domain protein PEA-15 prevents nuclear entry of ERK2 by inhibiting required interactions. *J Biol Chem* **279**: 12840-12847.

Wirschell M, Zhao F, Yang C, Yang P, Diener D, Gaillard A, Rosenbaum JL, Sale WS. (2008). Building a radial spoke: flagellar radial spoke protein 3 (RSP3) is a dimer. *Cell Motil Cytoskeleton* **65**: 238-248.

Wong W, Goehring AS, Kapiloff MS, Langeberg LK, Scott JD. (2008). mAKAP compartmentalizes oxygen-dependent control of HIF-1alpha. *Sci Signal* **1**: 1-9.

Wong W, Scott JD. (2004). AKAP signalling complexes: focal points in space and time. *Nat Rev Mol Cell Biol* **5**: 959-970.

Xu KF, Shen X, Li H, Pacheco-Rodriguez G, Moss J, Vaughan M. (2005). Interaction of BIG2, a brefeldin A-inhibited guanine nucleotide-exchange protein, with exocyst protein Exo70. *Proc Natl Acad Sci U S A* **102**: 2784-2789.

Yamaguchi T, Nagao S, Wallace DP, Belibi FA, Cowley BD, Pelling JC, Grantham JJ. (2003). Cyclic AMP activates B-Raf and ERK in cyst epithelial cells from autosomal-dominant polycystic kidneys. *Kidney Int* **63**: 1983-1994.

Yamaguchi T, Pelling JC, Ramaswamy NT, Eppler JW, Wallace DP, Nagao S, Rome LA, Sullivan LP, Grantham JJ. (2000). cAMP stimulates the in vitro

proliferation of renal cyst epithelial cells by activating the extracellular signal-regulated kinase pathway. *Kidney Int* **57**: 1460-1471.

Yamaguchi T, Wallace DP, Magenheimer BS, Hempson SJ, Grantham JJ, Calvet JP. (2004). Calcium restriction allows cAMP activation of the B-Raf/ERK pathway, switching cells to a cAMP-dependent growth-stimulated phenotype. *J Biol Chem* **279**:40419-40430.

Yang J, Drazba JA, Ferguson DG, Bond M. (1998). A-kinase anchoring protein 100 (AKAP100) is localized in multiple subcellular compartments in the adult rat heart. *J Cell Biol* **142**: 511-522.

Yang P, Diener DR, Yang C, Kohno T, Pazour GJ, Dienes JM, Agrin NS, King SM, Sale WS, Kamiya R, Rosenbaum JL, Witman GB. (2006). Radial spoke proteins of *Chlamydomonas* flagella. *J Cell Sci* **119**: 1165-1174.

Yang SH, Yates PR, Whitmarsh AJ, Davis RJ, Sharrocks AD. (1998). The Elk-1 ETS-domain transcription factor contains a mitogen-activated protein kinase targeting motif. *Mol cell Biol* **18**: 710-720.

Yazicioglu MN, Goad DL, Ranganathan A, Whitehurst AW, Goldsmith EJ, Cobb MH. (2007). Mutations in ERK2 binding sites affect nuclear entry. *J Biol Chem* **282**: 28759-28767.

Yu W, Fantl WJ, Harrowe G, Williams LT. (1998). Regulation of the MAP kinase pathway by mammalian Ksr through direct interaction with MEK and ERK. *Curr Biol* **8**: 56-64.

Zervos AS, Faccio L, Gatto JP, Kyriakis JM, Brent R. (1995). Mxi2, a mitogen-activated protein kinase that recognizes and phosphorylates Max protein. *Proc Natl Acad Sci U S A* **23**: 10531-10534.

Zhang Q, Carr DW, Lerea KM, Scott JD, Newman SA. (1996). Nuclear localization of type II cAMP-dependent protein kinase during limb cartilage differentiation is associated with a novel developmentally regulated A-kinase anchoring protein. *Dev Biol* **176**: 51-61.

Zhao J, Hoye E, Boylan S, Walsh DA, Trewhella J. (1998). Quaternary structures of a catalytic subunit-regulatory subunit dimeric complex and the holoenzyme of the cAMP-dependent protein kinase by neutron contrast variation. *J Biol Chem* **273**: 30448-30459.